Development of Conductometric Polymer Sensor

for Gaseous Hydrogen Chloride

Dissertation

zur Erlangung des Doktorgrades der Naturwissenschaften

(doktorum rerum naturalis, Dr. Rer. Nat.)

der Fakultät für Chemie und Pharmazie

der Universität Regensburg

Deutschland

vorgelegt von

Qingli HAO

aus Nanjing, China

im Dezember 2003

Development of Conductometric Polymer Sensor

for Gaseous Hydrogen Chloride

Dissertation

Submitted in conformity with the requirements

for the degree of doctor philosophy (Dr. rer. nat)

Presented by

Qingli HAO

(Nanjing, China)

December 2003

Faculty of Chemistry and Pharmacy, University of Regensburg, Germany

This study was performed in the group of Prof. Dr. Wolfbeis, Institute of Analytical Chemistry, Chemo- and Biosensors, University of Regensburg, during the period from October 2001 to December 2003 under the supervision of PD. Dr. Vladimir M. Mirsky.

Request for doctorate submitted in November of 2003

Date of defence: 17, December 2003

Board of examiners (Prüfungsausschuß):

Chairman (Vorsitzender):   Prof. Dr. Otto S. Wolfbeis

First Examiner (Erstgutachter):   PD. Dr. Vladimir M. Mirsky

Second Examiner (Zweitgutachter):   Prof. Dr. J. Daub

Third Examiner (Drittprüfer):   Prof. Dr. W. Kunz

Dedicated to my family

Table of Contents

1 Introduction

1.1 Overview of Organic Conducting Polymers

Organic conducting polymer (OCP) is one kind of polymers with spatially extended π–bonding system. The evolution of organic conducting polymers (OCPs) did not draw significant scientific attention before the mid 1970s, although they have been known for many years. Since the discovery that polyacetylene conductivity can be enhanced by seven orders of magnitude by doping with iodine in 1977,[1] a large effort has been focused on discovering other organic conducting polymers (OCPs). This covered making polymers conductive, improving the properties of the materials and the extensive applications followed in various fields. A new field of chemistry was born. The discovery of conducting polyacetylene and the significance of OCPs were recognized by the award of the Chemistry Nobel Prize in 2000 to Alan Heeger, Alan MacDiarmid and Hideki Shirakawa.[2-4]

OCPs combine the electronic and optical properties of semiconductors and metals with the attractive mechanical properties and processing advantages of polymers. OCPs possess many advantageous properties in chemical, electrical, physical and optical aspects, compared to normal polymers. These properties cover high conductance, luminescence, electrochromism and high thermal stability. This has triggered the development of novel OCPs, such as polyaniline (PANI), polypyrrole (PPY), polythiophene, polyphenylene, etc.,[2;3;5] and their application in batteries,[6-9] electronic devices, functional electrodes,[10;11] electrochromic devices,[12] optical switching devices, sensors and so on.[13-18] All these applications are based on OCPs on certain substrates. Different approaches are used to deposit OCP films onto a substrate, classified as "chemical method" and "electrochemical method". These preparation include spin-coating, dip-coating, drop-coating, thermal evaporation,[19] Langmuir-Blodgett (LB),[19;20] and self-assembly techniques (SA)[20-22] belonging to chemical approach.

Polyaniline (PANI) is probably the most important industrial OCP today. This is due to its facile synthesis and processing, environmental stability and low cost. In addition, PANI has two attractive properties: intrinsic redox state and reversible doping/de-doping of acid/base.

1.1.1   Synthesis of Organic Conducting Polymers

Various methods are available for the synthesis of conducting polymers. But the most widely used technique is based on the oxidative coupling. Oxidative coupling involves the

oxidation of monomers to form a cation radical followed by coupling to form a di-cation. Repetition leads to the desired polymer. This can be performed by chemical or electrochemical polymerization.

PANI and its derivatives may be synthesized by both chemical and electrochemical methods described above. Additionally, the synthesis of PANI can also be performed as inverse emulsion polymerization,[23;24] plasma polymerization,[25;26] and autocatalytic polymerization.[27]

Chemical Synthesis can be carried out in a solution containing the monomer and an oxidant in an acidic medium. The common acids used are hydrochloric acid (HCl) and sulfuric acid (H_2SO_4). Ammonium persulfate (($NH_4)_2S_2O_8$),[28] postassium dichromate ($K_2Cr_2O_7$),[29] cerium sulface ($Ce(SO_4)_2$), sodium vanadate ($NaVO_3$), potassium ferricyanide ($K_3(Fe(CN)_6$), potassium iodate (KIO_3) and hydrogen peroxide (H_2O_2)[30;31] are typically used as oxidants.

The optimal reaction conditions to obtain high conductivity and yield are: about 1 M aqueous HCl with an oxidant (ammonium persulfate)/aniline ratio of ≤ 1.15.[31] The optimal experimental temperature to avoid or reduce secondary reactions is $0 \sim 2°C$.[32] The reaction takes one to two hours. Experiments are performed under the following conditions: pre-cooling both aniline/HCl solution and the oxidant solution at about 0°C, adding drop by drop the latter to the former solutions with stirring, and washing with HCl acid after filtration, then drying under vacuum for about 48 h.[31] The green precipitate formed is called "polyemeraldine hydrochloride" (PANI-Cl). "Polyemeraldine base (PEB)" can be obtained by immersing PANI-Cl in aqueous ammonium hydrochloride for 15 h.

One of the disadvantages of this direct way results from the complicate solution containing an excess of oxidant and higher ionic strength in the medium. This leads to impurities of the final product.[33]

Electrochemical Synthesis can be carried out in three ways: (1) potentiostatic (constant potential) method; (2) galvanostatic (constant current) method; (3) potentiodynamic (potential scanning or cyclic voltammetric) method.

Standard electrochemical techniques include a three-electrode cell which contains a working electrode (WE), a reference electrode (RE) and a counter electrode (CE) or an auxiliary electrode (AE). Many kinds of materials can be used as WEs. Generally, the commonly used WEs are chromium, gold,[34] nickel, copper,[31] palladium, titanium, platinum, indium-tin oxide coated glass plates[35;36] and stainless steel,[25] Semi-conducting materials, such

as n-doped silicon,[37] gallium arsenide,[38] cadmium sulphide, and semi-metal graphite[39] are also employed for the growth of polymer films. The reference electrode (RE) is typically a saturated calomel electrode (SCE) or Ag/AgCl electrode. The CE or AE is usually made of a platinum wire or foil. Electrochemical synthesis can be done in aqueous or organic solutions.

Compared to chemical synthesis, electrochemical approach has definite advantages,[31;32;40] such as purity of the product and easy control of the thickness of OCPs deposited on WEs. In addition, the doping level can be controlled by varying the current and potential with time; synthesis and deposition of polymer can be realized simultaneously. Therefore, it rapidly becomes the preferred method for preparing electrically conducting polymers.

Different polymerization mechanisms have been put forward due to various synthesis methods. Many reviews[41;42] provided the polymerization mechanisms in chemical, electrochemical and gas-phase preparations. It seems that the electrochemical polymerization has been investigated more thoroughly compared to the chemical one; the reason could be the above described advantages of this technique.[31]

1.1.2 Polymerization Mechanism of Polyaniline

Both types of polymerization start with the formation of radical cations (Scheme 1.1-1 a), followed by coupling to form di-cation (Scheme 1.1-1 b) and the repetition leads to the aimed polymer containing reduced benzenoid (-B-) units and oxidized quinoid units (=Q=) (Scheme 1.1-1 c and d).[43;44] The latter reaction in (c) is autocatalyzed.[18] The general structure of PANI is shown in Scheme 1.1-1 (d),[16;18] where (1-y) is the average oxidation state.

Several oxidation states exist between the fully reduced state, so-called Leucoemeraldine Base (LB, where 1-y = 0), and the fully oxidized state, named Pernigraniline Base (PB, where 1-y = 1). The half oxidized state (1-y = 0.5), called Emeraldine Base (EB) state, is a semiconductor composed of an alternation sequence of two benzenoid units (-B-) and one quinoid unit (=Q=). EB can be non-redox doped with acid to a conducting Emeraldine Salt (ES) state of PANI, green colored.

Resonance forms of aniline radical cation

di-cation
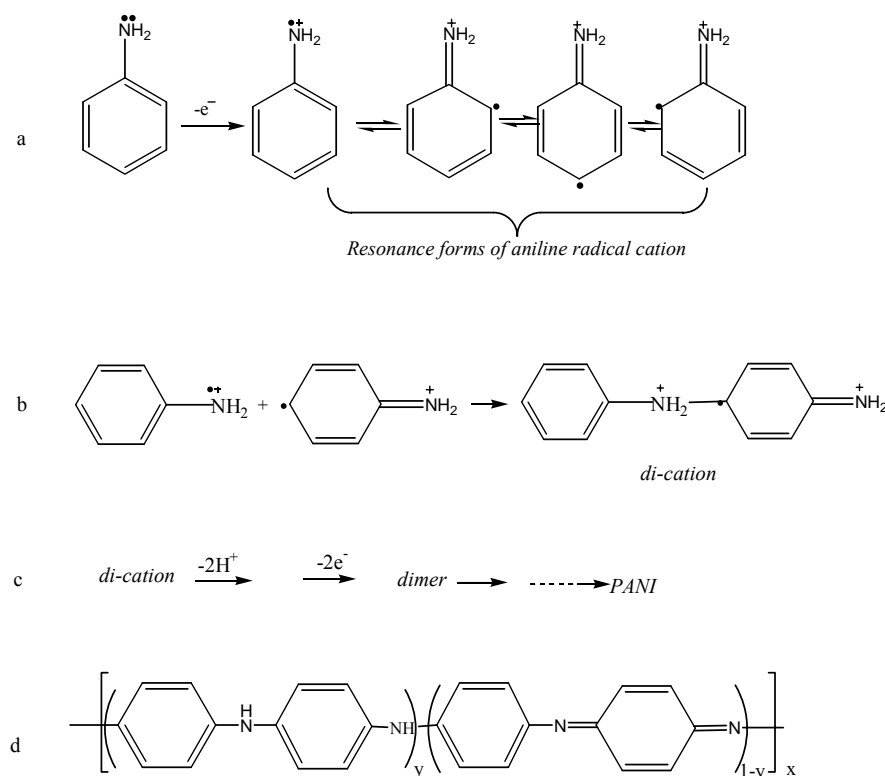
Scheme 1.1-1 Polymerization Mechanism of PANI

1.1.3   Mechanism of PANI Inter-Conversions

It is well known that there are several oxidation states of PANI which can exist in different forms (Table 1.1-1[18;45-47]). The various oxidation states of PANI were synthesized and characterized done extensively several years ago by many researchers.[28;48-56]

PANI is a specific conducting polymer because its conducting mechanism is caused either by the oxidation of poly(leucoemeraldine base) (PLB) or by the protonation of poly(emeraldine base) (PEB). The protonation/deprotonation process is also referred to as acid/base doping/dedoping process. Inter-conversions of PANI among various oxidation states are shown in Scheme 1.1-2.[46]

Oxidative doping can be performed by both the chemical and electrochemical method from the fully reduced state (PLB) of PNAI.[18] But the oxidative doping level in chemical process is very difficult to control. However, electrochemical doping solves this problem. It can be controlled very well by the potential applied between working electrode and counter electrode.[57] PLB is readily oxidized to PES with the counter ions of the electrolyte (acids) inserting in the polymer backbone.

Table 1.1-1 Different forms of PANI

Full Name	(1-y)	Redox state	Conductivity (S.cm^{-1})	Color
Leucoemeraldine Base (LB)	0	Full reduced	< 10^{-5}	Yellow or transparent
Emeraldine Base (EB)	0.5	Half -Oxidized	< 10^{-5}	Deep blue
Nigraniline Base (NB) (in non-aqueous media with additional halogen[58])	0.75	75 % oxidized	< 10^{-5}	Blue purple
Pernigraniline Base (PB)	1	Full oxidized	< 10^{-5}	Purple
Emeraldine Salt (ES)	*0.5*	*Half reduced- Oxidized*	*~ 15*	*Green*
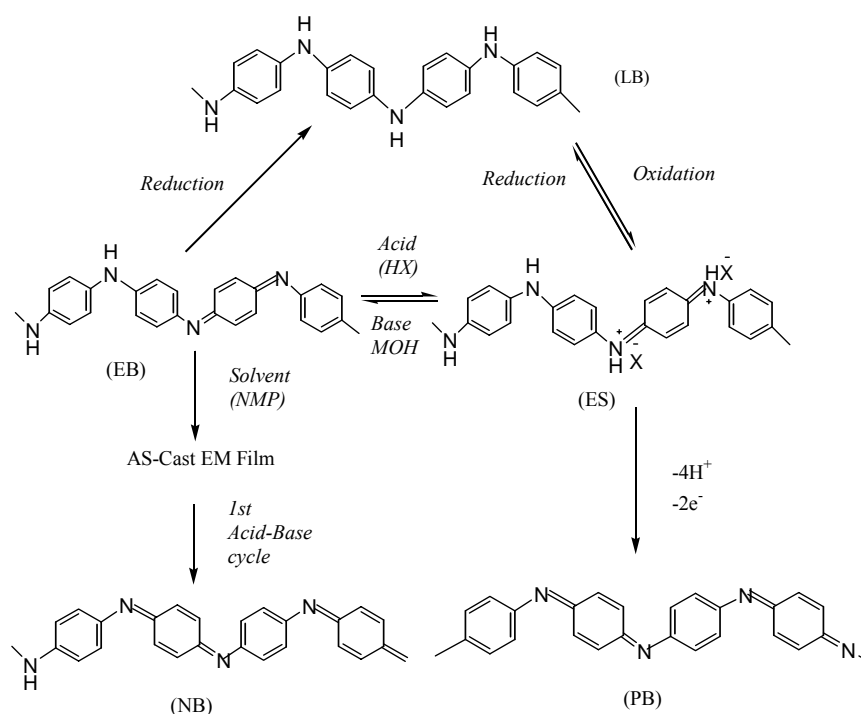
Scheme 1.1-2 Inter-conversions among various oxidation states and protonated/deprotonated states in PANI

Acid doping means acidic/basic doping/dedoping due to the protonation and deprotonation process of PANI. This is a reversible process which provides a great potential for the application of PANI in various fields. What is interesting is that, during doping and

dedoping processes, there is no change in the number of electrons in the backbone (chain) of PANI. Generally, a complete acidic doping process means the emeraldine base (EB) state can convert to the emeraldine salt (ES) state of PANI, which results from the protonation of the imine sites associated with quinonoid groups in the presence of a strong acid (HCl, H_2SO_4). This makes insulating PANI base of EB conductive. This doping process was demonstrated by Nicolas-Debarnot *et al.* [18] and shown in Scheme 1.1-3. At the last step, a formation of PEB bipolaron leads to a great increase in conductivity due to delocalization of charge and spins along the backbone of PANI.

Two types of doping exist in PANI during the electrochemical polymerization of aniline by cyclic voltammetry. According to polarization theory[51;59], PANI produced can exist in a base (EB) (A), a bipolaron (B) (ES), and two polarons (C) (PB). The EB form of PANI contains benzenoid and quinonoid rings in a ratio of 3:1; it is diamagnetic and insulating and its paramagnetic centers and conductivity would appear only if it is protonated (doped). Protonation leads to the appearance of positively charged paramagnetic polarons and diamagnetic bipolarons. Two polarons (C) can recombine to form one bipolaron (B). Conductivity can be a result of motions between polarons and bipolarons. Bipolarons prevail in the salt from of PANI (Emeraldine Base). All these inter-conversions can be presented clearly in cyclic voltammograms.[31;46;51]

Typical cyclic voltammogram of PANI includes two main redox couples. The anodic peak at $0.2 \sim 0.3$V (vs SCE) is due to the formation of a mono-cation radical; the anodic peak near 0.8 V (vs SCE) corresponds to the oxidation of ES followed by deprotonation of the polymer giving the fully oxidized pernigraniline form. This anodic process is responsible for the generation of di-radical di-cations in PANI structure resulting from the head to tail addition of monomer units.[60;61] In case of the potential > 0.8V, the di-radical di-cation acts as an energetic elector-pile capable of interacting with neutral aniline molecule to result in further growth. Middle peak (around 0.5 V) in cyclic voltammograms is a disputable peak. Dhawan *et al.*[43] suggested that was essentially due to an adsorption of quinone/hydroquinone generated during the growth of the polymer, and the intensity of this peak further increased with the increase of quinone/hydroquinone externally in the electrolyte; however, Chen W. – C[60;62] group and other groups[12;63;64] gave a different explanation: the presence of redox peaks around 0.5V (vs Ag/AgCl) in CVs is often considered as the argument for p-benzoquinone (BQ) and hydroquinone (HQ) formation.

Poly(emeraldine base) **PEB**)

+ 2 HCl | Formation of a coordinence bonding Between N and H⁺

Internal rearrangement (relaxation)

Redistribution of charge and spin

Poly(emeraldine salt) (**PES**)
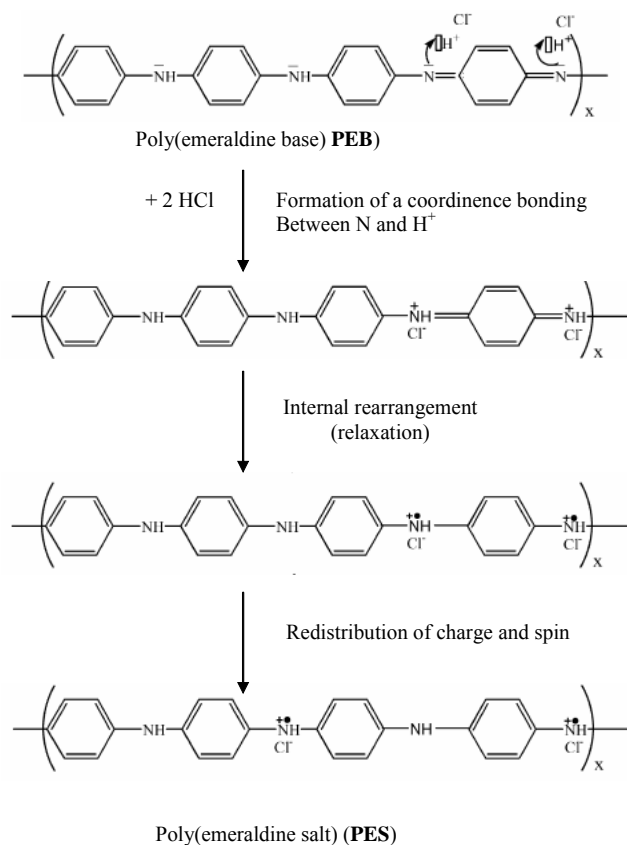
Scheme 1.1-3 Mechanism of acidic doping[18]

1.1.4 Properties of PANI

Low solubility is one of the properties of hydrochloride polyemeraldine salt (PANI-Cl). Most of other PESs doped with small size dopants have this drawback. Therefore, many approaches have been tried to improve the solubility of PANI salts. On the one hand, they can be achieved by using other dopants instead of HCl, H_2SO_4 in the monomer solution. For instance, lithium salts,[65] big-size dopants, or polymeric acids (such as polyacrylic acid[66-68]) are often employed. Additionally, voluminous acids (such as acrylic acid[69-71]) and long-chain sulfuric acids (for example, camphorsulfonic acid (CSA),[72-74] dodecylbenzenfulfonic acid (DBSA)[75-77]) have also been used as dopants of PANI.

On the other hand, introducing functional substitutions of hydrogen atom either in the aniline ring in various positions or in the nitrogen of amino group is another important method to improve the solubility of PANI films. The usual functional groups used are – R or –OR (R = alkyl). Some of such groups lead to modified polymers soluble in water, such as – OCH_3 and $–OC_2H_5$ instead of hydrogen in the aniline ring, but this also weakens conductivity to as low as $10^{-1} \sim 10^{-3}$ S.cm⁻¹. N-substituted PANI dissolves in some organic solvents,[78;79] but

has reduced thermal stability compared with PANI.[80] 'Self-doped' PANI, whose substitution is an acidic group like –SO$_3$H, -COOH and so on, has better solubility,[79;81] but lower thermal stability.[82;83]

Good thermal stability is another attractive property of PANI. It is recognized that PANI has good temperature stability up to 400°C in N$_2$.[84-86] Counter ions in the PANI chains influence the thermal properties of PANI. The introducing of –SO$_3$H in aniline ring can weaken the thermal stability of aniline.[82;83] Many studies reported the change of PANI structure during heating at high temperature. Several cross-linking structures resulting from degradation of PANI during heating were proposed. It is reported that cross-linking started at around 200°C controversially.[87-92]

"Anion effects" [93] are often referred to as the strong influence of counter ions on the properties of PANI. These effects are embodied on polymeric morphology and thermal stability, electropolymerization extent, and the electrochemical response.[94] The growth rate of a PANI film is apparently dependent on the type of anion as well.[95] Wang *et al*[96] observed that the reaction rate followed an order: H$_2$SO$_4$ > H$_3$PO$_4$ ≈ HF > > HBF$_4$ ≈ HClO$_4$ > HCl. A similar order in reaction rate was reported by several groups, e.g. H$_2$SO$_4$ >> HCl ≈ HNO$_3$ >> HClO$_4$ > HBF$_4$ > CF$_3$CO$_2$H by Zotti *et al*[97]; H$_2$SO$_4$ >> HCl ≈ HNO$_3$ >> HClO$_4$ ≈ CF$_3$CO$_2$H by Desilvestro and Scheifele[98]; and H$_2$SO$_4$ > > HCl ≈ HNO$_3$ > HClO$_4$ by Nunziante *et al*[99] and Duic *et al*[100]. In summary, anion effects can be grouped into two types from two sorts of counter ions. One contains BF$_4^-$, ClO$_4^-$, and CF$_3$COO$^-$, which results in a compact structure with fibres; while the other consists of SO$_4^{2-}$, NO$_3^-$ and Cl$^-$ anions, leading to an open granular structure. Tang *et al*[101] studied the anion effect on the over-oxidation of PANI.

1.2 Applications of Organic Conducting Polymers

An assessment of the application potential of PANI and other conductive polymers in organic electronics,[102;103] in chemical sensors,[104-106] biosensors[107-110] or as antistatic, corrosion protective[111-115] or as electrochromic coatings [43;107;116-121]resulted in its extensive investigations during the last decade. So far, hundreds of publications about various applications of OCPs can be divided into two main groups:[104] one is used as materials or elements for construction of various devices based on electronic, optoelectronic and electromechanical principles; the other is as sensitive materials in chemical sensors based on electronic, optical,[122] mass[123;124] or transduction mechanisms.

1.2.1 Gas Sensors Based on PANI

In my work, I would like to focus my efforts on the applications of OCPs, especially on the application of PANI and its derivatives, as gas sensitive layers.

Polyaniline (PANI) has been widely applied as a new sensitive layer for various gas sensors in both chemoresistors and optical sensors, since it undergoes significant electrical alteration and visible optical properties upon exposure to various gases.[125] The studied gases involve NH_3,[126-128] NO_x,[129-132] H_2S,[129;133] SO_2,[129;130] CO_2,[134] chloroform[135] and humidity.[130;136-139] Compared with inorganic materials (specially SnO_2), PANI film as a gas sensitive material has the apparent advantage of high sensitivity to analytes at room temperature.[18]

1.2.1.1 Gas Transducing Mode

Different transducing modes are used PANI as gas sensitive layer. There are electrical parameter measurement, measurement of optical parameter, measurement of electrochemical parameter, and measurement of electrical characteristics in field- effect transistor (FET).[104]

Electrical parameter measurement is probably the most common method, which is used when the resistance or conductance of PANI film changes under an analytic gas flow.[19;26;34;140-155] The change of polymer conductivity can be obtained by measuring one of these parameters, resistance (R), conductance (G) or conductivity (g), and current (I). This is due to conductance (or resistance) changes of the studied polymers based on acid/base doping/dedoping mechanism. The common sensor design bases on an interdigitated electrode[19;144;146] or array covered with PANI films.[34;156-158] But other designs could also be used, for instance, pellets of PANI on substance.[152;155] Many resistance/conductance measurements are carried out by two probe method.[19;159;160] Some of them are carried out by four point method.[160-165] The study based on this measurement is summarized in Table 1.2.1.1-1 (Part 1 and Part 2).

Recently, high and multi-frequency AC conductivity measurement techniques have been used for conducting polymer gas sensors.[166] The most important advantage of this technique is the possibility to distinguish different chemical species with a single sensor.[167] Organic vapours, such as methanol, acetone and ethyl acetate, could be detected by measuring the change of AC conductance of a PANI gas sensor at different frequencies.

Optical measurement is also one of the common methods for gas sensors due to the significant change in optical parameters of PANI film before and after exposure to gases.

Changes of UV absorption or transmittance, near infrared absorption or refractive index have been applied.[20;167-170]

For instance, an optical ammonia sensor based on PANI deposited chemically on the polyethylene surface was developed by using absorption spectroscopy.[167] This is based on the shift of the maximum of absorbance of PES from 800 nm to about 600 nm with increasing ammonia concentration. El-Sherif *et al*[169] have used a multi-mode optical fiber in which a small section of the original cladding material has been replaced by PANI or polypyrrole (PPY). The adsorption of gases or organic vapours results in refractive index and optical absorption fluctuations of the polymer, leading to an optical intensity modulation within the fibre. Results obtained in the case of HCl or NH_3 detection seem to be promising. The technique of surface plasmon resonance has been used[170] to monitor the interaction of gases like NO_2 or H_2S with Longmuir–Blodgett films of PANI deposited on glass/Ag/Ni. However the regeneration of these sensitive layers is incomplete. The studies based on optical property are summarized in Table 1.2.1.1-2.

Measurement of electrical characteristics in field-effect transistor (FET)[104] has been used for the detection of gases since the late 1980s,[171] including some gas sensors based on PANI studied by Janata J. *et al.,*[172-174] Barker P. S. *et al.*.[175;176] The gases investigated include NH_3, H_2, NO_x, SO_2 and H_2O.

Electrochemical method is performed by measuring an electrochemical parameter, current, potential, frequency, impedance, and so on. For instance, amperometric[177] and potentiometric[178] gas sensors belong to it (Summarized in Table 1.2.1.1-3).

Do *et al*[177] have realized gas sensors to detect NO_2. The sensitivity of NO_2 gas sensor decreased from 2.54 to 1.40 $mA.ppm^{-1}$ when the potential for prepg. PAn/Au/Nafion increased from 0.8 to 1.0 V and gas flow rate was 300 mL min-1. A novel SO_2 electrode made from PANI/Nafion membrane was developed by Syu *et al.*[179] The detection limitation of amperometric SO_2 sensor is at ppm levels. The detection of a few ppm of NH_3 and HCl was realized with a conductometric sensor based on a PANI/calixarene blend.[180] A humidity sensor based on PANI and PPY was built on basis of QCM (Quartz Crystal Microbalance).[181] The change of resonant frequency of QCM-based sensor on relative humidity was studied in presence of 0~85% RH with a response time less than 5 s.

Table 1.2.1.1-1 Electrical parameter measurement (R, G, I) – (**Part 1**)

Analyte	Synth. method	Deposition Method	Sensitive Layer (state)	Dynamic range (ppm)	Note (Sensitivity) (Min. Limit.)	Parameter	Reversibili-ty	Regene ration	Ref.
NH_3	chem	spin-coating	PANI(ES)+polystyrene; PANI(ES)+ poly(methy methacrylate)	10 ~500	$\Delta\log(G) < 1.84$ s (30 °C, 50°C)	G (S)	part	N_2	[182]
NH_3	chem	dip-coating	PANI-ClO_4 (ES)	1~2000	$\Delta R/R_0 =$ 1.23, (27°C); 0.6, (46°C); 0.2, (78°C)	R (Ohm)	part	a: air, argon; b: heating	[146]
NH_3	chem	dip-coating	PANI (ES)+MO_3	< 100	$R/R_0 =$ 3.3 ppm^{-1}	R (Ohm)	no data	no data	[183]
CO_2 (+H_2O)	chem	casting	PANI (EB)-PVA(poly(vinyl alcohol)	100 ~ 10^6 ppm (5%~ 70%)	$\Delta g/g_0$ 0.9 ~ 1.2 (3000ppm + 32%~40% H_2O)	g (S/cm)	part	air	[143]
Humidi-ty	electro-chem	electrochem	PANI	0~20%	no data	R (Ohm)	no data	no data	[181]
$CHCl_3$	chem	pressed pellet	PANI-Cl(ES)+Cu	10 ~100	$\Delta R/R_0 =$ 1.5 ~ 3.5	R (Ohm) 2-point	part	hexane	[140]
ethanol (+ H_2O)	electro-chem.	electrochem	PANI-DSA(decane Dulfonic acid)/H_2O (ES)	$2*10^3$~$35*10^3$ (+ 2328 ppm H_2O)	$\Delta G/G_0$ = 5.7%	G (S)	no data	no data	[148]
alipha-tic alcohol	chem	pressed pellet	PANI or derivatives chlorate, (ES)	3000	$\Delta R/R_0 =$ 45% - 94% (10min)	R (Ohm)	part	air	[155]

Table 1.2.2-1 Electrical parameter measurement (R, G, I) – (**Part 2**)

Analyte	Synthe-sis Meathod	Deposition Method	Sensitive Layer (state)	Dynamic range (ppm)	Note (Sensitivity) (Min. Limit.)	Parameter	Reversibili-ty	Regene ration	Ref.
HCl, HBr, HI,	chem	casting	PANI-PVC PANI-PS PANI-PVAc	$200 \sim 800$	$\Delta g = 0.1 \sim 0.4$ (S/cm) 30min	g (S/cm) (4-point)	no data	no data	[129]
Cl_2, Br_2, I_2	chem (4-point)	casting	PANI-PVC PANI-PS PANI-PVAc	$200 \sim 800$	$\Delta g = 0.03 \sim 0.07$ (S/cm) 30min	g (S/cm)	no data	no data	[129]
H_2S	chem	a: spinning	PANI Base (EB)	$4 \sim 100$	$\Delta I/I_0 = 0.15$ (ppm^{-1})	I(A)	part	air	[149]
		b: evaporation			$\Delta I/I_0 = -1.2$ (ppm^{-1})				
		c: LB			$\Delta I/I_0 = 0.04$ (ppm^{-1})				
SO_2	chem	a: spinning	PANI Base (EB)	$4 \sim 100$	$\Delta I/I_0 = 4.33$ (ppm^{-1})	I(A)	part	air	[149]
		b: evaporation			$\Delta I/I_0 = 0.02$ (ppm^{-1})				
		c: LB			No response				
NO_x	chem	a: spinning	PANI Base (EB)	$4 \sim 100$	$\Delta I/I_0 = 0.087$ (ppm^{-1})	I(A)	part	air	[149]
		b: evaporation			$\Delta I/I_0 = 5.0$ (ppm^{-1})				
		c: LB			$\Delta I/I_0 = 0.008$ (ppm^{-1})				

Table 1.2.1.1-2 Gas sensors based on optical method

Gas	Synthesis Meathod	Deposition Method	Sensitive Layer	Dynamic range (ppm)	Note (Sensitivity)	Parameter	Reversibility	Regeneration	Ref.
O_3 (ozone)	chem	dip-coating	PANI (LB)	50-100 (in air)	ΔA at 728nm; $\Delta A/A_{air}$, at 620 nm	absorbance (UV-vis)	part	air	[184]
NH_3	chem	dip-coating	PANI (ES)	10-1000	$\Delta T/T < 5\%$	transmittance (UV-vis)	part	N_2	[120]
NH_3	chem	dip-coating	PANI-ClO_4 (ES)	$180 \sim 18000$	A/A_0 2.7 ppm^{-1}	absorbance (UV-vis)	part (a); complete (b,c)	a: N_2; b: N_2 + HCl (acid); c: heating	[167]
NO_2	chem	LB	PANI (EB)	$50 \sim 700$	0.0175 ppm^{-1} (50 ppm)	reflectivity (SPR)	part	N_2	[170]
H_2S	chem	LB	PANI (EB)	$50 \sim 100$	0.1 ppm^{-1} (50 ppm)	reflectivity (SPR)	part	N_2	[170]
NH_3	chem	spinning; casting	PANI-Cl	$10 \sim 4000$	$\Delta T/T = 0.5\% \sim 13\%$	transmittance (Uv-vis)	part	N_2	[168]

Table 1.2.1.1-3 Electrochemical method (Gas sensor electrode)

Gas	Synthesis Meathod	Deposition Method	Sensitive Layer	Dynamic range (Min. Limit.) (ppm)	Note (Sensitivity)	Reversibility	Regeneration	Ref.
SO_2	chem	self-assembly	PANI base (EB)	$20 \sim 250$	$0.1 \sim 0.2$ µA/ppm	no data	no data	[185]
CO_2	electrochem	electrochem	PANI sulfate (ES)	$0.1 \sim 30$mM	/	yes	buffer	[186]
CO_2	plasma excitation	plasma polymerized	PANI	no data	$\Delta I/I_0 = 5$ at 2 l/min	yes	air	[26]

1.2.1.2 Preparation Methods of Sensitive Layers

The applications to gas sensors are based on certain substrates. The preparation techniques can be grouped to "chemical method" and "electrochemical method". Spin-coating, dip-coating, drop-coating, casting, thermal evaporation,[19] Langmuir-Blodgett (LB),[19;20] and self-assembly techniques (SA)[20-22] belong to chemical approach. Known from literature, the preparation methods influence the sensitivity of PANI films to gases. It was reported by Agbor *et al*[19] that, among spinning, evaporation and Langmuir-Blodgett techniques, the deposited PANI thin films all methods are sensitive to H_2S and NO_x of very low concentration level, but only spun and evaporated films response to SO_2.

1.2.2 Current Scientific State of Gas Sensors Based on PANI

Among so many publications in this area, most of them deal with the detection of ammonia (NH_3) alongside with a few studies about chloroform[135], ethanol,[148] water vapour and NO_2.

PANI film as a NH_3 sensitive layer has several advantages, compared with poly(pyrrole) (PPY),[146] such as higher sensitivity and faster response to NH_3, additionally, relative reversibility is also one advantage for PANI film as NH_3 sensitive material. According to literature, the common regeneration way of gas flow is popularly used in practice. But it is not quite satisfactory. The regeneration by heating up to $104 \sim 107$ °C was used to recycle NH_3 sensor by Kukla *et al.*[146] It was helpful to regenerate the sensor after adsorbing NH_3 for a short time, but, it was not successful for the gas adsorption longer than 10 min.

Matsuguchi *et al*[145] reported that PANI blend prepared chemically with soluble matrix polymers not only improved the poor processability of chemically formed PANI, but also reduced the response time. This was attributed to the porous morphology caused by the component of the blend. However, the poor reversibility and response time have not been satisfactory for practical use yet.

In case of NO_2 sensors based on PANI, the influence mechanism of NO_2 on the resistance of PANI film is relatively complicated. It is reported that this depends on the kind of PANI used. When the polymer used is in the state of PES, exposure to ammonia may lead to a decrease of polymer conductance, for instance, Li *et al.*[183] observed such a phenomenon when a self-assembled PANI film doped with molybdic acid was used on exposure to NO_2. On the other hand,

Agbor *et al*[19] reported that the increase in conductance of PANI base resulted from the presence of NO_2 gas. In the first case, NO_2 plays the role of an oxidative dopant which oxidizes PES to the higher oxidative level of PANI. The higher oxidation state of PANI is not as conductive as PES.[46] As for the second case, Li *et al*[183] suggested that poly(emeraldine base) (PEB) could be oxidized by NO_2 to PES, which resulted in the increase of polymer conductance. Here, I would like to put forward a more plausible explanation, since there is only protonation/deprotonation doping between EB and ES. NO_2 molecules could react with moisture remaining in the polymer to form a small amount of nitric acid (HNO_3); further, nitric acid dopes PEB to the conducting state of PES, leading to an increase of conductance.

1.2.3 Unsolved Problems in the Field of Gas Sensors

Slow penetration of gases into the bulk of OCPs causes the hysteresis and relatively long response time (tens of seconds to minutes).[187] On the other hand, the desorption of analytic gases from polymer bulk is also very slow in the flow of nitrogen or air. According to the literature,[131;132;188] this is the most popular way to regenerate a sensor in practice. Although many kinds of gas sensors based on PANI have been studied or developed, not all regeneration processes are equally successful. Partial- or semi-reversibility occurs frequently when desorption is carried out by pressed air or N_2.[146;170] The regeneration process of these gas sensors has not been investigated. Finally, poor reversibility of the response converted the system into a lab-toy and excluded any commercial applications.

Only a few publications on HCl gaseous sensor are based on PANI (OCPs).[189;190] As we know, hydrogen chloride is one of the products upon cables burning. So it would be of significance to develop HCl sensors based on OCPs for the application in the fire alarm system. Maybe you still remember the worst disaster happened in Austria, Kaprun in the winter of 2000: toxic fumes and smoke generated by the burning carriages caused 160 people dead. If the fire were possible to be detected in time, many such catastrophes would have been avoided.

1.3 Combinatorial Approach

High – throughput screening and combinatorial chemistry have been successfully extended from pharmaceutical applications to other scientific fileds.[191-195] It is a promising tool for

speeding up the search for and the development of new or advanced materials. Most technologies of combinatorial chemistry rely on solid-phase synthesis. It can be realized in different formats and addressable techniques. Typically, a dispensing of reagents into micro- or nano-titerplates is used[196]. Further investigation can be performed by different techniques[197], including binding and inhibitor assays, screening of biological activity, masspectroscopy, chromatography, optical[196;198] or electrochemical[199] methods. Several exceptions, described in literature, include a light-directed immobilization[200] and an addressation by use of microfluidic systems.[201;202]

Only a few authors described electrical addressation.[203-205] The first automated system for combinatorial synthesis and high throughput investigation of electrical properties of OCPs was built in our laboratory.[156;157] We focused our effort on the application of the combinatorial approach with electrical addressation for the synthesis of electrochemically polymerized materials and multilayer structures to the development of sensors. To our knowledge, this is the first time to use such high-throughput screening in electrochemistry.

1.4 Objective of the Work

The aim of this thesis is, on the basis of organic conducting polymers as HCl sensitive layers, to develop a reversible, selective and highly sensitive conductometric polymer sensor for the application in fire alarm system.

It is planned to overcome problems by investigation the reasons of poor reversibility and by combinatorial testing of large variety of polymer materials.

The main investigation in this work is performed on single electrodes for the characterization of polymers. Then a new combinatorial approach should be used to electrochemically synthesize various OCPs. By this techniques, the most promising conducting polymers as sensitive materials for HCl sensors will be evaluated.

2 Experimental

2.1 Reagents and Materials

Reagents

All chemicals and solvents used were purchased from Aldrich (Steinhein, Germany), Fluka (Buchs, Switzerland) or Merck (Darmstadt, Germany), except 3,4-ethylenedioxythiophene (EDOT) offered kindly by Bayer AG and used as received. Aniline (ANI), N-methyaniline (NMA) and pyrrole (PY) were purified by vacuum distillation, and stored in a refrigerator at about 4 °C for further use. The other chemicals were of analytical grade unless otherwise stated, and utilized without further purification. All experiments, if not specified, were carried out at room temperature (22±2°C).

Buffers

The following table outlines the buffers used in this work (Table 2-1). All buffers were prepared with MILLIPORE water, and used immediately after preparation. The pH was adjusted with 0.1 M and 1 M HCl or 0.1 M and 1 M NaOH when necessary.

Table 2-1 Buffer solutions

Buffer	Composition	pH	Experiment
A	100 mM KCl 5 mM citric acid; 5 mM potassium dihydrogen phosphate; 5 mM dipotassium hydrogen phosphate; 5 mM Borax; 5 mM Tris	1 ~ 12	Influence of pH and electrode potential on the conductance of PANI or its copolymer
B	1M mM KCl 5 mM citric acid; 5 mM potassium dihydrogen phosphate; 5 mM dipotassium hydrogen phosphate; 5 mM Borax; 5 mM Tris	1 ~ 12	Influence of ionic strength of buffers on PANI conductance
C	25 mM sodium dihydrogen phosphate 25 mM disodium hydrogen phosphate	7.0	Fructose sensor
D:Base Buffer	100 mM sodium carbonate 100mM sodium hydrogen carbonate	9.0	Post-treatment

Two universal buffer solutions (A, B) were used for investigation the influence of pH and potential dependence on polymer conductance, which contain citric acid, potassium dihydrogen phosphate, dipotassium hydrogen phosphate, sodium tetraborate (Borax), trishydroxymethylaminomethane (Tris), and potassium chloride with different concentrations. In addition, Phosphate buffer of pH 7.0 was also prepared for detecting fructose.

Electrodes

Thin film electrodes on glass or silicon support formed by deposition of gold or platinum, were provided by R. Bosch GmbH (Germany). The thickness of metal layer is about 250 nm; the electrode area is 0.38 mm^2 for circle electrodes or 0.25 mm^2 for interdigitated electrodes. Two types of interdigited electrodes were used, 2-stripe and 4-stripe electrodes with a gap of 10 μm and 5 μm, respectively (shown in Fig. 2.1-1). Before use, the electrodes were cleaned by ultrasonic treatment in chloroform and by hot piranha solution (1:3 mixture of 30% H_2O_2/conc. H_2SO_4, v/v), then rinsed thoroughly with pure water and dried in the nitrogen gas flow. (*Caution: this solution reacts violently with most organic materials and must be handled with extreme care!*)

700 mm
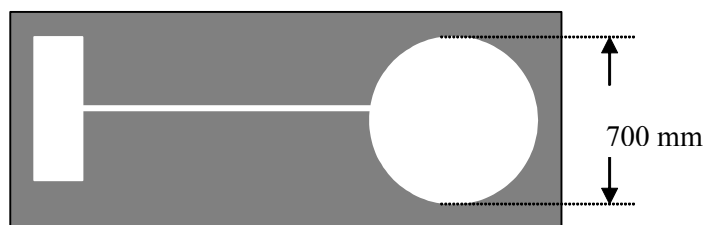
(a) single circle electrode

100 μm

100 μm
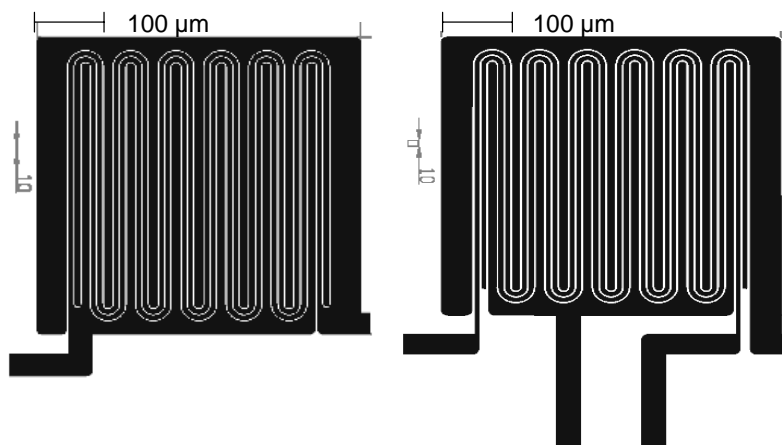
(b) 2-stripe electrode;   (c) 4-stripe electrode

Fig. 2.1-1 Electrode schemes (a, b, c)

2.2 Modes of Electropolymerization

Most electrochemical polymerizations were performed in a potentio/galvanostat Autolab PGSTAT-12 (EcoChemie). Three main modes, cyclic voltammetry, constant current and constant potential were used for bare electrodes. In the case of modified electrodes as working electrodes, a potential pulse was employed for polymerization.

Cyclic voltammetry can be performed at a certain sweep rate, if A PGP 201 potentiostat was used, the maximum sweep rate was 500mV/min during cyclic voltammetry. For PANI and its derivatives, the potential range was applied from -0.3 V ~ +1.0 V if not specified differently. The polymerization of EDOT was carried out in the range of -0.3 V ~ 1.2V.

Constant potential (**chronoamperometry**) was used for electrochemical polymerization after the initial tests. Polymerization charges through WE were controlled automatically with the software of Autolab. Usually, an experiment begins with 60s equilibration at 0 V, followed by constant potential over a certain time. The polymerization of aniline and its derivatives was usually performed at 0.9 V vs SCE; potential in the range of 0.6 V ~ 1.2 V was also applied for investigation of properties of PANI, its derivatives and PEDOT.

At *constant current mode*, a current density of 30 A/m^2 was used for the polymerization of aniline and for its derivatives if not otherwise specified.

Potential pulse was used to improve the electropolymerization if a sublayer of 4-aminothiophenone (4ATP) was pre-coated on a gold electrode. This is to protect 4ATP and to avoid simultaneous polymerization. Four potential pulses (0 V, 0.6V, 0.9V, 0.3V) were used for the polymerization of aniline or its derivatives on a modified gold electrode. This electrode was pro-coated with a self-assembled monolayer of 4ATP obtained from ethanol solution of 20 mM 4ATP. The first step at 0 v was done for 1min to equilibrate the three-electrode system in the solution; then the polymerization procedure began at 0.6 V versus SCE (0.553 V versus Ag/AgCl) for 3min firstly which is to protect the monolayer of 4-ATP from polymerization of its dimmer at higher potential (0.7V versus Ag/AgCl)[206;207]. The next electrochemical step was followed at 0.8 ~ 0.9V for a certain time to deposit the required polymer on the surface of the ATP-modified electrodes. At last, 0.3 V was applied for 30 s to get conducting PES.

2.3 Electrochemical Synthesis

Preparation of Single-monomer Solutions

The monomer solutions of aniline or its derivatives were prepared in MILLPORE water without special directions. The monomer EDOT (3,4-ethylenedioxythiophene), pyrrole (PY) and thiophene are insoluble in water and were therefore dissolved in acetonitrile. Aqueous solutions of monomers comprised additionally one of the following acidic dopants: HCl, $HClO_4$, H_2SO_4, H_3PO_4 or CH_3COOH; organic solutions of monomers included 0.1 M $LiClO_4$. The concentration of monomers in H_2SO_4 solutions was 0.1M for aniline, N-ethylaniline (NEA), N-butylanline (NBA), and the ring-substituted anilines: 2-ethylaniline (2EA), 3-ethylaniline (3EA), 2-propylaniline (2PA), 2-tert-butylaniline (2*t*BA), 2-sec.butylaniline (2*s*BA), 3-aminobenzzoboric acid (3-ABBA), anthranilic acid (ABA), 3-Aminobenzoic acid (3ABA), 3-Aminobenzenesulfonic acid (3-ABSA); for monomer N-methylaniline (NMA), two concentrations used were 0.1 M and 0.2 M in H_2SO_4, HCl, $HClO_4$, H_3PO_4 or CH_3COOH solutions (pH = 0). In case of HClO4 as a dopand, the concentration of monomers was 0.2 M in the solutions of pH = 0.

Preparation of Binary Monomers Solutions

The solutions for co-polymerization consisted of aniline and another monomer in MILLPORE water containing 0.5 M sulfuric acid. Usually, the total concentration of aniline and its derivatives was 0.1 M if not specified otherwise. The molar ratio of aniline and its derivative was varied from 100:1 to 1: 3 for the experiments on single electrodes.

Gold or platinum electrodes on silicon or glass substrates were used as WEs. A traditional three-electrode cell was built with a platinum wire as counter electrode and a saturated calomel electrode (SCE) as reference electrode. All solutions used for electrochemical polymerization were deaerated with purging Argon either through or above the solutions before or during all of the experiments.

All electrochemical experiments started with 60 seconds equilibration, followed by electrochemical polymerization by one of four modes described above. After electropolymerization, the electrode was taken out, rinsed extensively with MILLPORE water or CH_3CN for organic solutions, and dried in a N_2 flow.

2.4 Methods of Characterization

Various methods were used to characterize electrochemically synthesized polymers.

2.4.1 Traditional Electrical Method (DC, 2-point)

Polymers on two-stripe interdigitated electrodes were characterized by traditional electrical two- point method, to measure the total resistance including bulk resistance and contact resistance. These measurements were performed with a multi electrometer (Keithley 175).

2.4.2 Electrochemical Impedance Spectroscopy

PANI and its copolymers with 3-ABBA or 3ABA, Poly(ANI-3ABBA) and Poly(ANI-3ABA), were measured by Electrochemical Impedance Spectroscopy (EIS). They were performed in different frequency ranges at fixed DC potential with 10 mV sine voltage. The potential range is over 0 V ~ 1.0V. All the experiments were carried out in the three-electrode cell. Various types of impedance curves of Z_r vs Z_i were obtained under different conditions. From the acquired curves and their fitting curves, the parameters, real and image impedance (Z_r, Z_i), solution resistance and capacitance, were obtained. EIS was carried out by using of a potentio/galvanostat Autolab PGSTAT-12 (EcoChemie). Data analysis was performed by using the Autolab software (Version 4.9).

2.4.3 Optical Microscopy and Scanning Electron Microscopy

An investigation of unique conductive properties of the deposited polymers requires information about the morphology after deposition on electrodes. In this work, the influence of counter ions, polymerization conditions, electrode materials and adhesive sub-layers on morphology of these polymers was studied. The surface morphology of the polymers was investigated and evaluated by means of optical microscopy (Leica, Xe lamp, Germany) and Scanning Electron Microscopy (SCE) (Topcon SM-510, Japan; Physics Department of University of Regensburg) in the micrometer scale.

2.4.4 Thermal Gravimetric Analysis and Differential Scanning Calorimetry

Thermal properties of PANI films and PANI-HCl were investigated by thermal gravimetric analysis (TGA) and differential scanning calorimetry (DSC). Thermal stability of the polymers was measured using TGA 7 (Perkin Elmer) at a heating rate of 1 ºC/min in nitrogen atmosphere, from 25 ºC up to 210 ºC or 400 ºC. DSC measurements were performed on a DSC 7

(Perkin Elmer), between 25 ºC and 400 ºC, with the heating rate of 1 ºC/min, under nitrogen. (This work was performed in the lab of Prof. K. Heckmann in our department.)

2.4.5 Infrared Spectra

FTIR measurements with PANI polymers (KBr pellet) were acquired on a seria FTS 3000 spectroscopy device. These were carried out in the Lab of Prof. Reiser at the institute of organic chemistry.

2.4.6 Elemental Analysis

For the determination of composition of the synthesized OCPs after treatments, a large amount of PANI-SO$_4$ was polymerized electrochemically on a large gold electrode, and then mechanically removed from the electrode surface, rinsed extensively with MILLIPORE water, and dried in a vacuum desiccator overnight. A fractional of PANI-SO$_4$ was treated with base buffer (pH = 9.0) overnight. Then, samples of at least 10mg probe were used for the analysis of C, H, N and S in a Vario-EL V4-01 Elementar Analyse Systeme GmbH (Analytical center, our faculty).

2.4.7 Apparatus for Investigation of Temperature Effects

Three home-made setups were used to study thermal properties of conducting polymers we synthesized. Sep-up 1 and 2 were used for the experiments on single electrodes; Setup 3 was used for those on 96-electrode arrays.
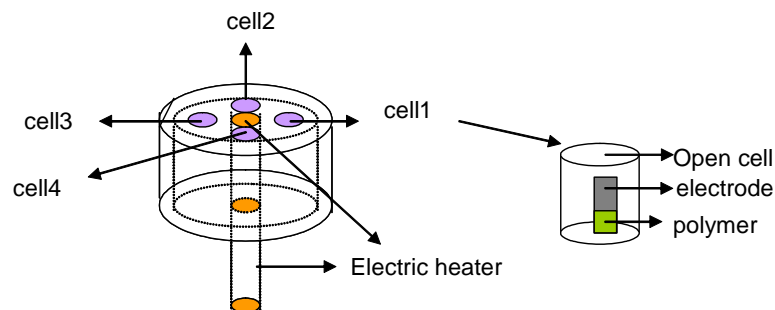

Fig. 2.4.7-1 Layout of Setup 1

Setup 1 consists of a simple electric heater with thermostat and a steel multi-cell with four open cylindrical cells of 300 mm height and 70 mm diameter. Individual electrodes can be placed in the cells and heated in the temperature range of 100 ~ 300 ºC calibrated. It was used to study

thermal desorption (thermal regeneration) of gas sensors and thermal dependence of polymeric conductance based on individual electrodes, respectively.

Setup 2 was used to study thermal adsorption of gaseous HCl to conducting polymer films on single electrodes. The main part for this setup, besides conductance measurement, was a small laboratory oven where a glass gas cell with a removable lid was fixed. An electrode holder, who had four contacts out of the oven for four-point measurement, was integrated into the lid. In order to reduce or avoid experimental errors caused by temperature change of incoming gases, part of the steel tube was mounted in the oven to transport and preheat gases before entering the cell. Experiments were performed in the temperature range of 30 ~ 120 ºC, controlled by this oven.

Setup 3 is composed of electrochemical polymerization cell and a cell for gas test combined with a thermostat (made by V. Kulikov). One can use it for the measurement at constant temperature, thermal dependence of polymer conductance and thermal adsorption or desorption. One PC workstation is connected by using the GPIP card with this setup for controlling procedures and collecting data.[156] Temperature can be controlled with software (programmed by V. Kulikov).
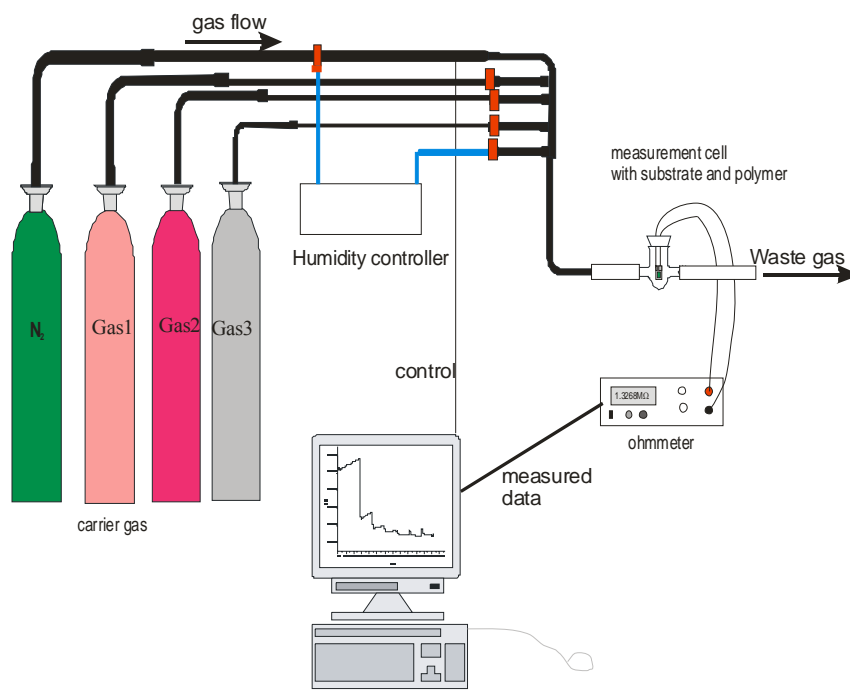
2.4.8 Gas Test

Fig. 2.4.8-1 Diagram of gas test

After electropolymerization, the electrodes were immersed into a sodium carbonate buffer (100 mM, pH = 9.0) overnight, then rinsed with water and dried by nitrogen. An investigation of gas effects was performed with a home-made automated gas mixing system based on valves from MKS Instruments (shown in Fig. 2.4.8-1). All gases were obtained from Linde GmbH, Munich, Germany. The compositions of gases used are listed in Table 2.4.8-1.

Table 2.4.8-1 Gas specifications in cylinders

Gas diluted with nitrogen	Concentration (ppm)	Volume (L)	Provider
HCl	500	200	Linde
HCl	250	200	Linde
NH_3	250	200	Linde
CO_2	500	500	Linde
N_2	10^6	500	Linde
Synthetic air (N_2+O_2)	$0.8*10^6 + 0.2*10^6$	500	Linde

Gas flow is controlled by the gas-mixer software automatically. Four channels are available for dry gases; additional humidity controller (homemade) part is necessary for the test of humid gases (shown in Figure 2.4.8-1). When gas tests were performed in the presence of humidity, two channels were used for main flow gas (nitrogen or synthetic air). Nitrogen in one of these two channels flows through humidity controller and goes on to mix with nitrogen from the second channel. If necessary, the second gas can be output from the third channel and mixed with humid nitrogen. *(Be careful! Always turn on the channel where nitrogen flows through water first, and then the others. Otherwise, water could flow back to the channels by the higher pressure of dry gases and block gas flows.)*.

The total gas flow rate is set not to excess the maximum pressure of any device in the system. In the case of our gas cell for single electrode (shown in Fig. 2.4.8-1), the maximum flow rate cannot exceed 1000 ml / min. All the gases used were diluted with nitrogen or synthetic air to

the required concentration for the experiments in the gas-mixer. Individual flow rates for gases required to be mixed can be calculated according to the equation below:

$$C \text{ (gas)} = \frac{r(gas)}{r(total)} * C_0 \text{ (gas)} \qquad\qquad \text{Eq 2-1}$$

Here, C (gas) is the required concentration of tested gas for sensors; C_0 (gas) is the original concentration of this gas in cylinder. The flow rate of certain gas and total flow rate for gas cell are labeled r (gas) and r (total), respectively. The flow rate of nitrogen can be calculated from the subtraction of total flow rate and the other gas flow rate. For the tests of humid gases, the relative humidity is calibrated already beforehand, so the humidity of the mixture can be calculated as follows:

$$\text{Humidity (RH) \%} = \frac{r(wetnitrogen)}{r(total)} * 100\% \qquad\qquad \text{Eq 2-2}$$

2.5 Development of New Experimental Approaches

2.5.1 Electrochemical Surface Plasmon Resonance Spectroscopy

As shown in Fig. 2.5.1-1, electrochemistry and surface plasmon response (SPR) measurements were performed with a combination of the SPR-spectrometer BIOSUPLAR-2 (MIVITEC GmbH, Regensburg, www.BIOSUPLAR.de) and a PGP201 potentiostat/galvanstat Radiometer. The SPR system couples a modified electrochemical SPR cell providing simultaneous optical and electrochemical measurements to study the electrochemical growth of organic conducting polymers. Moreover, it was connected with the gas system to check the sensitivity of conducting polymers to gases after electrochemical polymerization with simultaneous SPR.

The core of BIOSUPLAR spectrometer was a measurement prism installed on a swivel carriage. This prism was used for excitation of surface plasmon (SP) waves on the metalized surface of a sensor chip placed onto its top face. Usually, the sensor chip consists of a polished glass plate about 1-1.2 mm thick with the vacuum-deposited metallic thin film. Gold films were used in this work. The linearly polarized light from a laser diode was directed through the prism onto the gold electrode. The intensity of the reflected light was measured by a photodiode with a copper lock-in amplifier technique.
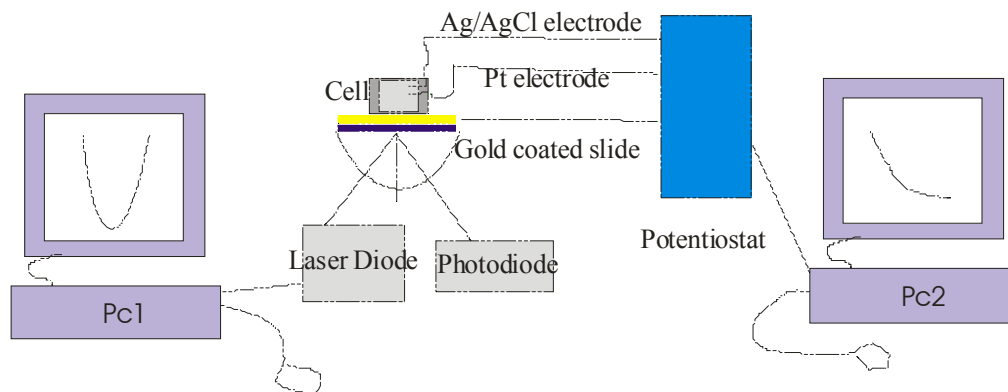
Fig. 2.5.1-1 Setup for In–situ Characterization of the Films Growth and Properties

Gold films (50 nm) on the glass slides (n= 1.562 at 650nm) were used as both surface plasmon medium and the working electrodes for electropolymerization. In case of electrochemical polymerization, a small drop of silver fluid was painted to improve electrical contact at one corner of the gold surface. Before use, gold coated glass slides were cleaned with hot piranha solution, as mentioned before in Chapter 2.1, rinsed with Mill-Q water and dried.

The glass slide was pressed onto the top face of the glass prism via a contact fluid with corresponding refractive index. The gold surface of the slide was covered with a silicon rubber sheet with a hole for the electrolyte contact. Then a sample cell was sealed against the gold surface with that silicon rubber circle.

A special electrochemical cell (shown in Fig. 2.5.1-2), containing a fixed reference and auxiliary electrode from Ag/AgCl and platinum wire, respectively, was used to study the films growth during polymerization, connected with PGP201. While a special gas cell with two fine rubber tubes was used for gas test. The layout of this whole setup is described in Fig. 2.5.1-1.
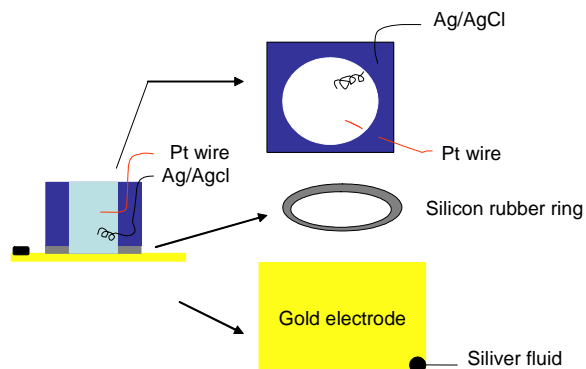

Fig. 2.5.1-2 Layout of Electrochemical Cell of SPR

2.5.2 Simultaneous Two- and Four-Point Techniques for Conductance Measurement

A simultaneous use of the two- and four-point techniques allows to separate the total resistance between two electrodes into the contact and bulk parts. A combined two- and four-point measurement was designed and described by Kulikov *et al.*[34] A circuit providing simultaneous two- and four- point conductivity measurements is shown in Fig. 2.5.2-1. Four points from the device (Keithley-2400) are connected to four connectors of a four- interdigitated electrode (See Fig.2.5.2-2).

These two methods will be used simultaneously to test the resistance of polymer deposited on interdigitated electrode surface. The resistance of conductive polymers on the electrodes is named R_P measured by 4-point technique between the two inner electrodes in our case (Fig. 2.5.2-2); R_{C1} and R_{C2} are contact resistance from the interface among polymer films, substrate, and gaseous analyte, and so on. The resistance R_2, measured by the two-point technique, is a sum of contact resistance and bulk resistance of the polymer between the two outer electrodes. Therefore, the contact resistance can be excluded by four-point techniques.

A source monitor unit (Keithley-2400) applies a fixed current between outer of the four electrodes and measures potential drop between two inner electrodes. Additionally, a high-impedance voltmeter (Keithley-617), measuring the output voltage of the current source, allows to calculate resistance, corresponding to the two-point measurement technique. The data will be saved automatically on a PC and two resistances versus time curves from these two methods will be shown on a screen.
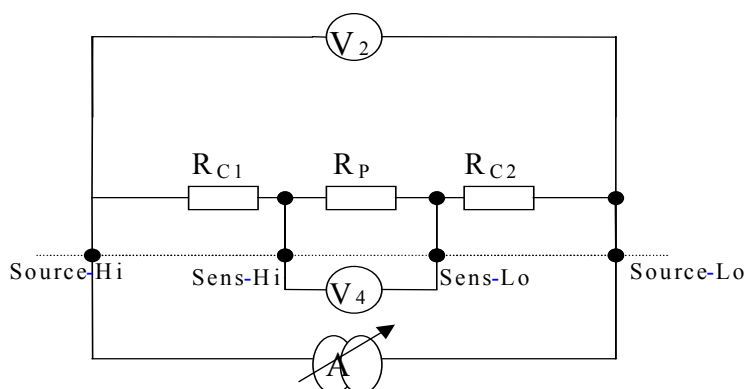
$$R(\text{4-point})= R_P; \quad R(\text{2-point})= R_{C1}+R_{C2}+R_p$$

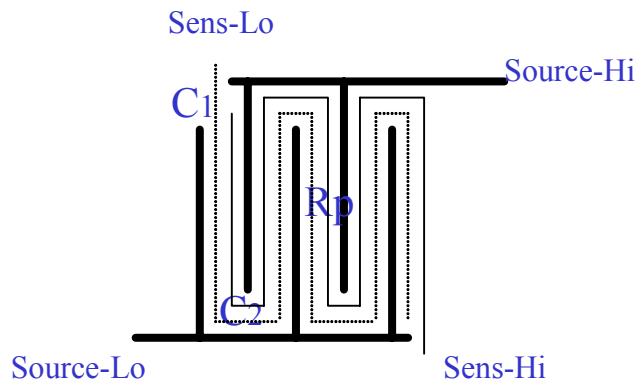**Fig. 2.5.2-1** Diagram of simultaneous two- and four- point measurements

Fig. 2.5.2-2 Four-wire interdigitated electrode

2.5.3 Combinatorial Electrochemical Polymerization and High-throughput Characterization of Gas Effects

Overview of Combinatorial Setup

The developed set-up for combinatorial electropolymerization and high-throughput screening of electrical properties consists of three main parts (Fig. 2.5.3-1): a dosing station, an electronic block with a computer, and an electrode array. All parts of the set-up are synchronized and controlled by a computer program.

The dosing station provides a mixing of monomers and additives in defined ratio, a delivery of this mixture into the cell for electropolymerization and cleaning of the flow system. All processes of the dosing station are automatically performed according to the parameters (content of mixture, timings, cleaning) written in the file library preparation.

Up to four different reagents (monomers and additives) are injected by syringes of dosing pumps (DP, Schott Titronic Universal) from reservoirs (A-D) into the mixer bin (MB) with a magnetic stirrer. Then the mixture is transported into the reaction cell (RC) by a peristaltic pump (P1, Gilson Minipuls 3), and the electropolymerization process starts. The electropolymerization is performed step by step on each interdigitated electrode of the electrode array (EA), so that every electrode is coated by one or more polymer layers of specific chemical content defined in the library preparation file. If required, the electrodes can be coated simultaneously. After each polymerization step, the dosing station provides cleaning of the reaction cell, mixer bin, and transporting tubes.
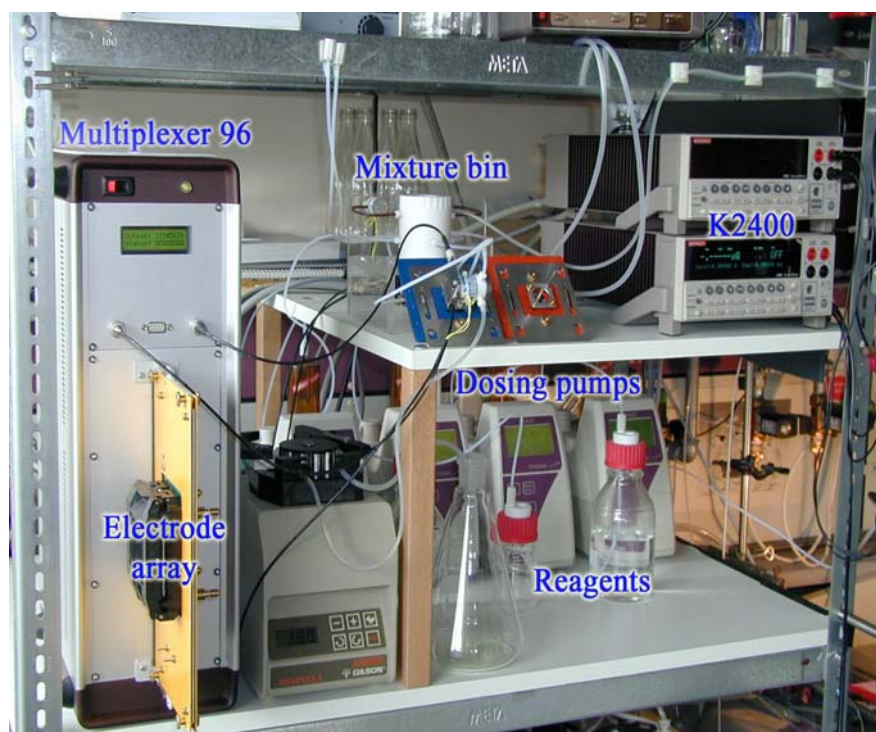
Fig. 2.5.3-1 Set-up for electropolymerization and screening of synthesized polymers.

The second part of the set-up is an electronic block consisting of a home-made high-impedance electronic multiplexer MX96, a source monitor unit (SMU, Keithley K2400), an interface board with a test clamp socket (Yamaichi), and of a miniature thermostat for the polymerization cell. The SMU provides electropolymerization, which can be done galvanostatically, potentiostatically or by potential cycling, and measurements of electrical properties of obtained polymer structures. The Ag/AgCl electrode with a salt bridge filled by saturated KCl solution is used as a reference electrode and a platinum wire as the auxiliary electrode.

Electrode array is based on an oxidized Si wafer with dimensions of 61 x 61 mm, on which a metallic layer is deposited (platinum or gold and corresponding adhesive layers). The metallic layer was treated by lithography to form array of 96 electrode groups (Fig.2.5.3-2). Every group consists of specially designed [208] interdigitated electrodes allowing two- and four-point measurements of electrical properties. To protect connections between contact pads and interdigitated electrodes from undesirable electropolymerization, the electrode array is coated by an insulating layer with 96 windows, placed in central parts of the interdigitated electrodes.
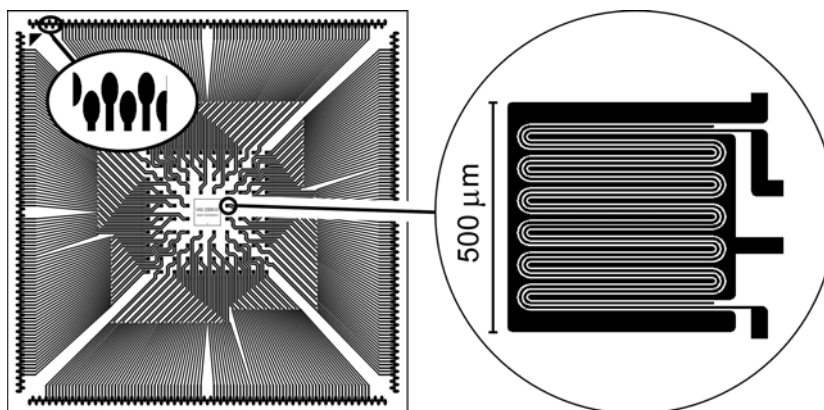
Fig. 2.5.3-2 Electrode array containing 96 interdigitated structures for four-point measurement.

Procedure for Gas Exposure

Slow kinetics is designed for determination of gas sensor equilibrium and can be done by measurement conductance 2p+4p outlined below, where X is the specified gas concentration.

Fig. 2.5.3-3 Slow kinetics of HCl test

Fast kinetics is designed for determination of gas sensor response, gas effect reproducibility and reversibility and can be done by time measurement outlined below, where X is the specified gas concentration.
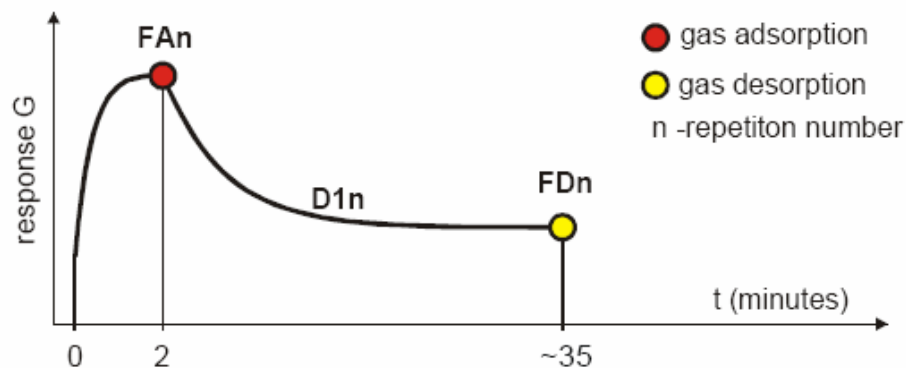
Fig. 2.5.3-4 Fast kinetics of HCl test

Measurement procedure for HCl Test

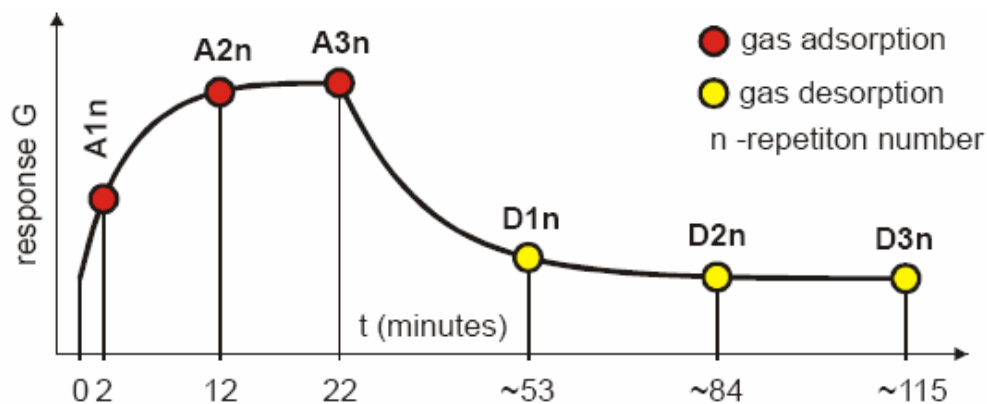The measurement based on combined I-V and kinetics conductivity measurements (four-point configuration). The gas concentrations were indicated for HCl from 2.5 ppm to 40 ppm. Total gas flow rate 600ml/minute.The measurements started after the array coated with polymers had been pre-heated at 125°C for 20 min. The measurement procedure is shown in Table 2.5.3-1.

Table 2.5.3-1 Measurement Procedure

Procedure step	HCl conc. (ppm)	conductivity meas.(G)	Slow kinetics	Fast kinetics	I-V sweep	Measur. time (minute)
1	0	✔			✔	~12
2	2,5	✔	✔ 2 times	✔ 2 times		~230
3	3,5	✔				4
4	5	✔				4
5	7	✔				4
6	10	✔				4
7	14	✔				4
8	20	✔				4
9	28	✔				4
10	40	✔	✔ 2 times	✔ 2 times	✔	~230
11	40	✔				~10
					Required time	~12:45

Table 2.5.3-2 Protocol for data evaluation and presentation

Characteristics	Calculation	Ideal case	Graphs
I-V characteristics:			
• Initial (G0) • after exposure to **low** gas concentration • after exposure to **high** gas concentration	• Linear approximation of conductivity (G_{AP}) in the range <–50 mV, +50 mV>		• I vs V (C=0) • I vs V (C_{max}) • GAP initial vs. X • GAP max vs X
Slow kinetics parameters			
Drift during gas exposure: Drift changes during gas exposure: Drift without gas: Drift changes, without gas: for GC min and GC max	KA1=A2/A1 KA2=A3/A2 KA3=KA2/KA1 KD1=D2/D1 KD2=D3/D2 KD3=KD2/KD1	1	KA1 vs. X KA2 vs. X KA3 vs. X KD1 vs. X KD2 vs. X KD3 vs. X
Reversibility of gas effects			
• from slow kinetics, 1-st and 2-nd additions • from fast kinetics for GC min and GC max	$RVS_1 = (D3_1-G0)/G0$ $RVS_2 = (D3_2-D3_1)/D3_1$ $RVF_1 = (FD_1-D3_2)/ D3_2$ $RVF_2 = (FD_2-FD_1)FD_1$	0	$RVS_{1,2}$ vs. X $RVF_{1,2}$ vs. X
Reproducibility of gas effects			
• from slow kinetics • from fast kinetics for GC min and GC max	$RPS = (A3_2-D3_1)/(A3_1-G_0)$ $RPF = (FA_2-FD_1)/(FA_1-D32)$	1	RPS vs. X RPF vs. X
Analysis in Langmuir model			
• Fitting ΔG by Langmuir • Relative effects: ΔG • Relative effects: ΔG /G_0	Langmuir Fitting: $\Delta G=\alpha*C/(C+C_{1/2})$ $\Delta G_{max}/G_0$ (for max gas concentration) $\Delta G_{min}/G_0$ (for min gas concentration)	1	$(G-Go)_{max}$ vs. X $((G-Go)/Go)_{max}$ vs. X $k=1/C_{1/2}$ vs. X Good-Lang vs. X
Sensitivity (Linear model) G-Go = f(gas concentration)			
• Linear fitting: ΔG = f(c) • Absolute sensitivity: d(ΔG)/dc • Relative sensitivity: d(ΔG/Go)/dc Linearity	Slope calculation: dG/dc, d(ΔG)/dc, d(ΔG/Go)/dc Correlation coefficient	max 1	Slope d(ΔG)/dc vs X Slope d(ΔG/Go)/dc vs X Correlation vs X

Data Evaluation and Presentation

Data evaluation was carried out on the basis of the follow protocol (Table 2.5.3-2). X is the parameter to be varied (for example, concentration of a dopant, ratio etc.). The parameters to display the properties of gas sensors, reversibility, absolute sensitivity, relative sensitivity, reproducibility…, can be estimated by using software.

(This was designed by Dipl. Ing. V. Kulikov.)

3 Results and Discussion

3.1 Electrochemical Synthesis of Conducting Polymers

More than thirty conducting polymers were prepared electrochemically and tested as sensitive layers for gaseous HCl. Most of polymers were electorpolymerized by three methods including cyclic voltammetry, constant current and constant potential. The results from cyclic voltammetry are summarized in Table 3.1 (see Appendix I). As synthesized, these materials are macromolecular cations, and hence for the reason of charge compensation, they take up counter ions from the electrolyte, so called primary dopants. The type of counter ions has influence on the polymerization. To coordinate our further work in combinatorial setup, we mainly limited our experiments in aqueous system.

3.1.1 Homo-Polymers

Polyaniline and its derivatives:

Polyaniline (PANI) and poly (N-methyl aniline) (PNMA) films were prepared electrochemically from various aqueous solutions at different conditions. The cyclic voltammograms of polymerization are shown in Table 3.1.1-1 and Table 3.1.1-2, respectively. To get the same oxidation state of polymers, we stopped the potential run at 0.4 V vs SCE for polymerization of aniline (ANI), and at 0.6V vs SCE for polymerization N-methyl aniline (NMA). This resulted in the formation of polyemeraldine films doped electrochemically with anions X- (ClO4-, HSO4-, Cl-).

According to the described later results on morphology and sensitivity to hydrochloride gas, sulfuric acid seems to be the optimal electrolyte for polymerization of aniline in aqueous solution. Therefore, aniline derivatives were also polymerized in H_2SO_4 solution (Appendix I: Table 3.1).

Table 3.1.1-1 Cyclic voltammograms of electrochemical polymerization of aniline on various electrodes from various solutions.

WE	Substrate	Surface	Aniline/HClO4	Aniline /H$_2$SO$_4$	Aniline/HCl
Au	Si	bare			
		ATP			
	glass	bare			
		ATP			/
Pt	Si	bare			
		ATP			

Table 3.1.1-2 Cyclic voltammograms recorded during the electropolymerization of NMA from various aqueous solutions with 50 mV/s sweep rate

WE	Substrate	Surface	NMA/HClO₄	NMA /H₂SO₄	NMA/HCl
Au	Si	bare			
		ATP			
	glass	bare			/
		ATP			/
Pt	Si	bare			/

It can be observed in Table 3.1.1-1 that, in general during electrochemical polymerization, all PANI films present the similar pattern of cyclic voltammograms (CVs) of

films deposited on various substrates from different aqueous solutions; three main redox couples with anodic peak potential values at around 0 ~ 0.2 V, 0.5 - 0.6V and 0.8 ~ 1.0 V(vs SCE) are observed. This result is in good agreement with previous studies,[43;60;74;209-211] These peaks correspond to the inter-conversions of different PANI forms. The highest peak near 0.8 V (vs SCE) corresponds to the oxidation of ES followed by deprotonation of the polymer giving the fully oxidized pernigraniline form. In case of the potential > 0.8V, the di-radical di-cation acts as an energetic elector-pile capable of interacting with neutral aniline molecule to result in further growth.

Table 3.1.1-2 presents cyclic voltammograms of electropolymerization of NMA at different conditions. Despite small differences under various conditions, the behavior of PNMA is different from that of PANI. The initial process of PNMA growth on both Au and Pt electrodes at the first several circles involved two weak peaks in the range of 0.4 ~ 0.6 V. With subsequent cycling of potential, these two peaks merged into a single composite while the cathodic scan still showed the existence of the two processes. In the region of higher potential, different peak shapes are observed for different acidic electrolytes. In the cases of H_2SO_4 and HCl, the peaks at 0.8 ~ 1.0V in H_2SO_4 solution or at 0.8 V in HCl solution were getting higher with subsequent cycling after the initial 5 cycles; while the peak at around 0.7 ~ 0.8 V in $HClO_4$ solutions disappeared gradually with the increase of the number of cycles, which resulted from diffusion process.[212]

3.1.2 Co-Polymers

Most of copolymers were obtained from the mixture of aniline and its derivatives in H_2SO_4; the copolymers containing PEDOT or PPY were deposited from the mixtures of aniline (ANI) and EDOT or ANI and PY in CH_3CN. The total concentration of monomers is 0.1 M. The ratio of aniline and the other monomer is varied from 100:1 to 1:3 (See Appendix I, Table 3.1-1). The details of experiment were described in Chapter 2. The comparison of cyclic voltammograms between individual polymers and their copolymer can be used to distinguish copolymerization and polymerization of both individual polymers.

Fig. 3.1.2-1 and Fig. 3.1.2-2 show the cyclic voltammograms comparison between different copolymer and its individual polymers, respectively.
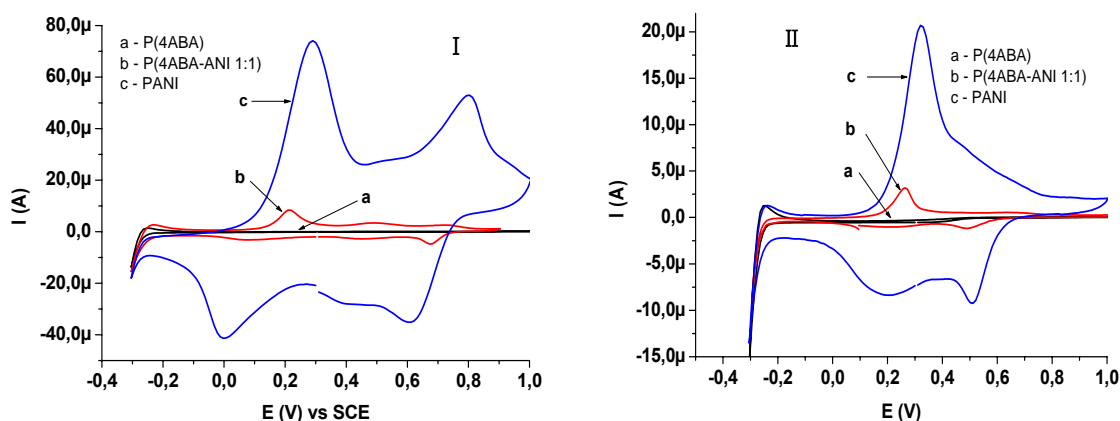
Fig. 3.1.2-1 Cyclic voltammograms (the 10th cycle) of P(4ABA) (a), poly(ANI-4ABA 1:1) (b) and PANI (c) films on Pt electrodes in the aqueous solution of 0.5 M H_2SO_4 with (I) or without (II) monomers in the range of -0.3 V ~ 1.0 V with potential sweep rate of 50 mV/s

In Fig. 3.1.2-1(I and II), curve a, b, and c present the electrochemical properties of P(4ABA), poly(ANI-4ABA 1:1) [P(4ABA-ANI 1:1] and PANI on platinum electrodes in the aqueous solutions with or without monomers. The polymerization of individual 4-ABA (curve I-a) was too slow to form visible polymer film on the electrode, and only slight anodic peak at about 0.8V presenting the formation of radicals of 4-ABA is shown in the 10th of cyclic voltammograms. The reaction is much slower than its copolymerization (curve I-b) and that of PANI (curve I-c). In curve I-b, there are three pairs of redox peaks at 0.2 V, 0.5 V and 0.7V, respectively, which are different from curves a and c. In Figure 3.1.2-1 (II), differences of peak potential may be observed in II-b and II-c. The anodic peak (*b* in II) at around 0.2 ~ 0.3V proved the conversion between leucoemaldine and emaldine stages of copolymer of P(ANI-4ABA) in H_2SO_4. It shifted to the left compared with the corresponding peak of PANI (0.3 ~ 0.4V). All these electrochemical properties imply the formation of co-polymers of P(ANI-4ABA).

Figure 3.1.2-2 shows the cyclic voltammograms of individual polymer poly(3-aminobenzoboronic acid) [P(3ABBA)] and its copolymers with aniline at different molar ratios in 0.5 M H_2SO_4 solution. All curves were obtained at the same sweep rate of 50 mV/s. The curves of the same number of cycles are shown in Fig. 3.1.2-2, I. The magnification of the curves (a, b, c) is depicted in Fig. 3.1.2-2 (II). These were acquired on the polymers containing higher component of 3ABBA (aniline to 3ABBA is 0 (a), 1:2 (b), and 1:1(c)).

Obviously, the anodic current is increasing with the increase of aniline content in the mixtures. The shapes of cyclic voltammograms of copolymers deposited from the mixture with higher content of 3ABBA tend visibly to the cyclic voltammogram shape of P(3ABBA); on the contrary, the shapes of cyclic voltammograms of those containing higher content of aniline display the cyclic voltammogram property close to PANI.
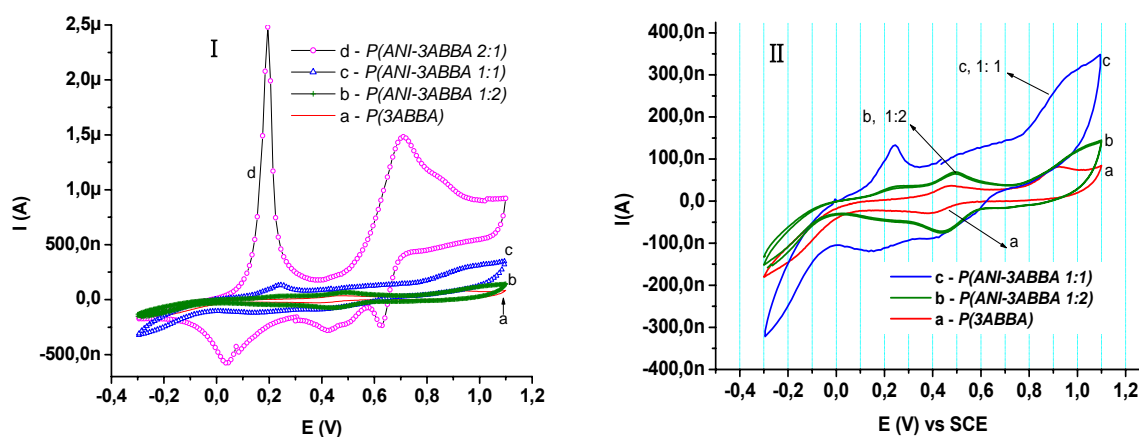

Fig. 3.1.2-2 Cyclic voltammograms of Pt/P(3ABBA) (a) and copolymer Pt/P(ANI-3ABBA) with different ratios of aniline to 3ABBA (b 1:2; c 1:1; d 2:1) in 0.5 M H_2SO_4 in the range of -0.3 V ~ 1.1 V with potential sweep rate of 50 mV/s.

(I: All curves; II: Detailed curves)

The same result is valid also for other polymerization mixtures. The electropolymerization reaction is getting slower in mixtures than that of aniline alone (Table 3.1). This is attributed to low electro-activity of aniline derivatives which contain some substituent groups in the ring. At potentiostat or potentiodynamic conditions, the lower the ratio of aniline to another monomer in the mixture, the lower the electropolymerization speed.

3.2 Electrochemical Characterization

3.2.1 Cyclic Voltammetry of PANI Films

Cyclic voltammetry is one of the most important tools to be used for characterizing electrochemical properties of polymers and polymerization. Fig. 3.2.1-1 demonstrates the electrochemical properties in cyclic voltammograms of PANI in 0.5 M H_2SO_4 solution with or without monomer. Figure (a) shows the cyclic voltammograms of electropolymerization

from 0.1M aniline in 0.5 M H_2SO_4 solution; (b) shows cyclic voltammograms of PANI film on a platinum electrode obtained from (a) in monomer-free H_2SO_4 solution. Both were carried out over the potential range from – 0.3 V to 1.0V with the sweep rate of 50 mV/ s.
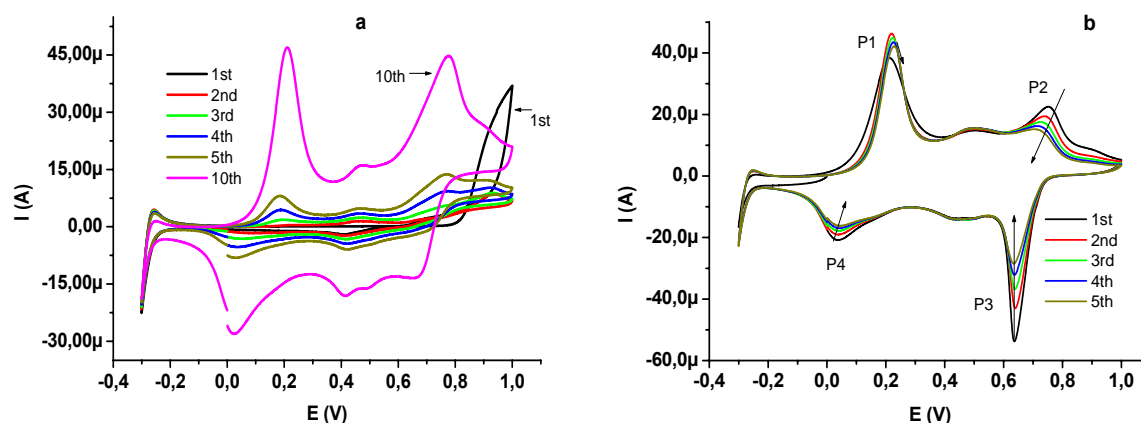

Fig. 3.2.1-1 Cyclic voltammograms of Pt / PANI in 0.5 M H_2SO_4 with (a) and without (b) monomer in the range from – 0.3 V to 1.0 V with a sweep rate of 50 mV/s.

The anodic current increases gradually with the increase of cycle numbers (Figure 3.2.1-1 (a)). It can be observed that in the first cycle of (a), the current begins to increase sharply at approximately 0.8 V (vs SCE) in the direct sweep, and limited by the potential cycling range. Here, 0.8 V is the start electro-oxidation potential of aniline, after inversion at 1.0 V, the anodic current decreases quickly during the reverse scan from 1.0 to 0.9 V because of the decrease in the reaction kinetics. The following cathodic peak at 0.4 V characterizes the electrochemical response of the electrodeposited PANI film; it is associated with the reduction of the oligomers obtained in the positive sweep. This is the typical behavior already observed for the PANI electro-deposition under various experimental conditions.[74;213]

From the second potential cycle, three redox couples appear. The peak at 0.2 V reveals the inter-conversion from leucoemeraldine to emeraldine with the change of color from yellow to green; the middle couple is at around 0.45 V; and the last couple at higher potential (0.75 V) originates from the generation of di-radical di-cations in the PANI structure resulting from the head to tail addition of monomer units. It's obvious that the anodic current at the oxidation potential of the second cycle is much lower than in the first cycle; this is mainly due to the increase of electrode surface area because of the film formation in the first cycle. The current of all anodic peaks in Fig. 3.2.1-1 (a), as well as other cyclic voltammograms of polymerization in Table 3.1.1-1, increases faster and faster with the number of potential

cycles; this demonstrates the autocatalytic polymerization of aniline.[214;215] The result is in agreement with the result from electropolymerization at constant potential (Fig. 3.2.1-2). The initial current is around 9 μA, and decreases sharply during first 10 s. Then it increases quickly with the increase of reaction time.
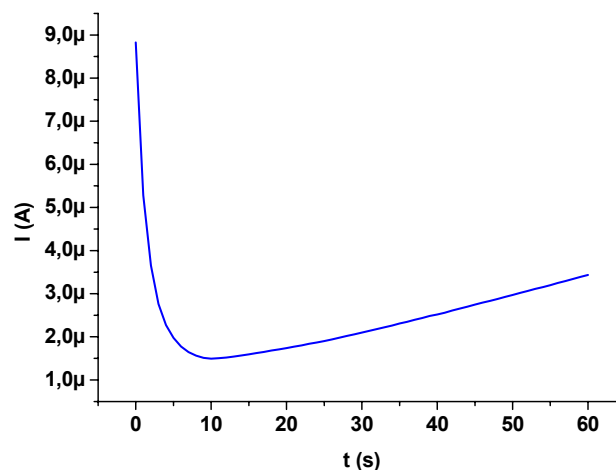

Fig. 3.2.1-2 Electropolymerization of 0.1 M aniline in 0.5 M H_2SO_4
on platinum electrode at 0.9 V

In Figure 3.2.1-1 (b), three pairs of oxidation-reduction peaks are observed in cyclic voltammograms at similar oxidation potentials to those during polymerization of aniline after 5 cycles in figure (a). The difference in CVs between (a) and (b) is that, in Fig. 3.2.1-1 (b), the oxidation current after P2 decreases sharply with increasing potential when the potential is over 0.65 V in (b); however, the oxidation current in (a) continues to increase quickly if the potential is over 0.65 V.

The latter is attributed to the electrochemical oxidation of aniline on the PANI film itself. Additionally, in Fig. 3.2.1-1 (a), the current increases with the increase of scanning number; it proves that PANI in the presence of aniline can not be over-oxidized when the scan potential is more than 0.65 V vs SCE. On the contrary, PANI in a solution without aniline is getting degraded during the potential scan between -0.3 V and 1.0 V because the oxidation current of the anodic peak decays with increasing number of potential cycles at the highest potential. It results from the over-oxidation of PANI.[211] This phenomenon can also be observed in other cases if the PANI films are formed on different electrode surfaces in different electrolytes (Table 3.1 and Table 3.1.1-1).

3.2.2 Anion-Exchange in PANI Films

To study the anion-exchange property of PANI, a series of experiments on PES state of PANI films were done in solutions of 1 M HCl, $HClO_4$ or 0.5 M H_2SO_4; they were performed by using cyclic voltammetry from -0.3 V to 1.0 V with sweep rate of 50 mV/s. All the films were formed on gold electrodes from various acidic solutions; they were obtained by cyclic voltammetry over the same potential range. The acids used for polymerization were called primary dopants. Three types of anions from corresponding acids were compared: Cl^-, HSO_4^- and ClO_4^-. After electrochemical polymerization, PANI films were scanned first in the primary acidic solution without monomer; then they were transferred to the solution with another salt, measured and transferred into the third solution, etc. Afterwards, the electrode was scanned again in the solution containing the primary dopant. The films were always rinsed with MILLIPORE water before they were immersed into different solutions. The order of procedures is numbered as Step1, Step2.....The curves from the fifth cycle for every experiment are shown in Fig. 3.2.2-1, 3.2.2-2, and 3.2.2-3 respectively, if not specified differently.
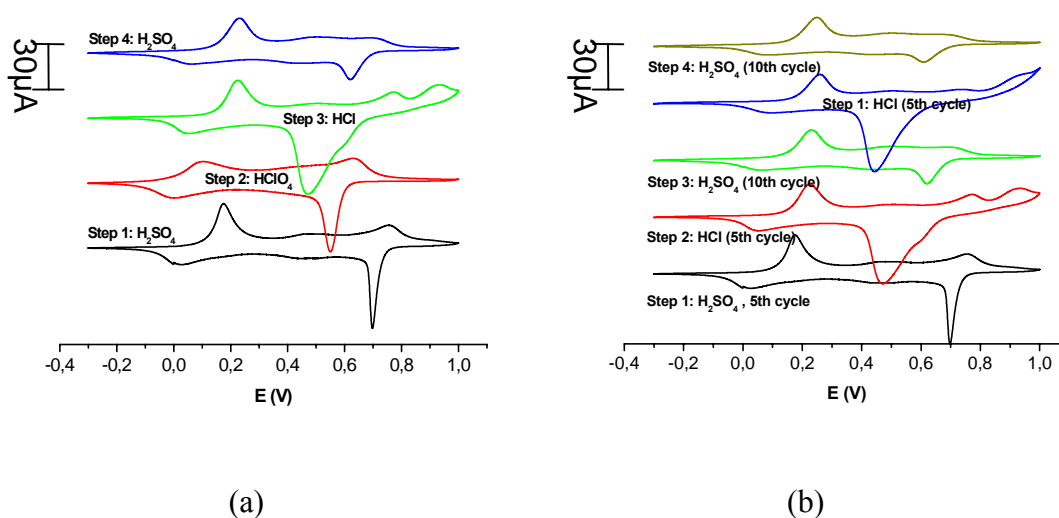

(a)   (b)

Fig. 3.2.2-1 PANI-SO_4 film on Si/Au electrode was cycled at the potential range of -0.3 V ~ 1.0V (vs SCE) successively in various acids. Sweep rate is 50 mV/s.

a: H_2SO_4 (Step 1)- $HClO_4$ (Step 2)– HCl (Step 3)- H_2SO_4 (Step 4)

b. H_2SO_4 (Step 1) – HCl (Step 2) - H_2SO_4 (Step 3) – HCl (Step 4) - H_2SO_4 (Step 5)

It is difficult to make a conclusion concerned for the exchange of HSO_4^- and ClO_4^- from Fig. 3.2.2-1 (a), mainly because of the similar shapes of CV graphs. But there are differences between the curves in the first two steps. All peaks in $HClO_4$ solution (Step 2)

shift to the left; the first anodic peak becomes wider and the anodic current decreases. However, after the electrode was transferred to H_2SO_4 (step 4) again, all peaks shifted back to the right, similar to the first curve in H_2SO_4 (step 1). The reduced or missing second anodic peak is due to the over-oxidation of PANI. Additional ten sweep cycles were carried out in $HClO_4$ at Step 2. No definite changes were observed in the CV graphs. This effect is more pronounced in HCl solution (step 3): the typical CV of PANI-Cl film appeared in the second cycle, and it took at least 52 s (1 cycle) to start the exchange; however, it did not change completely back to the property of PANI-HSO_4 film during 5 cycles (260 s) at Step 4.

In order to certify the exchange between HSO_4^- and Cl^- in PANI-HSO_4, two cycles of exchange experiments (1st cycle: Step 1 and Step 2; 2nd cycle: Step 3 and Step 4) were carried out for those two solutions. The results from 5 steps are shown in Fig. 3.2.3-1 (b). At Step 2 and 4, the typical CV belonging to PANI-Cl occurred in the third cycle at Step 2 and in the second cycle at Step 4, respectively; this means it takes at least 52 s for primary HSO_4^-, 104 s for the partially exchanged primary HSO_4^- to be exchanged by Cl^-. However, at Step 3 and 5, no changes happened during the first five cycles; partly changed CV shapes after sweeping 10 cycles (520 s) were shown in Fig. 3.2.3-1 (b).

The anion-exchange in primary PANI-Cl and PANI-ClO_4 films were investigated in a same way. The results are demonstrated in Fig. 3.2.2-2 and Fig. 3.2.2-3.

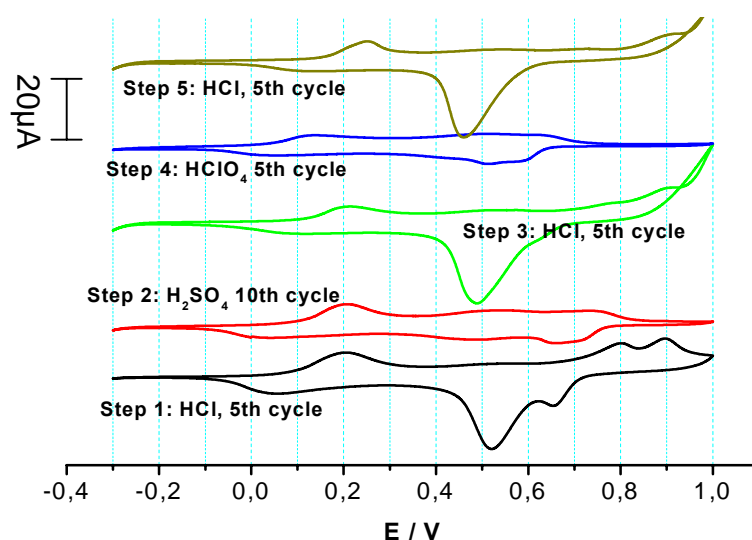

Fig. 3.2.2-2 PANI-Cl film on Si/Au electrode was cycled in the potential range of -0.3 V ~ 1.0V (vs SCE) in successively changed acids. Sweep rate is 50 mV/S. HCl (Step 1) - H_2SO_4 (Step 2)- HCl (Step 3) – $HClO_4$ (Step 4) - HCl (Step 5)

Fig. 3.2.2-2 presents the anion-exchange in primary polymer PANI-Cl between Cl⁻ and another anion HSO_4^- or ClO_4^-. The similar CVs of PANI in HCl solution were observed at Step 1, 3, 5. The difference of the curves at Step 3, 5 from at Set 1 is the missing of oxidative peak and the slight shift of cathodic peaks. This is due to the over-oxidation of PANI, as described before. The curve at Step 2 was acquired at the 10 th cycle, and it showed the CV shape of PANI-Cl in hydrogen chloride; the same phenomena of slow exchange was observed at Step 4 for the curve obtained at the 10 th cycle in $HClO_4$. However, the typical CV shape of PANI-Cl in HCl solution already appeared in the first cycles of Step 3 and Step 5 (less than 26 s).
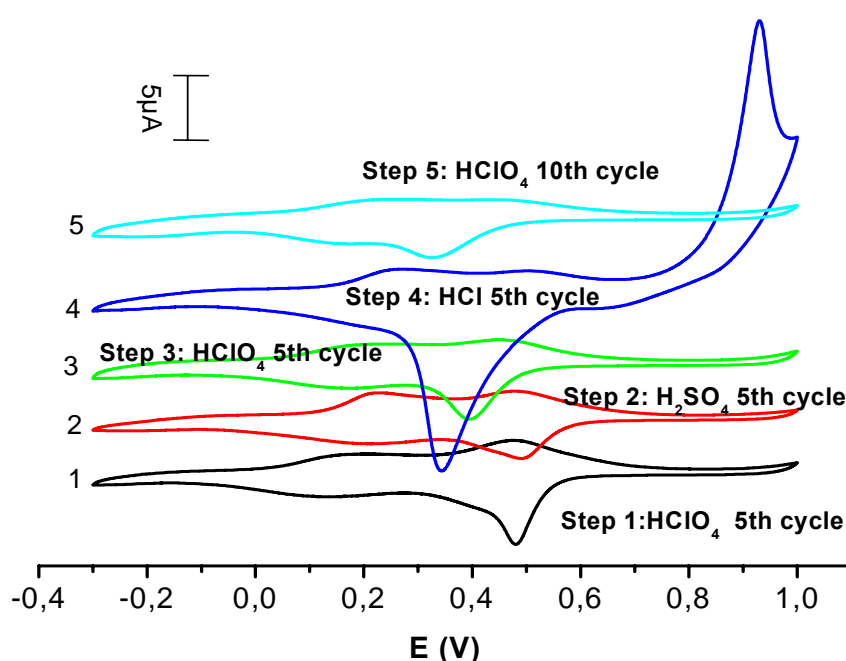

Fig. 3.2.2-3 PANI-ClO₄ film on Si/Au electrode was cycled at the potential range of -0.3 V ~ 1.0V (vs SCE) in successively changed acids. Sweep rate is 50 mV/S.
HClO₄ (Step 1) - H₂SO₄ (Step 2) - HClO₄ (Step 3) -HCl (Step 4) – HClO₄ (Step 4)

The same investigation of anion exchange has been done on the primary PANI-ClO₄ (Fig. 3.2.2-3). During the first three steps, slight changes between every two steps occurred to the cyclic voltammograms. It is difficult to distinguish whether there are anion exchanges in the PANI film between ClO_4^- and HSO_4^- or not. However, primary dopant ClO_4^- in PANI film can be exchanged by Cl⁻ easily. It was realized in the beginning of the first cycle (less than 26 s), shown in Fig. 3.2.2-3 (Step 4).

These results are different from the expected phenomena according to the 'structural memory' effect suggested by Nekrasov et $al.$[216] In the theory of 'structural memory' effect, the sizes of ions determine the ionic mobility. As we know, the (thermal) radii of ClO_4^-, HSO_4^- and Cl^- are 0.225 nm, 0.221 nm and 0.168 nm, respectively, so the mobility of these anions changes in this order: $ClO_4^- < HSO_4^- < Cl^-$. We expected before the experiments, that the exchange of primary ClO_4^- in the PANI-ClO_4 film with Cl^- anion could be slower than that of HSO_4^- in PANI-HSO_4 with Cl^-. However, the different result was obtained. This means that there are some unspecified reasons overwhelming the ionic mobility.

The results are summarized, according to the information from Fig. 3.2.2-1, Fig. 3.2.2-2 and Fig. 3.2.2-3, that the anion-exchange between ClO_4^-, HSO_4^- and Cl^- are different.

- Primary dopants, ClO_4^- and HSO_4^- in PANI can be easily exchanged by Cl^- with different start exchange time, less than 26 s for ClO_4^- anion and 104 s for HSO_4^-; the opposite exchange seems to be very difficult, and takes longer time (more than 520 s).

- Primary chlorate anion in PANI can be partially exchanged by other two anions during the first 10 cycles (520 s); the polymers with partially exchanged anions are easily recovered in the first cycle (less than 52 s) in HCl solution (containing primary dopant of this polymer).

- The uncertain conclusion is that probably there is no exchange or exchange at a lower extent between these ClO_4^-, HSO_4^- during the first 10 cycles, since no specified change of CV graphs is observed.

3.3 Morphology of Conducting Polymer Films

An exploration of the unique conductive properties of OCPs requires some information on their morphology after deposition on electrodes. In this work, individual polymer films of PANI were compared with its copolymer films from the mixture of aniline and other monomers which were prepared as mentioned before. A focus was put on the comparison of PANI films with poly (N-methyl aniline) (PNMA). The influence of counter ions, polymerization conditions, electrode materials and adhesive sublayers on morphology of these polymers was studied.[217] The results were evaluated by means of optical and electron microscopy in the micrometer scale. A group of gold electrodes was pre-coated by a sublayer of 4-aminothiolphenol[218] prior to polymerization. The electropolymerization was performed at constant potential (+0.6, +0.7 or 0.9 V vs. SCE), at constant current (0.1, 0.5, 5 or 10 μA), or at potential sweep between –0.3 and +1.1 V (versus SCE) with scan rate of 50 mV/s. PNMA

films were electrochemically formed from aqueous solutions containing 0.2M N-methylaniline (NMA) and 2 N H_2SO_4, $HClO_4$, HCl, H_3PO_4 and CH_3COOH. To get similar oxidation state of the polymers, a potential of +300 mV was applied for 60 s after electropolymerization.

3.3.1 Influence of Polymerization Conditions

Electropolymerization in galvanostatic and in potentiostatic mode was compared. To minimize effects of the layer thickness, the polymerization reaction was stopped at the same value of polymerization charge. Variation of the current density 100 times (between 0.3 and 30A/m^2) does not lead to any visible modification of the polymer morphology (Fig. 3.3.1-1) – in both cases, formation of smooth, light-green, transparent polymer layers with individual dark-green, non-transparent grains was observed. Polymerization at constant potentials of 0.7 or 0.9V, stopped at the same value of polymerization charge, results in similar polymer morphology. The polymer thickness in these experiments, estimated according to Faraday's equation was about 0.3 mm (assuming that the whole amount of oxidized monomers is included in polymer chains, stoicheiometry is 2.5 electrons per monomer,[219] and the polymer density is similar to the density of NMA). The results are shown in (Fig. 3.3.1-2 a, b). Polymerization up to a higher charge leads to the same polymer morphology (Fig. 3.3.1-2 c). Therefore, the structure of PNMA films polymerized on gold electrodes at a fixed polymerization charge does not depend on electrochemical polymerization conditions. The equation to be used for the calculation of polymer thickness is expressed as follows:

$$D = \frac{QM}{zFA\rho}$$
Eq. 3.3.1-1

where, Q is the transferred charge; M (NMA) is 107.16 g/mol; A is the area of electrode (0.38 mm^2); ρ = 0.989 g*cm^{-3}; F is the Faraday's constant 96500 C/mol; z = 2.5, number of electrons per monomer.
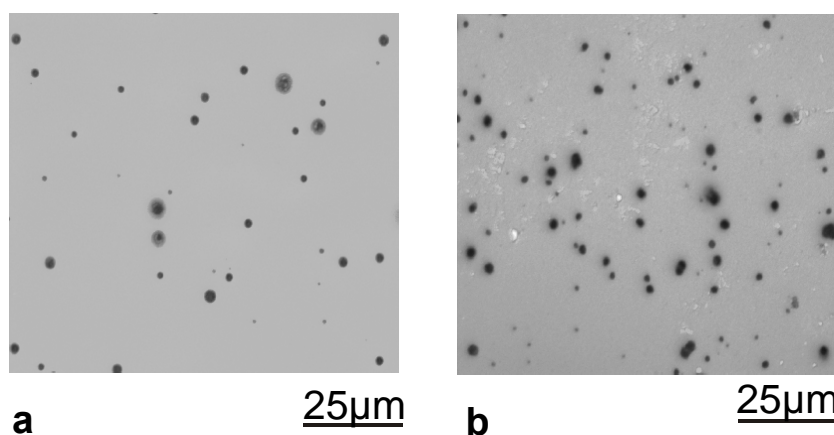
Fig.3.3.1-1 Optical microscopy of PNMA-perchlorate films polymerized on bare gold electrodes galvanostatically at 30 A/m^2 (a) and 0.3 A/m^2 (b) until the total polymerization charge density of 800 C/m^2.
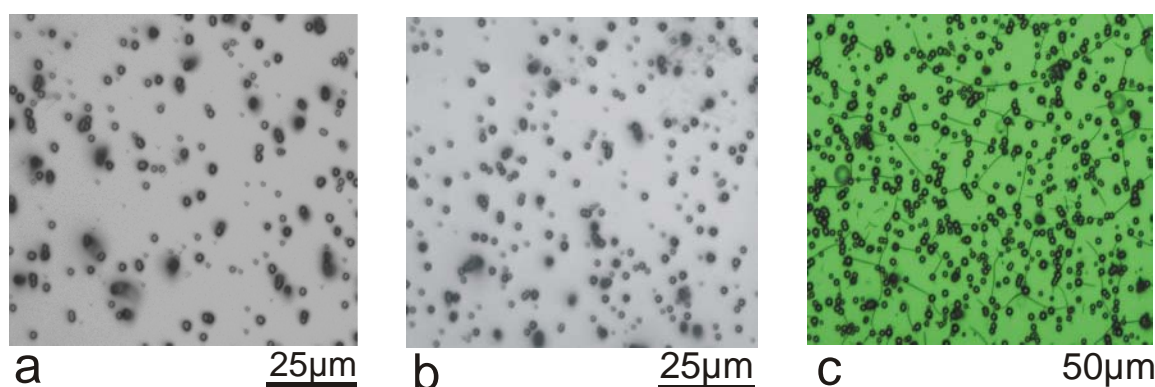

Fig. 3.3.1-2 Optical microscopy of PNMA-perchlorate films formed on bare gold electrodes galvanostatically at 15 A/m^2 (a) and potentiostatically (b, c) at +0.9V. The total polymerization charge density is 4 kC/m^2 (a, b) or 8 kC/m^2 (c).

A comparison between Fig. 3.3.1-1 and Fig. 3.3.1-2 demonstrates an effect of the polymerization charge on the film structure. The results were obtained by electro polymerization in perchlorate. The polymer layers are smooth with individual polymer grains on the surfaces. Continued polymerization leads to an increase of the grain size and to the formation of visible cracks in the polymer layer (Fig. 3.3.1-2c). The same effect was observed with the same polymers obtained by cyclic voltammetry between –0.3V and 1.1 V with sweep rate of 50mV/s. The results are shown in Fig. 3.3.1-3; a and b show the morphology of PANI-ClO$_4$ after 2 and 20 cycles, respectively.
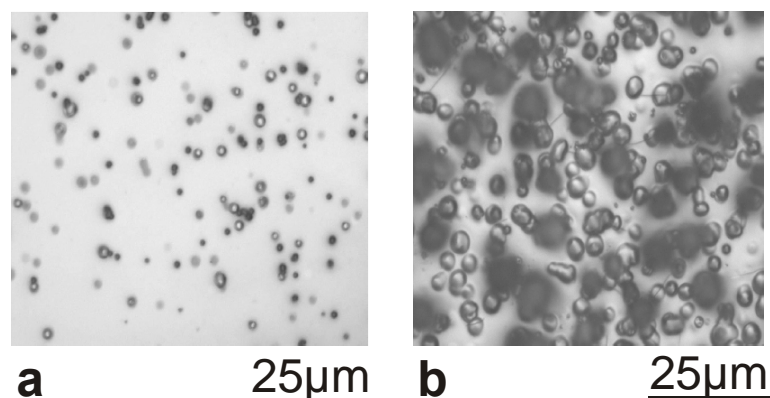
Fig. 3.3.1-3 Optical microscopy of PNMA-perchlorate films formed on bare gold electrodes
by cyclic voltammetry between –0.3V and 1.1 V with sweep rate of 50 mV/s
during two (a) and twenty (b) cycles.

3.3.2 Influence of Anions

N-methylaniline has basic properties (pK=5.02[220]) and can be protonated easily. PNMA could have similar properties. Polymerization under acidic conditions leads to the formation of salt and to the inclusion of anions into the polymer. The anions effect the electrochemical properties of PNMA films.[221] One can expect an influence of the anions on the polymer morphology. In this case, we performed electropolymerization from solutions of N-methyl-aniline in acetic, hydrochloric, phosphate, sulfuric- and perchloric acids. This was done galvanostatically, potentiostatically and by cyclic potential sweep. Although the formation of PNMA-acetate was clearly monitored electrochemically and although it was possible to observe a formation of a blue-green substance near the electrode, no visible trace of the polymer appeared on the electrode (polymerization was performed up to the charge of 8 kC/m^2). This may be caused by its poor adhesion to the electrode surface and/or in its high solubility in the polymerization solution. Electropolymerization of PNMA-chloride did at first not lead to any traces of polymer on the electrode either, in spite of formation of blue-green color substance and clear electrochemical indications of electropolymerization; increasing the polymerization charge up to 8 kC/m^2 resulted in the formation of polymer grains on the electrode surface (Fig. 3.3.2-1 a).
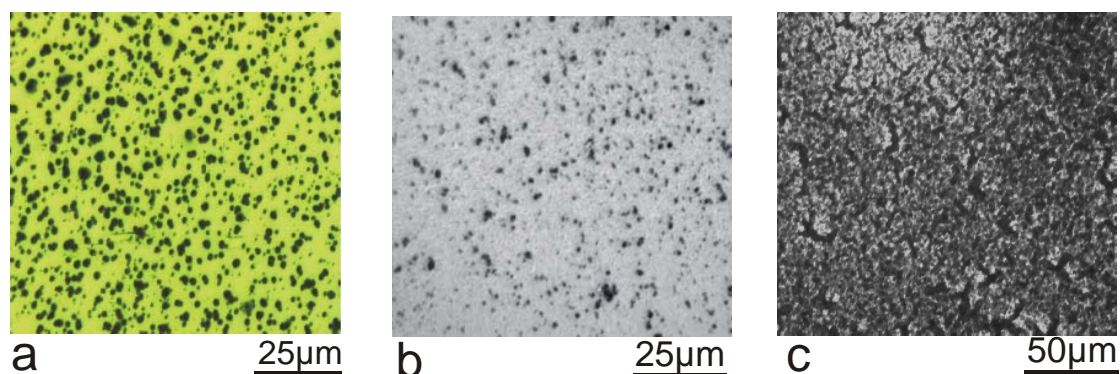
Fig. 3.3.2-1 Optical microscopy of PNMA films deposited on bare gold electrodes from 2 N aqueous solutions of hydrochloric (a), phosphoric (b) and sulfuric (c) acids. Polymerization performed at constant potential of + 0.9 V.

Electrochemical deposition of PNMA-phosphate under the same conditions was much easier: formation of polymer film on the electrode was observed at a polymerization charge density of 4 kC/m^2 (Fig. 3.3.2-1 b). However the layer was not stable and detached from the electrode upon a slight disturbance. The polymer grains were much smaller than those of PNMA-chloride. Visually, the polymer was of a gel-like consistence. Electropolymerization of PNMA sulfate under the same conditions also led to the formation of a polymer layer on the electrode surface, but the layer was formed by much larger and uniform grains and looked like a crust (Fig. 3.3.2-1 c). It was possible to get PNMA sulfate films on the electrodes and even to measure surface conductivity of these films and its increase upon addition of acidic gases. However, mechanical disturbances of the polymer films also resulted in the loss of the polymer. This low adhesion was especially evident if the electrode area was small; this behavior is shown in the Fig. 3.3.2-2. The poor adhesion of PNMA-sulfate to solid electrodes was also discussed in literature.[222;223]
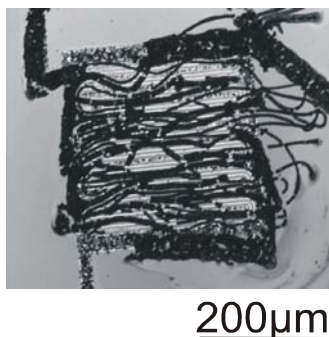

Fig. 3.3.2-2 Poor adhesion of PNMA sulfates to bare gold electrodes. Polymerization conditions: 15 A/m^2, polymerization time 20 min.

The most homogeneous films were observed for PNMA perchlorate. This polymer formed a glass-like structure on the electrode surface (Fig. 3.3.1-1 ~ 3), especially for thin polymer layers (Fig. 3.3.1-1 a). Cracks are clearly visible in thick polymer layers (Fig. 3.3.1-2 c), indicating solidity and brittleness of these films. Obviously, due to optical homogeneity of the polymer, light scattering in the films and on the interfaces is very low leading to the high optical transparency. Individual grains form on top of the polymer layer; a decrease of the polymerization charge leads to the minimization of these grains and to the formation of practically smooth polymer layers. Due to higher adhesion and/or lower solubility of PNMA-ClO_4, the formation of the films on gold electrodes and manipulations of the films were much easier than those for PNMA with other anions investigated.

The readily visualized difference in the adhesion of polymeric films having different counter-ions allowed us to draw a comparison even without a peeling test. Adhesion increases dramatically in the series: PNMA acetate, PNMA chloride, PNMA phosphate, PNMA sulfate and PNMA perchlorate.

3.3.3 Influence of Electrode Material and Surface Pretreated

a. Si / Au / PANI-SO_4 (1000 fold)   b. Si / Pt / PANI-SO_4 (1000 fold)
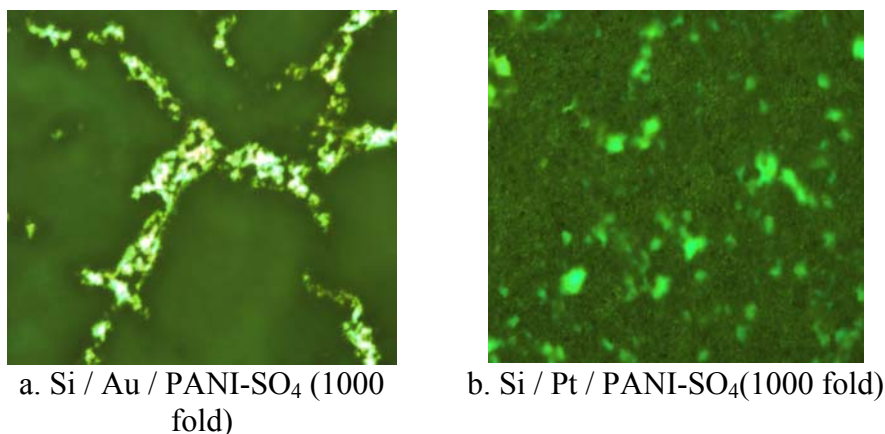
Fig. 3.3.3-1 Optical microscopy images of PANI deposited by cyclic voltammetry from 0.5 M H_2SO_4 acid on (a) Au and (b) Pt round electrodes, respectively.

PANI films obtained from aqueous solutions containing 0.1 M ANI and 0.5 M H_2SO_4 were electrochemically deposited at 0.9 V on gold and platinum electrodes, respectively. The total charge through each electrode is 0.3 mC [800C/m^2]. The optical microscopy images are shown in Fig. 3.3.3-1 (*a*, *b*). The morphology on both electrodes looks similar; both are porous and granular. But on the gold surface (a), there are many cracks in the polymer film which can not be found on platinum surface, while only a porous structure is observed in the

picture (b). It seems that the adhesion between polymer and platinum surface is stronger than that between polymer and gold. This has also been observed for other polymers.

Investigation of PNMA-sulfate and PNMA perchlorate formed on platinum electrodes demonstrated that the film morphology is the same as on the gold electrodes formed with the same polymerization charge and anion. Therefore, the electrode metal does not affect the film morphology. Adhesion of the polymers to platinum is much stronger than to gold; this corresponds with the well-known fact of strong adsorption of organic compounds onto metals of the platinum group.

Poor adhesion of electrochemically formed polymers to gold electrodes can be improved essentially by deposition of a sublayer of thiolated monomer.[34;224-226] It can be done by modifying the hydrophobicity of the surface influencing on the nucleation density of the polymer growth[225] or by using short thiols as electrically permeable adhesive layer. In this study we used 4-amino-thiophenol as an adhesive sublayer. The idea is based on the formation of strong, almost covalent binding of thiol compounds to gold surfaces.[227] Then, the application of polymerization potential leads to the copolymerization of the monolayer with monomers from the solution, thus causing the formation of polymer chains chemically immobilized on the gold electrodes. This principle was successfully applied to the deposition of PNMA in the present work.

The PNMA sulfate layers deposited on the sublayer were more homogeneous and displayed a certain grain structure (cf. Fig. 3.3.2-1 c and Fig. 3.3.3-2 a). The much higher adhesion of the polymer allowed us to perform electron microscopy even at the developed stage of the polymer growth (Fig. 3.3.3-2 b); without a sublayer it was impossible (Fig. 3.3.2-2). Fig. 3.3.3-2 b shows that the growth of polymer leads to the formation of rough structures with many sprouts tending to form bridges (Fig. 3.3.3-2 b). The formation of "nanorods" of PNMA-sulfate between electrodes was observed (Fig. 3.3.3-2 c) at high magnification. They look very similar to the nanotubes reported for PANI doped with hydrogensulfated fulleronol or sulfonated dendrimers.[228] It is interesting that also polypyrrole can form micro-tubular structures in the presence of sulfonated counterions.[229] All the dopants used belong to the family of sulfonates.

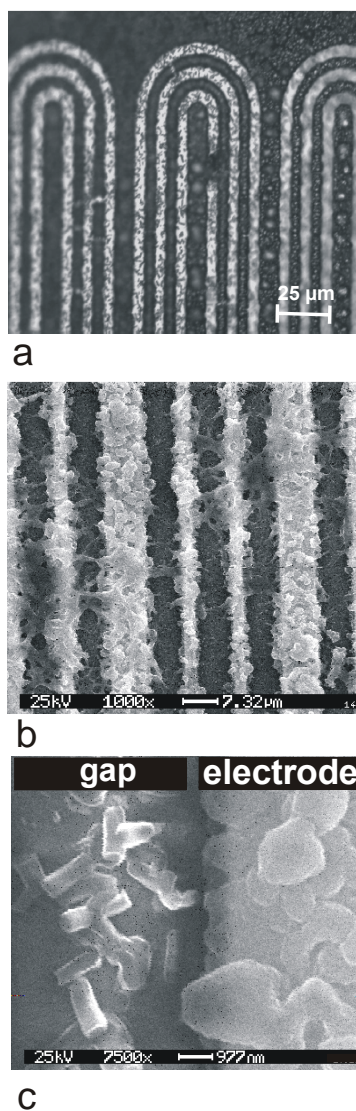**Fig. 3.3.3-2** Optical (a) and scanning electron (b, c) microscopy of PNMA-sulfate films on gold electrodes precoated by 4-amino-thiophenol. The formation of "nanorods" can be seen at high magnification (c). Polymerization conditions are the same as in Fig. 3.3.2-2.
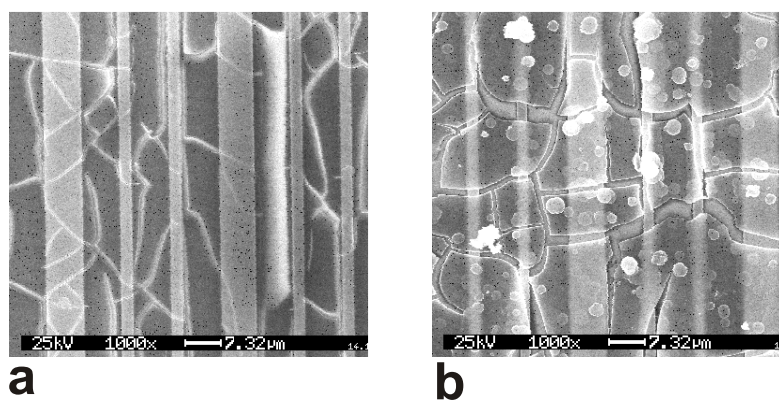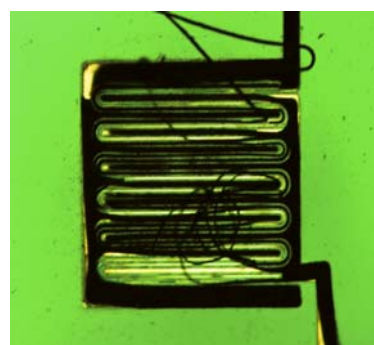

Fig. 3.3.3-3 Scanning electron microscopy of PNMA-perchlorate films, formed on gold electrodes precoated by 4-amino-thiophenol at 0.9V for 8 (a) and 20 (b) min.

PNMA perchlorate films on gold electrodes with a 4-amino-thiophenol sublayer did not show any morphological difference compared to films deposited directly on gold electrodes. In both cases a glass-like structure was observed (Fig. 3.3.1-1, Fig. 3.3.1-2 and Fig. 3.3.3-3), and an increase of the polymerization charge led to the formation of individual grains on the polymer surface, followed by an increase of their size and formation of cracks (Fig.3.3.3-3 b).

3.3.4 Influence of Geometric Structure of Electrode

a. round glass/ Au/ PANI-ClO$_4$ b. interdigitated glass/Au/PANI-ClO$_4$

Fig. 3.3.4-1 PANI-ClO$_4$ films deposited on bare gold electrodes with different shapes.
(a) round; (b) interdigitated

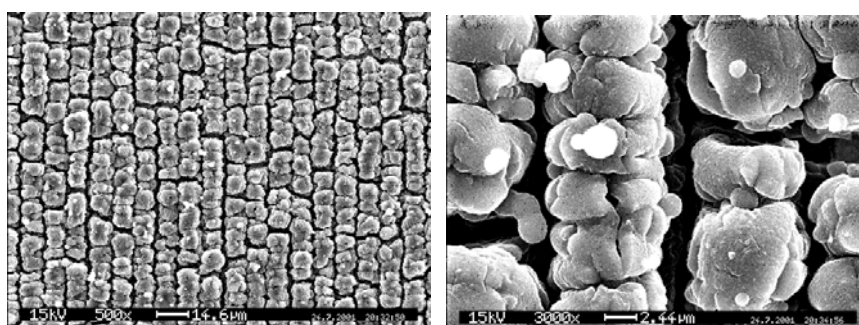**Fig. 3.3.4-2** SEM picture of PNMA at an angle of 60°. It can be recognised that the grains start growing together. **Left**: 1000 times magnification; at the edge of the electrode; **right**: 4000 times magnification; in the middle of the electrode.[230]

Electrode geometry has been found to influence the morphology of polymers. In Fig. 3.3.4-1, the same polymer deposited on an interdigitated electrode is easier to peel off from

thinner gold surface (b) than that on a round electrode (a), although both present the compact morphology. Interestingly, in Fig. 3.3.4-2, a grain structure of PNMA-ClO$_4$ was observed on a two-interdigitated platinum electrode by a former colleague; this is quite different from glass-like structure (Fig. 3.3.3-3) we observed under the same electrochemical condition except the difference of electrode geometry. The electrode in Fig. 3.3.4-2 was two–interdigitated electrode with the same width of two stripes (about 5µm). Obviously, the polymer grains started growing together like mushrooms.

3.3.5 Influence of Composition of Monomers

According to the morphology of various polymer films obtained from aqueous solutions, we observed some common structures and special structures for different monomers. The results are summarized in Table 3.3.5-1.

Table 3.3.5-1 Morphology of conducting polymers
from various monomers at 0.9V vs SCE

Dopant	PANI	PNMA	Copolymer	
			Higher content of PANI	Lower content of PANI
H$_2$SO$_4$	Porous and globular film	Porous and globular	Porous and globular film	More compact film
HClO$_4$	Uniform and compact film	Glass-like; compact film	/	/

As Wang [96] and Zotti [97] found, some ions (BF$_4^-$, ClO$_4^-$, CF$_3$COO$^-$) led to a compact structure of PANI (with a fiber structure) and other anions (SO$_4^{2-}$, NO$_3^-$ and Cl$^-$) promote an open structure (with a granular structure), we also observed the similar morphology of PANI-SO$_4$. However, we always obtained a compact and uniform structure for PANI-ClO$_4$ films instead of a fiber structure. Interestingly, a fiber structure can be observed on PANI grown from H$_2$SO$_4$ solutions too (shown in Fig. 3.3.5-1), which is a surprising result for the former studies of other groups.[97;231]
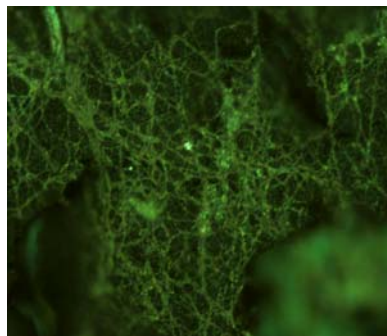
Fig. 3.3.5-1 Optical microscopy images of PANI deposited by cyclic voltammetry on Si/Au electrodes from 0.5 M H_2SO_4 acid in the potential range from -0.3V to 0.9V with sweep rate of 50 mV/s.

Additionally, it was observed during the experiment of ion-exchange for PANI, that the morphology of conducting PANI in micrometer scale did not be changed when the primary counter ions were exchanged by other anions. This coincides with the 'structural memory' effect. The morphology of copolymers from aniline and its derivatives has also been studied by using optical microscopy. It contains both characteristics between PANI and the other individual polymer, which allows to the mixture ratio of both monomers. Generally, the morphology of the copolymers from mixture with higher content of aniline showed a more porous and heterogeneous nature, close to that of PANI; on the contrary, the lower ratio of aniline and its derivative led to a more homogenous structure. This is in agreement with the study of Thiemann C. *et al.*[232]

3.4 Multilayer Structures Based on Conducting Polymers for Gas Sensor

Conductive polymers can be used as electrically-conductive bonds to bond flip clips and substrate bond pads[233;234] or be bonded between nanotubes and substrates[235] instead of metal bonding, which overcomes the limitations of a metal layer and expands the range of applications. But for practical usage, each individual conducting polymer shows some limitations. So the preparation of conducting copolymers, composites,[236;237] blends[238], bi-layers[239;240] or multi-layers[241] has been extensively studied recently for the improvement of the physical, chemical, mechanical, and electrical properties of polymers. Thus it is very significant that such conductive polymer bonds would be fabricated to bind on other polymers for the applications of sensors or electrical devices. Stimulated by those ideas, we demonstrated an application of a step-by-step electropolymerization for preparation of multi-layer conducting polymers, containing multi-function elements. These integrated structures can be employed for gas sensors.

The development of multilayer in this work is based on an interdigitated electrode. Two differently functional conductive polymers should be prepared electrochemically. One is sensitive to HCl gas (Here we use PANI), the other is not sensitive to gas but with high conductivity (Here is PEDOT), which both are obtained by a step-by-step all-electrochemical approach (a step-by-step all-electrochemical polymerization approach) to prepare gas sensors for HCl. Considering the growth of conducting polymers on an interdigitated electrode, we designed the formation architecture of PEDOT / PANI / PATP / Au as shown in Fig. 3.4-1.
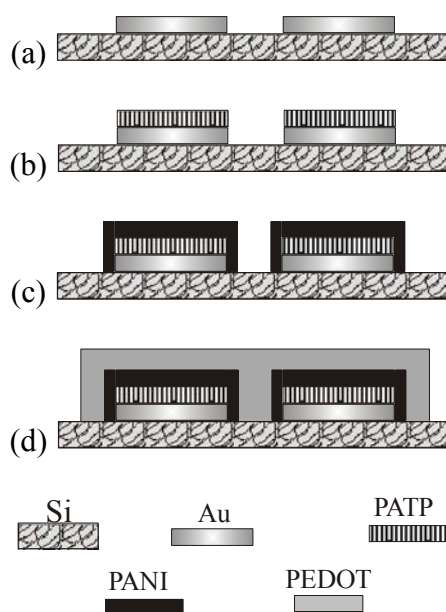

Fig. 3.4-1 Preparation of multilayer structure of conducting polymers
on gold interdigitated electrodes

To get a better adhesion of polymers to gold surface (Fig. 3.4-1 a), a sub-layer consisting of a self-assembled monolayer of 4-aminothiophenol (4-ATP) can be deposited on the gold electrodes (Fig. 3.4-1 b). After electro-polymerization of PANI (Fig. 3.4-1 c), very thin green PANI films would be formed only on the surface of gold lines pre-coated with 4-ATP; at the second step of electrochemical polymerization, a conducting layer of PEDOT will be deposited on the top of PANI layer up to overlapping on the gaps (d). This is the model of a multilayer structure from conducting polymers.

The working electrode was a gold two stripes interdigtated electrode with glass substrate, which was modified by a 4-ATP monolayer on bare Au electrodes after the appropriate surface treatment. The electropolymerization was conducted in two different solutions which each were in the standard three- electrode cell as used before. One was 0.2 M aniline and 2.0 M $HClO_4$ aqueous solutions, the other was CH_3CN solution containing 0.04 M

EDOT and 0.1 M LiClO$_4$. Electrochemical polymerization was performed using Autolab instrument. Resistance or conductivity was measured by the use of 4261A LCR HP meter. The response and sensitivity behavior to HCl gas was detected by the change in the resistance. The measurement system consists of a digital multimeter (Keithly 2400) for measuring the resistance, a gas flow system with two channels (one is for HCl, and the other is for N$_2$) and a PC for data acquisition. The atmosphere in the gas chamber was maintained at room temperature and a humidity of 0%. Nitrogen was the transporting and diluting gas for HCl, moreover it was used to refresh the sensor film.

The PANI/PEDOT multi-layers were obtained as following:

- *PANI/PATP/Au*: The PANI film was obtained on 4-ATP/Au modified interdigitated electrode by potential pulses (0.6V for 2min; 0.9V for. 40 min) electropolymerization. After rinsing with MILLIPORE water, and drying in a nitrogen gas flow, the resistance measurement and morphology study of the PANI films were preceded immediately.

- *PEDOT/PANI/PATP/Au*:   The electrode with PANI film was then transferred into the second solution containing EDOT monomer deaerated already. A sky-blue PEDOT film was prepared quickly under the condition of constant potential 1.2V. In order to get appropriate PEDOT films, the electropolymerization lasted 60s until the entire gold electrode window was covered completely by the deep sky-blue PEDOT film. After rinsed with ethanol and dried in the nitrogen gas flow, the electrode was used for the measurements of conductivity and the study on morphology. For the measurement of the sensitivity and response to HCl gas, the electrode was immersed in 0.1M NaHCO$_3$-Na$_2$CO$_3$ (pH = 9.0) buffer for about 24 h.

In the experiment, the solution of aniline in perchloride acid was used for PANI preparation because the morphology of PANI-ClO$_4$ is compact and uniform. Optical microscopy and resistance measurements were used to characterize the functionality of all structures of this multilayer system.

The process and results are shown in Fig. 3.4-2 and Table 3.4-1. The polymer growth was controlled by the charge amount through cathodic electrode, and an ultra-thin green PANI-ClO$_4$ layer, around 500 nm, was observed only on the electrode lines; no overlapping

of polymeric layers was found (Fig. 3.4-2 a, b), which was confirmed by the high resistance value: higher than 20 MOhm either in air or in N_2 / HCl atmosphere (Table 3.4-1).

(a) PANI (100 fold)   (b) PANI (200 fold)   (c) PEDOT/PANI(100 fold)
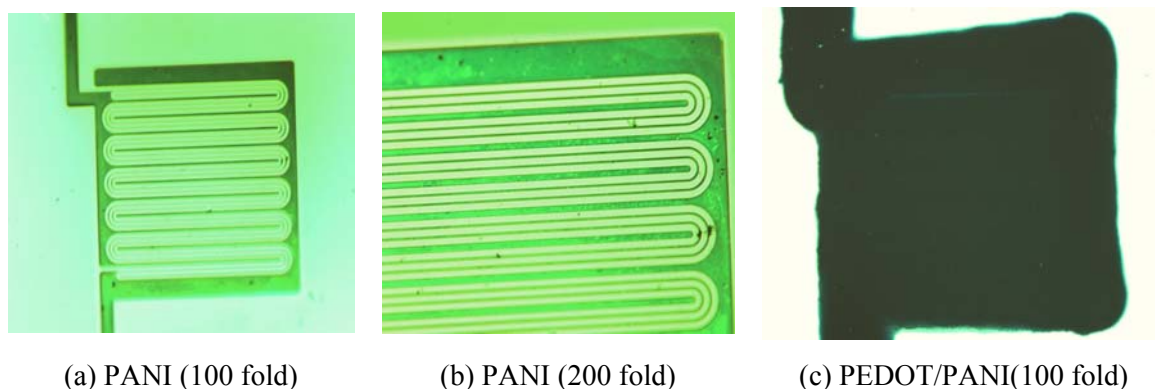
Fig. 3.4-2 Photomicrographs of PEDOT/PANI multilayer at two steps.

a and b: PANI grown on the separated gold modified electrodes

c: PEDOT polymerized on the surface of PANI and gaps

The electrical properties of the polymers coated electrodes for analysis of the multilayer structure are shown in Table 3.4-1.

Table 3.4-1 Electrical properties of polymers coated on electrodes

Polymer	Resistance (ohm)	Sensitivity to alkaline	Sensitivity to HCl gas
single PEDOT	75	no	no
single PANI	about 200	yes	yes
PANI in bilayer	> 20M	no	no
PEDOT/PANI	100-180	yes	yes

When the first step of polymerization was over, the working electrode was moved to the second solution containing EDOT, and followed the next electrochemical polymerization step. The subsequent electrochemical deposition of PEDOT was performed to get a conductive bridge between the PANI–coated electrodes as designed in Fig. 3.4-1d. It has been proved with microscopy (Fig. 3.4-2c) and resistance measurements (Table 3.4-1). The polymerization of PEDOT layer was carried out up to overlapping of PEDOT films over the whole electrodes, which led to a dramatic decrease of the resistance down to 120 ~ 180 Ohm. Thus the PEDOT bridge provides good electrical contacts of PANI lines. A complete

experiment and result for the formation of multilayer structure from Au/4-ATP/PANI/PEDOT is shown in Fig. 3.4-3.
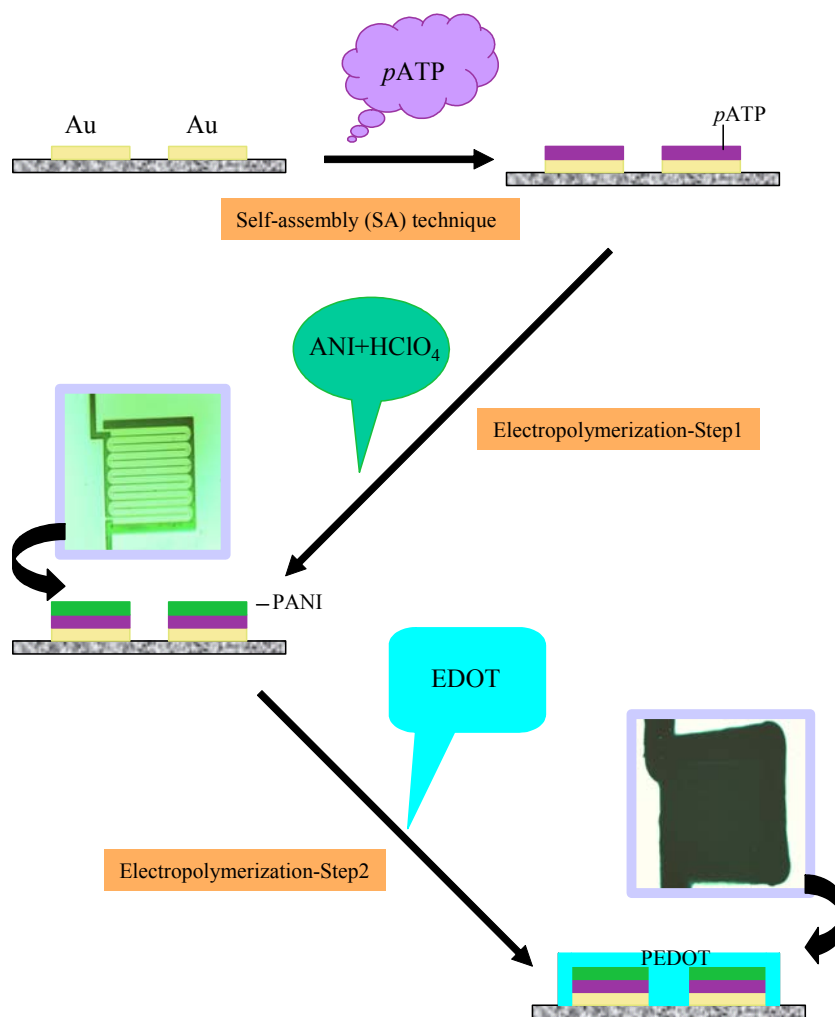
Fig. 3.4-3 Formation of multilayer structures of conducting polymers

The sensitivity and response of this kind of multilayer to hydrogen chloride (HCl) has been studied. The resistance measurements obtained from the multilayer of Au/p-ATP/PANI/PEDOT were compared with resistance changes on interdigitated electrodes (IDEs) overlapped with an individual polymer, PEDOT or PANI, in presence of HCl gas. The IDEs coated with PANI film displayed a conductance increase in the presence of gaseous HCl. However, the resistance of the IDEs covered with individual PEDOT did not change after or before put in the HCl gas atmosphere, and treating with the alkaline did not lead to any change in resistance either. So it is quite chemically stable. The result in Table 3.4-1 demonstrates thoroughly high conductivity of PEDOT independent on pH and gaseous HCl,[236;237] and high sensitivity of PANI to HCl. Based on these facts, we can suggest that

PANI provides sensing properties while PEDOT provides an electronic bridge between PANI-coated gold electrodes.

On exposure to HCl gas in different concentration and for different time, the resistance of PEDOT/PANI multilayer apparently decreased, and then increased when the HCl gas was replaced by nitrogen. The results were shown in Fig. 3.4-4. The sensitivity of Au/p-ATP/PANI/PEDOT multilayers to gaseous HCl and its reversibility imply the feasibility of the gas sensor application based on such multilayer structures.
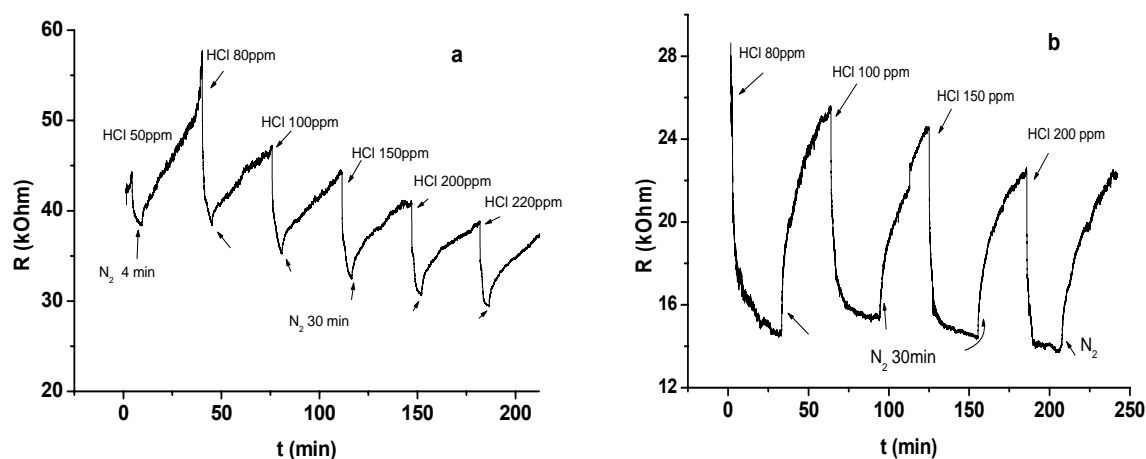

Fig. 3.4-4 Response of PEDOT/PANI multilayer exposed in different concentration of HCl gas for 5min at first (a), and then increase to 30min (b). The total flow rate is 250 ml/min; N_2 purging gas flow rate: 250 ml/min.

In Fig. 3.4-4, the gas response and sensitivity of Au/p-ATP/PEDOT/PANI resulted from ultra-thin layer of PANI actually due to the chemical stability of PEDOT against gaseous HCl. PANI can be doped or dedoped on exposure to acidic or basic environment, and this reversible mechanism is due to the presence of -NH group in the PANI backbone, protonation of which results in an increase of polymeric conductivity and the change of color.[49] On exposure to HCl gas, the HCl molecules firstly penetrated the PEDOT layer, and then contacted the interior dedoped PANI, and subsequently doped it to the salt of the emeraldine base, which caused the conductivity of PANI increasing. When nitrogen flow is replaced HCl gas, HCl molecules were desorbed gradually, now that N_2 is a chemical stable gas for PANI.[19] Although the PANI layer was grown only on the separated PATP/Au electrode lines, there was a PEDOT conducting polymer bridge which was bonded on the separated PANI/PATP/Au electrode lines. Therefore, through the complete circuit, individual

changes from the resistance of the PEDOT/PANI multilayer, which was observed from un-doped state and doped state, could be presented successfully in the device.

Stability of such multilayer structure used as a gas sensor for HCl has also been studied. After stored in the open air of our lab for more than one year, the sensitivity of this sample was tested in the presence of gaseous HCl under the same conditions as tested before. The result is shown in Fig. 3.4-5. The sample is still sensitive to gaseous HCl although the signal after long storage is slight noise than the original; the reversibility is as good as before. This means this multilayer structure is very stable and the lift time is long enough.
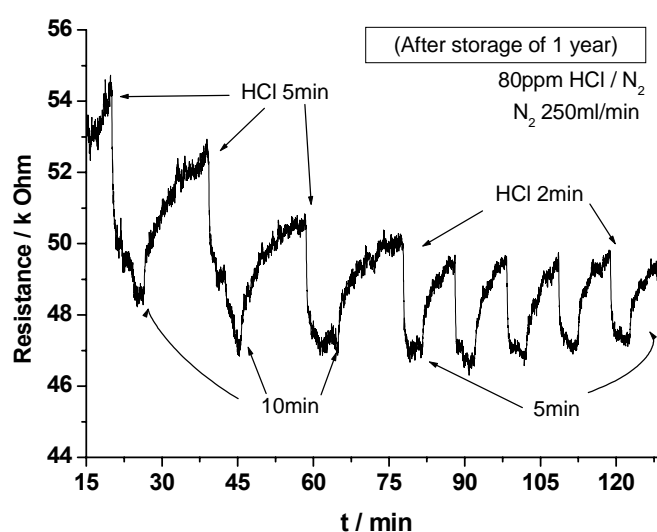
Fig.3.4-5 Response of Au/pATP/PANI/PEDOT to HCl after storage of 1 year in the lab

In this work, an application of layer-by-layer electropolymerization for the formation of two electrically coupled polymeric layers which could be used as a gas sensor. The conducting multilayer polymer, PEDOT/PANI/PATP/Au, described here is very instructive and intriguing because there are three outstanding characteristics to be mentioned.

- It was obtained by means of step-by-step electrochemical polymerization, in which different electrochemical methods could be selected in order to control the properties of every layer;

- Two functionally different polymers were used. One possesses sensitive properties and the other provides electrical bonding. In our design, conductive PANI is sensitive to HCl gas, and PEDOT is a new attractive conducting polymer with high conductivity but also with high chemical and thermal stability, which acts not only as a conductive

bridge to connect separated PANI, but also as a protecting coat film for PANI against oxidation.

- Additionally, the approach can be extended for the formation of multilayers or for fabricating p-n junctions for applications in chemical sensors, organic electronic devices or in other fields.

3.5 Application of Simultaneous Two- and Four-point Techniques to Characterization of Conducting Polymers

The principle of simultaneous 2- and 4-point method was tested on gold and platinum interdigitated electrodes which were electrochemically coated with PANI. An estimation of the polymer thickness from Faraday's equation gives about 1 μm. The electropolymerization has been done directly on bare platinum electrodes or on gold electrodes precoated with 4-aminothiophenol (4-ATP). An investigation of gas effects was performed with the home-made automated gas mixing system described in Chapter 2.4.8. A total gas flow rate of 250 ml/min was used throughout. Hydrogen chloride was diluted with nitrogen to a final concentration of 80 ppm for the experiments with gold electrodes or 20 ppm for the experiments with platinum electrodes.
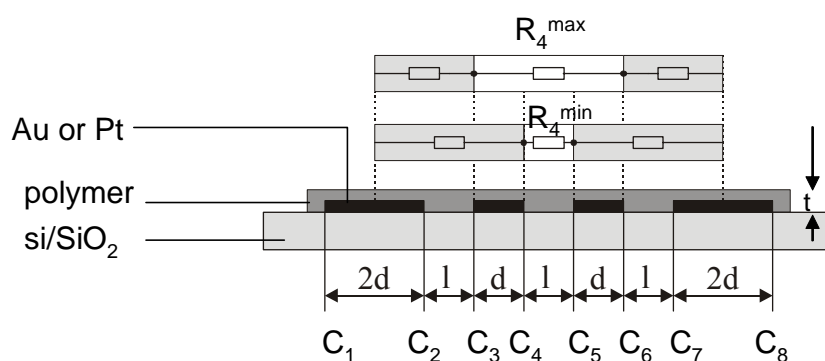
Fig. 3.5.1 Model of distribution of bulk resistance between four electrodes

Fig. 3.5.1 describes the distribution of bulk resistance between four figures in a four-interdigitated electrode. Let's assume that the polymer on the electrode is uniformly deposited, and consider the resistance of a fractional polymer with the width of l as R_0. Taking into account that $l = d$, and that the thickness of the polymer layer is less than the distance between the electrodes, the minimum and maximum resistance from two-point method (R_2^{min} and R_2^{max}) should be $5R_0$ (between C_2 and C_7) and $9R_0$ (between C_1 and C_8); the minimum and

maximum resistance (R_4^{min} and R_4^{max}) from four-point technique should be R_0 (between C_4 and C_5) and 5 R_0 (between C_3 and C_6). Therefore, the value of bulk resistance measured by the four-point technique can be between 1/9 and 3/5 from the bulk resistance contributed into the two-point measurements. From geometric considerations, for thin ($t<l$) polymer layers, the part of the polymer resistance between the inner electrodes ($\eta=R_4/R_2$) should be between 1/9 and 3/5. Therefore, if the ratio $R_2/R_4 > 9$, we can make a conclusion on measurable contribution of the contact resistance to the R_2. A modification of bulk resistance should only lead to proportional changes of R_2 and R_4; a constant contact resistance results in a deviation from this proportionality.

The resistance values measured by two- and four-point techniques are shown in Table 3.5-1. For platinum and the precoated gold electrodes, the values of R_2/R_4 were between 2 and 5. This corresponds to the expected range of geometrical effect (from 5/3 to 9) thus indicating a good electrical contact between polymer and electrodes. However, the high R_2/R_4 value measured for the polymer on gold electrodes without precoating cannot be explained by geometrical factors ($R_2/R_4 >> 9$). This demonstrates clearly a high contribution of contact resistance into the R_2.

Table 3.5-1 Initial resistance of PANI-coated electrodes
as measured by two- (R_2) and four- (R_4) points techniques

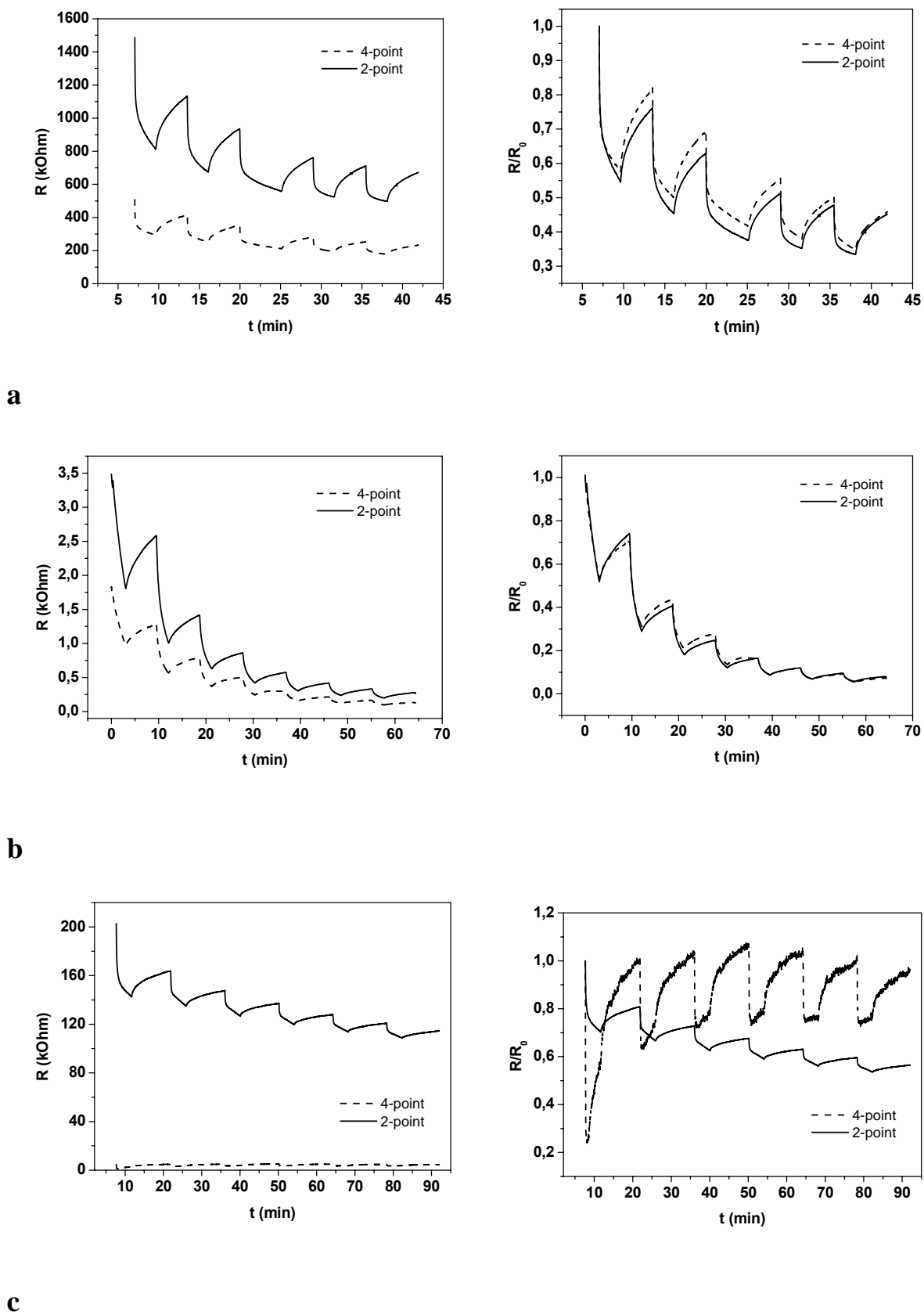| electrode material	polymer layer	precoating by 4-aminothiophenol	R_2, MOhm	R_4, MOhm	R_2/R_4
Au	PANI-ClO$_4$	yes	1.5	0.5	3
Au	PANI-SO$_4$	yes	3.4	1.7	2
Au	PANI-SO$_4$	no	26	0.4	65
Pt	PANI-SO$_4$	no	1.0	0.3	3
Pt	PANI-ClO$_4$	no	2.2	0.4	5

a

b

c

Fig. 3.5-2 Response of PANI films on gold electrodes to subsequent exposures of gaseous HCl, measured by simultaneous application of 2- and 4-point techniques. The curves are shown in absolute values (left) of the resistance or the values normalized for the initial values

(right). Preparation of polymer layers: polymerization from aniline/$HClO_4$ solution, the electrode was precoated by 4-aminothiophenol (a); polymerization from aniline/H_2SO_4 solution, the electrode was precoated by 4-aminothiophenol (b); polymerization from aniline/H_2SO_4 on bare gold electrodes.

a

b
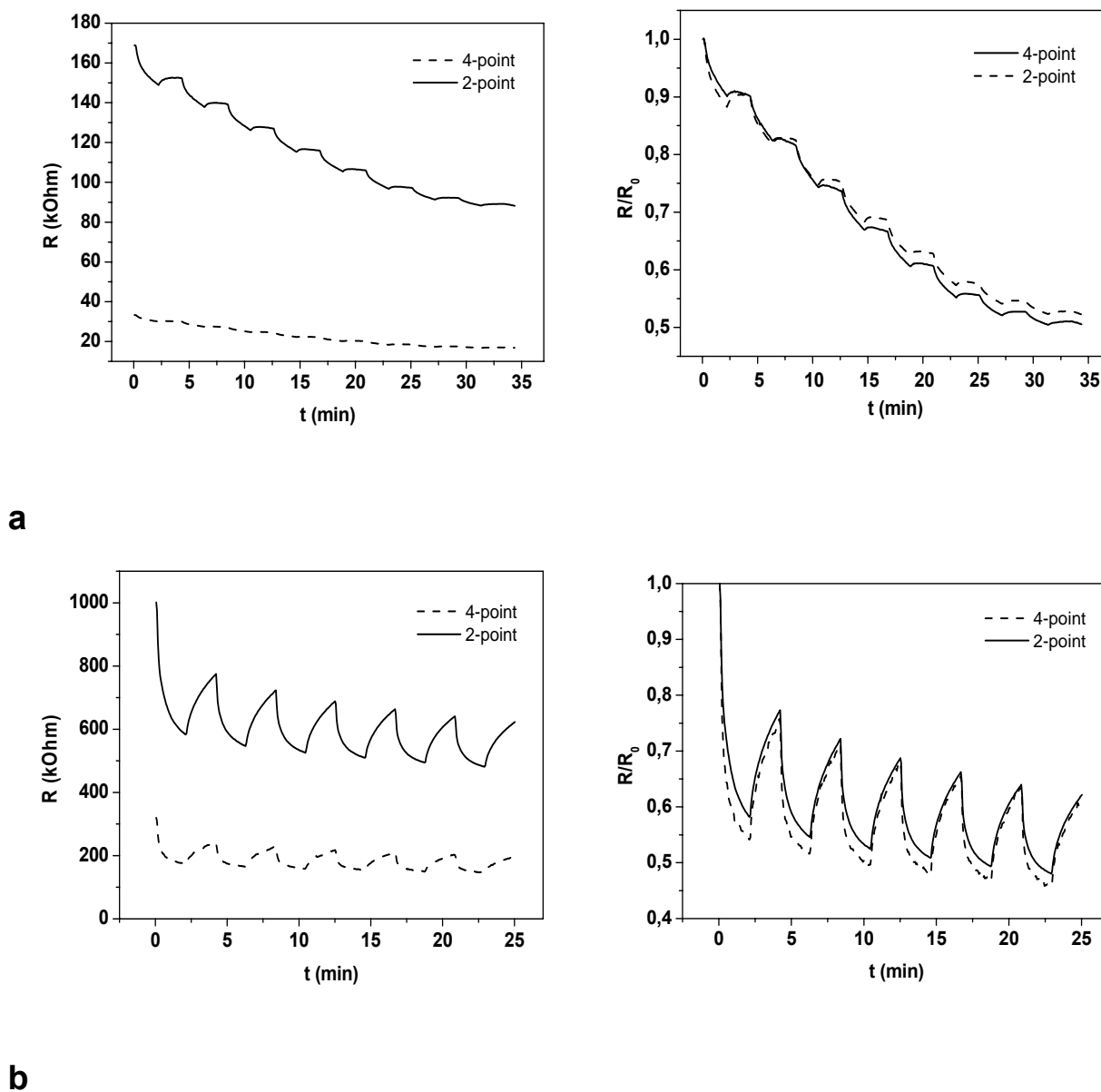
Fig. 3.5-3 Response of PANI films electropolymerized on bare platinum electrodes to subsequent exposures of gaseous hydrogen chloride, measured by simultaneous application of 2- and 4-point techniques. The curves are shown in absolute values (left) of the resistance or the values normalized for the initial values (right). Polymerization from (a): aniline/$HClO_4$ solution; (b): aniline/H_2SO_4 solution

The conclusion, that R_4/R_2 is varied between $1/9 \sim 3/5$, has been confirmed by measurements of gas effects on R_2 and R_4. An exposure to gaseous hydrogen chloride results

in a considerable decrease in the bulk resistance of polyaniline.[242;243] Changes of the resistance, measured by the two- and four-point techniques, are shown in Fig. 3.5-2 and Fig. 3.5-3, left. A normalization of these data for the initial resistance (Fig. 3.5-2 and Fig. 3.5-3, right) demonstrates a proportionality of the resistance changes for both measurements techniques, if platinum electrodes were used (Fig. 3.5-3) or if the gold electrodes were precoated by 4-ATP (Fig.3.5-2 a, b). In these cases, the contact resistance is much less than the bulk resistance and the two-point technique gives information on the bulk resistance. Direct deposition of polymer on bare gold surface leads to an evident deviation from the proportionality between R_2 and R_4 (Fig. 3.5-2, c). In this case the contact resistance is much higher than the bulk polymer resistance, and the two-point technique measures mainly the contact resistance.

Conclusion

It was reported that a sublayer of 4-aminothiophenol improved binding of polyaniline to the gold electrode[226] and decrease polymerization potential of aniline.[244] A similar approach has been used for the improvement of insulating properties of polyphenol.[245] Here, we demonstrated that this approach also minimizes a contact resistance between metal electrodes and electropolymerized polymer. We think that the electropolymerization of aniline on the 4-aminothiophenol coated electrodes leads to the polymer growth starting from the monolayer formed by this thiolated aniline, thus leading to the formation of thiol-terminated chains of PANI. A high affinity of thiols to gold provides strong adhesion of polymers and good electrical contact between electrode and polymer. This approach can be widely used in different devices based on conducting polymers, such as organic electronic devices or conductometric gas sensors. Platinum electrodes possess a high affinity to many organic compounds, and therefore form good electrical contacts with PANI without an additional adhesive sublayer.

3.6 Kinetics of Polymer Response to Hydrogen Chloride

Response curves of PANI on exposure to gaseous HCl are shown in the last sub-chapter. All gas effects were only partially reversible. The conductivity changes result from the protonation or de-protonation of imide form in PANI chains. Emeraldine base (EB) of PANI after treated with alkaline consists of the repeat units of B-N=Q=N-, where B denotes benzenoid and Q stands for quinoid rings. On exposure to HCl gas, the primary PANI chains can be partly doped by HCl molecular thus converting to the salt of emeraldine base (B-NH-

B-NH-), which causes the conductivity of PANI to increase. The conductivity decreases when HCl is replaced by nitrogen flow.

The analysis of kinetics was studied for adsorption and desorption of gaseous HCl to polymer surfaces. A wide concentration range of gas HCl from 5ppm to 200ppm is tested. The attempts to use more exponential functions demonstrated rather poor fitting. Then a bi-exponential function,

$$y = A_1*(1-e^{(-x/t1)}) + A_2*(1-e^{(-x/t2)})$$

Eq3.6-1

was used. The results are shown in Fig. 3.6-1.

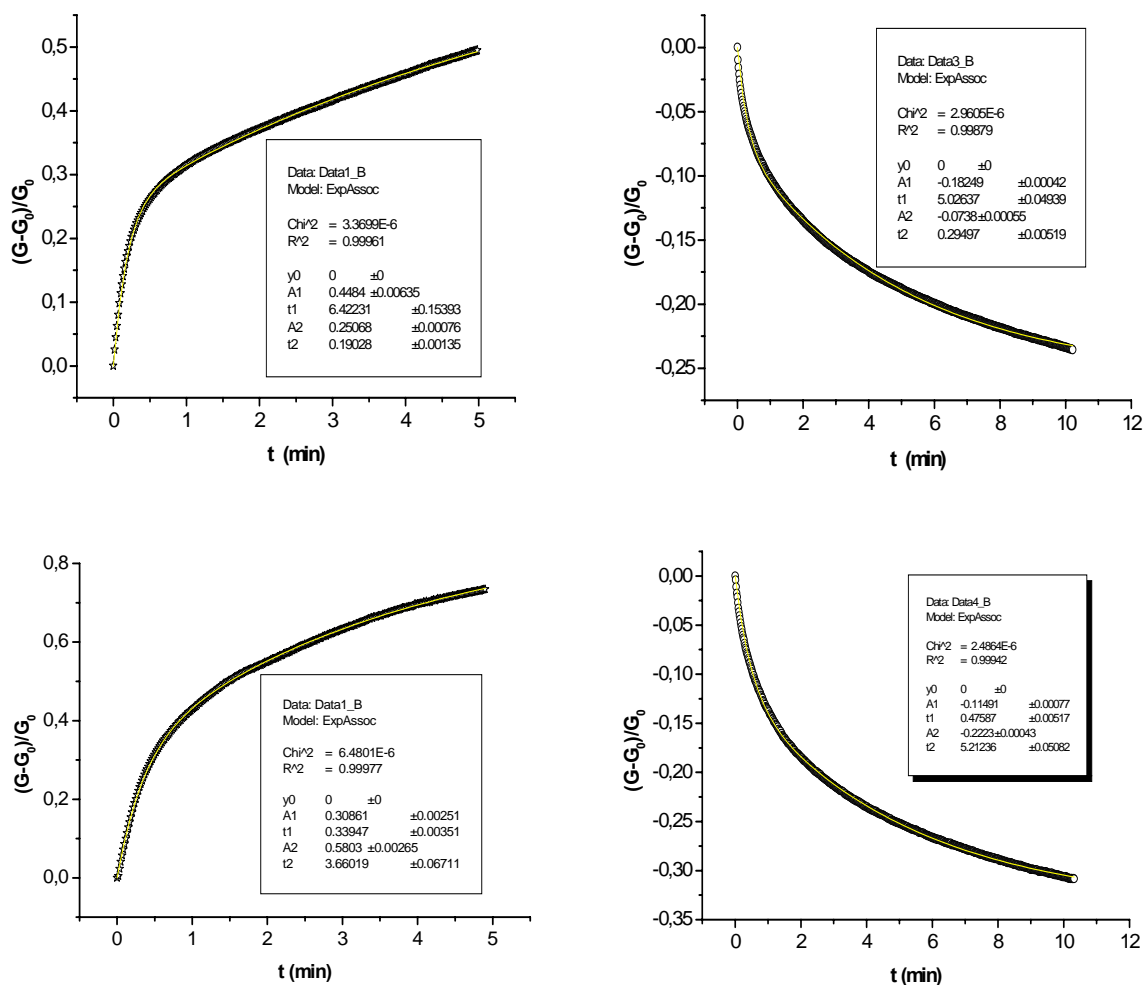**Fig. 3.6-1** Bi-exponential fitting of conductivity kinetics on adsorption (left) and desorption (right) of gaseous HCl onto / from PANI. Gas concentration: 10 ppm (upper) or 5 ppm (lower)

Although the response curves shown in Fig. 3.6-1 were fitted perfectly by bi-exponential kinetics function, no systematic dependence of the fitting parameters on gas concentrations was observed. Therefore, the kinetics probably is not exponential.

3.7 Surface Plasmon Resonance (SPR) Spectroscopy

3.7.1 Characterization

Experiments were performed by using the combined setup described in chapter 2.5.1. The polymerization was carried out at a constant current of 30 µA. The studied polymer layers were deposited from a deoxygenated 1.0 M HCl solution containing 0.1M NMA or 0.1M aniline respectively. After 1000 µl of each solution were transferred to the cell, the SPR measurement was started in the BIOSUPLAR program, and a recording was continued until a stable baseline reached. Afterwards, the electrochemical polymerization at constant current started, and changes of SPR signal with simultaneous electropolymerization were recorded. Film thickness was controlled by the electrolysis time which relates to the calculated charge passing through the electrode. Growth process of polymer films was monitored by SPR measurement; simultaneously chronopotentiometric graphs were recorded. SPR measurements include two modes, one recording SPR angular scan curves during polymer growth (R-θ), the other recording SPR kinetic curves at a fixed angle (R-t) chosen to study film growth.
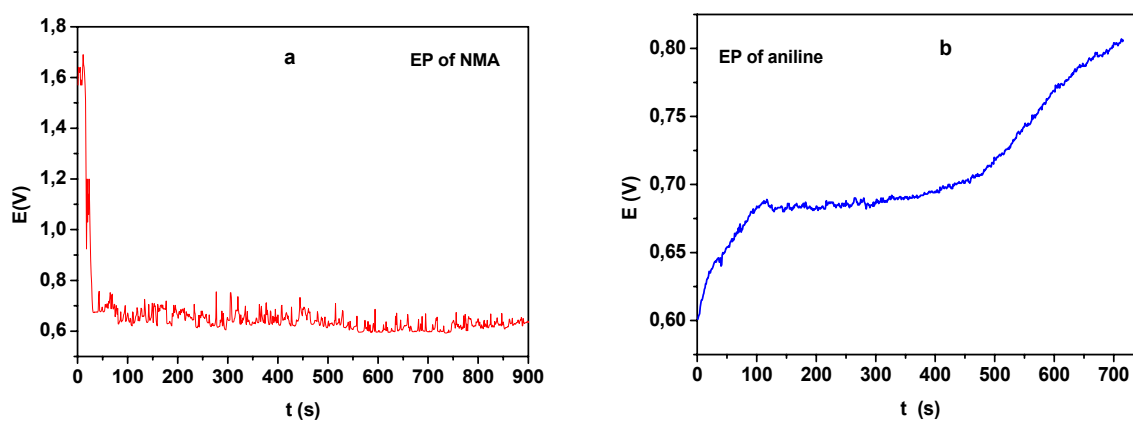

Fig. 3.7.1-1 $t \sim E$ curves for PNMA (a) and PNAI (b) polymerization at 30 µA vs Ag/AgCl electrode on a gold working electrode.

Fig. 3.7.1-1 shows the potential response during polymerization of NMA (a) and aniline (b), respectively. SPR angular scan curves (R-θ) of both polymers are shown in Fig. 3.7.1-2 a, b.

As we can see in Fig. 3.7.1-1, the oxidation potential of NMA (a) decreased from a high initial potential of 1.6 V to the range of 0.7 ~ 0.6 V after 30 s, while the potential in (b) was rising with increasing of time.
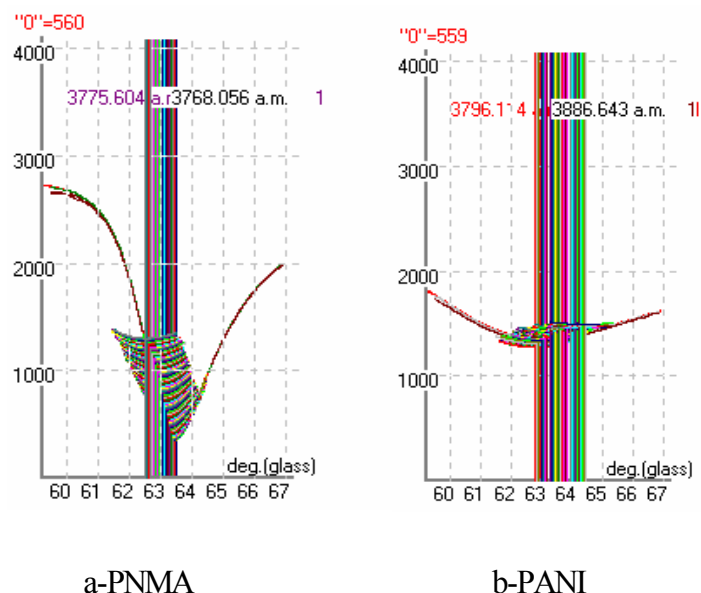

a-PNMA   b-PANI

Fig. 3.7.1-2 Experimental SPR angular scan curves recorded
during the growth of polymer films. a PNMA; b. PANI

In Figure 3.7.1-2, the resonance minimum in (a) shifts gradually toward a lower angle during the growth of PNMA film, while it shifts to a higher angle during the growth of PANI film in (b). Furthermore, distinct changes in the resonance depth and width are also shown in both cases of PNMA and PANI: they are getting wider and lighter. In principle, the shift in the angle of the resonance minimum can be associated with the change in both the refractive index of a film and the film thickness; while the shape change of SPR curves depends mainly on the variation in the imaginary part of dielectric constant of the film.[246]

Fig.3.7.1-3 shows the SPR kinetic curves of both experiments. A linear kinetic curve of PNMA indicates the smooth growth of the PNMA film during electrochemical polymerization at 30 µA. In contrast to the polymerization curve in Figure 3.7.1-1 (a), a sharp potential decrease is observed at the first seconds, and then it becomes constant at around 0.65 V versus Ag/AgCl. The kinetic curve from the polymerization of PANI–Cl shows a higher slope of the SPR-*t* curve during the first 100 seconds, and then the slope of kinetic curve decreases intensively (Fig. 3.7.1-3 b), which is correlated to the potential changes during the electrochemical polymerization of ANI in Fig. 3.7.1-1 (b).
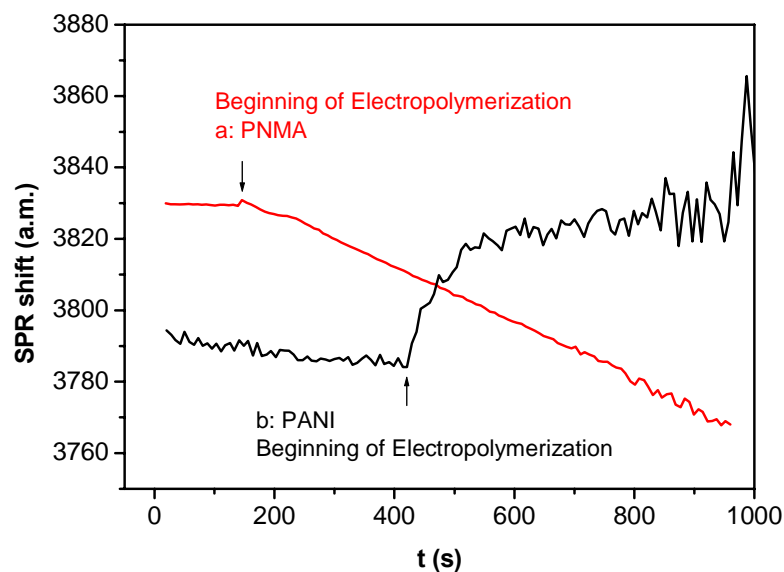
Fig.3.7.1-3 SPR kinetic curves of the electrochemical polymerizations of NMA and aniline, respectively. (a) PNMA; (b) PANI

The change of SPR angles ($\Delta\varphi$) is proportional to the product from (n_{polmer}-n_{water}) and the thickness of the film ($d_{polymer}$), i.e. $\Delta\varphi \sim (n_{polmer}$-$n_{water})* d_{polymer}$. If SPR angle increases, $\Delta\varphi > 0$, that means the refractive index of polymer is bigger than that of water, i.e. ($n_{polmer} > n_{water}$); conversely, if $\Delta\varphi < 0$, $n_{polmer} < n_{water}$ can be induced. Therefore, we conclude that the refractive index of PNMA (n_{PNMA}) is less than n_{water}, while the refractive index of PANI (n_{PANI}) is higher than that of water (n_{water}).

3.7.2. PNMA-Based Gas Sensor with SPR Transduction

The sensors used in fire detection, should provide a fast response to the concentration of evaluated gases. The studied sensor based on PNMA-Cl was exposed to gaseous HCl for 30 s. At this stage of the work, it was the only possibility to get at least partial reversibility of the response. Additionally, thirty – second exposure of HCl may minimize and avoid the swelling process of the polymer. [247] The concentration range of HCl between 2.5 ppm and 160 ppm was studied. Nitrogen flow of 600 ml/min was used for the regeneration of the sensor. The results are shown in Fig. 3.7.2-1 and Fig. 3.7.2-2.
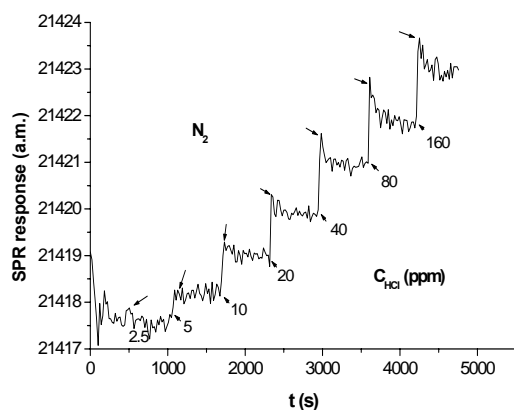
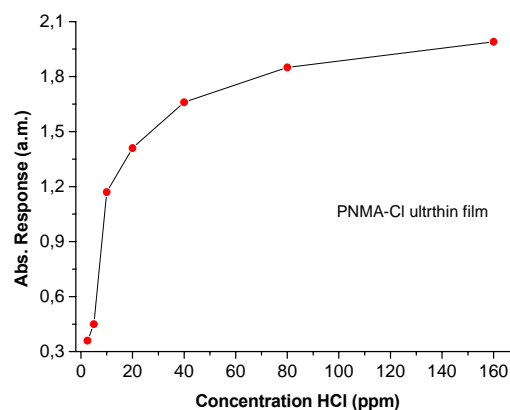**Fig. 3.7.2-1** SPR kinetics of PNMA-Cl on exposure to gaseous HCl

Fig. 3.7.2-2 Absolute SPR response ($\Delta\varphi$) depending on the concentration of gaseous HCl

A detectable increase of SPR angle of PNMA-Cl was observed on exposure of gaseous HCl in Fig. 3.7.2-1, moreover, the increase shift is dependent on the concentration of HCl (Fig. 3.7.2-2). In addition, the SPR spectra fitting by the Fresnel's equation (performed at the Institute of Semiconductor Physics in Kiev) demonstrated that the exposure of PNMA films to HCl led to about 10% decrease of the film thickness and 50% increase of the film refractive index.

Surface plasmon resonance is a simple technique for gas sensing. According to our knowledge, this is the first SPR based HCl sensing. The advantage of PNMA-based HCl sensor with SPR transduction is the nano-scale thickness of sensitive PNMA (20 nm). But the signal of PNMA-based sensor was not high. Further efforts should therefore be focused on the development of new sensitive materials to HCl with high sensitivity. This approach can be extended to detecting other gases.

3.8 Electrochemical Impedance Spectroscopy

The most informative electrochemical technique for characterization of electro-inactive SAMs is Electrochemical Impedance Spectroscopy (EIS)[248]. This technique is also useful for conducting polymer layers on electrodes.

Several conducting films were measured by Electrochemical Impedance Spectroscopy (EIS) at fixed DC potential in the range of 0 V ~ 1.0 V during a frequency scan. All the experiments were carried out in the three-electrode cell. Various types of impedance curves of

Z_r vs -Z_i were obtained under different condition. The usual result is a Nyquist impedance plot of half a semi-circle: the high frequency part gives solution resistance and the width of the semi-circle gives the real impedance of the studied layer, i.e. polarization resistance. More detailed analysis would demand time consumable ultra–low–frequency measurements.

3.8.1 Fitting of Nyquist Diagrams of Impedance
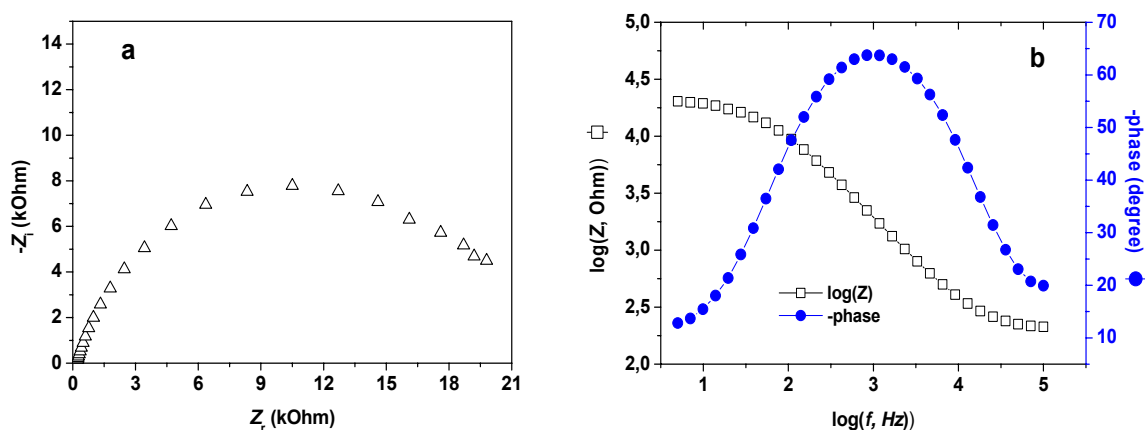
Fig. 3.8.1-1 AC impedance curves for P(ANI-3ABA) film measured in 0.5 M H_2SO_4 at 0.1 V during the frequency scan of $10^5 \sim 5$ Hz.
(a) Nyquist diagram; (b) Bode plot

Fig. 3.8.1-1 shows the impedance curve and bode plot of copolymer P(ANI-3ABA) with a ratio of 1 to 1. It was done at 100 mV over a frequency scan range from 10^5 Hz to 5 Hz. The Nyquist diagram was fitted with the basic Randles circuit as shown in Fig. 3.8.1-2. It consists of a charge transfer resistance, R_{ct}, and parallel to an organic film capacitance C_l, and then assumed to be in series with the uncompensated solution resistance R_s. According to the fitting results, for the experiment shown in Fig. 3.8.1-1, R_{ct} is 16 kOhm; R_s is 230 Ohm, and C_l is 90 nF. The electronic state of P(ANI-3ABA) is conductive.
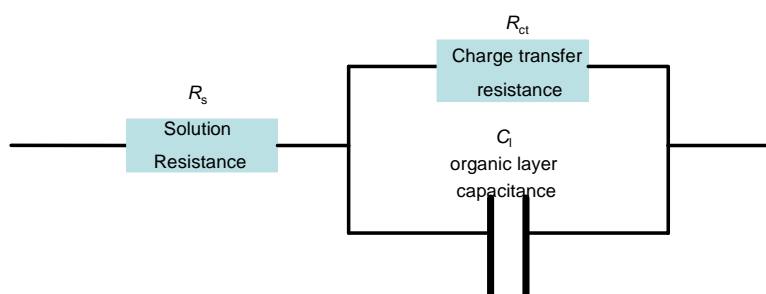
Fig. 3.8.1-2 Simple Randles Equivalent Circuit

3.8.2 Potential Dependence of R_{ct} and C_l

On the basis of Randles circuit, charge transfer resistance R_{ct} and organic layer capacitance C_l were obtained for all studied polymers in the potential range from 0 V to 1.0 V. The polymers, PANI, P(ANI-3ABBA) and P(ANI-3ABA), deposited from relative H_2SO_4 solutions were studied, respectively. The potential dependences of R_{ct} and C_l for these films are shown in Fig. 3.8.2-1 and Fig. 3.8.2-2.

From Fig. 3.8.2-1 (*a*, *b* and *c*), one may observe the difference in electrical state among three polymers. Firstly, sharp difference in the scale of resistance shows that the conductance (G = 1/R) at a same potential for the three polymers obeys the order: P(ANI-3ABA 1:1) > PANI > P(ANI-3ABBA 1:1). Secondly, the conductive state of PANI occurs in the potential range between 0 V and 0.7 V, while the conductive states of P(ANI-3ABA) and P(ANI-3ABBA 1:1) layers appear in the more narrow range of 0 V ~ 0.6 V and 0 V ~ 0.5 V, respectively. On the other hand, the potential dependence of capacitance shows a similar trend for the three polymers.
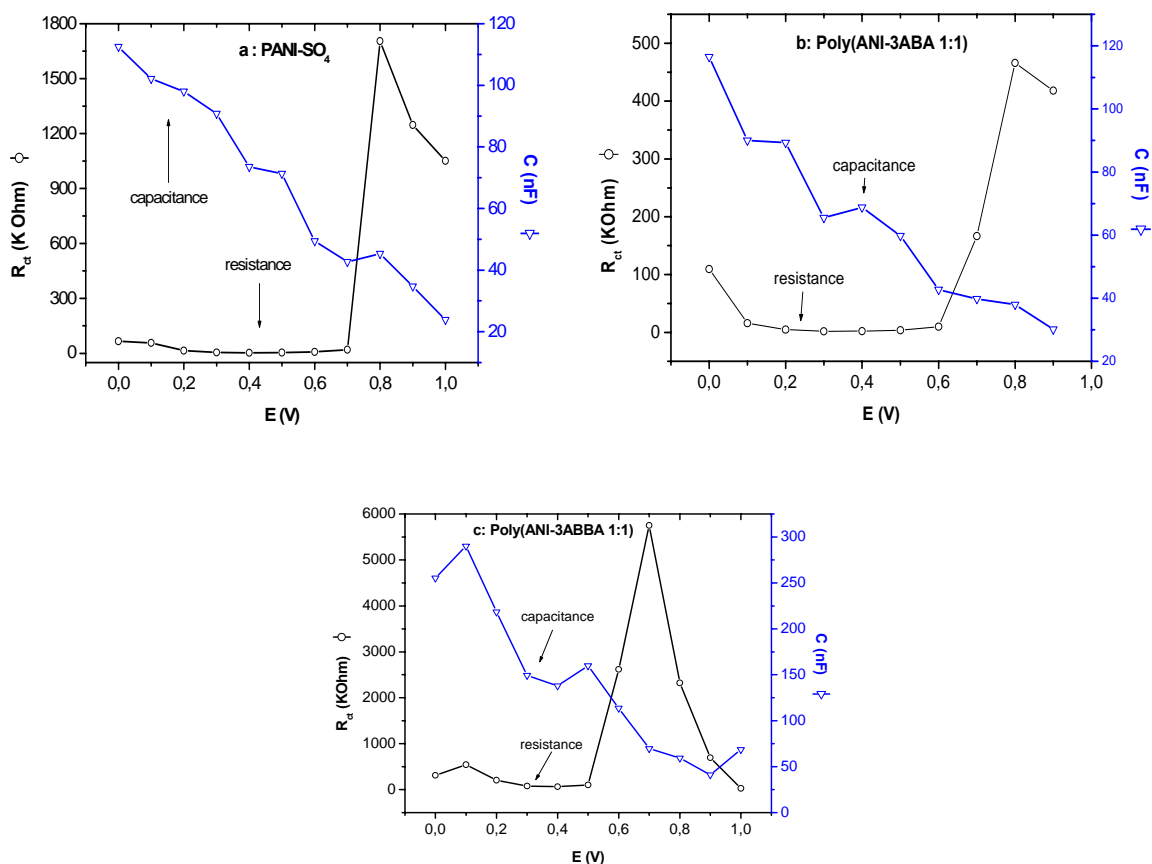
Fig. 3.8.2-1 Potential dependence of R_{ct} and C_l for PANI (a), P(ANI-3ABA) (b) and P(ANI-3ABBA) (c) in 0.5 M H_2SO_4

Fig. 3.8.2-2 *a* and *b* present the change of R_{ct} and *Cl* with the change of potential for P(ANI-3ABBA) layers deposited from the monomer mixture of aniline and 3ABBA (1:1 and 2:1, respectively). From figure *a*, similar potential dependence of R_{ct} was observed for both polymer layers. Both show nonconductive states in the high potential range. But the potential at the highest resistance is different: 0.7 V for P(ANI-3ABBA 1:1) and 0.8V in the case of P(ANI-3ABBA 2:1). Furthermore, the potential conversion to the nonconductive state for P(ANI-3ABBA 1:1) is lower than for the polymer with ration 2:1 (0.6V and 0.7 V correspondingly). Fig. 3.8.2-2 (*b*) demonstrates a decreasing trend of polymer layer capacitance change accompanying the increase of measurement potential for both polymers.
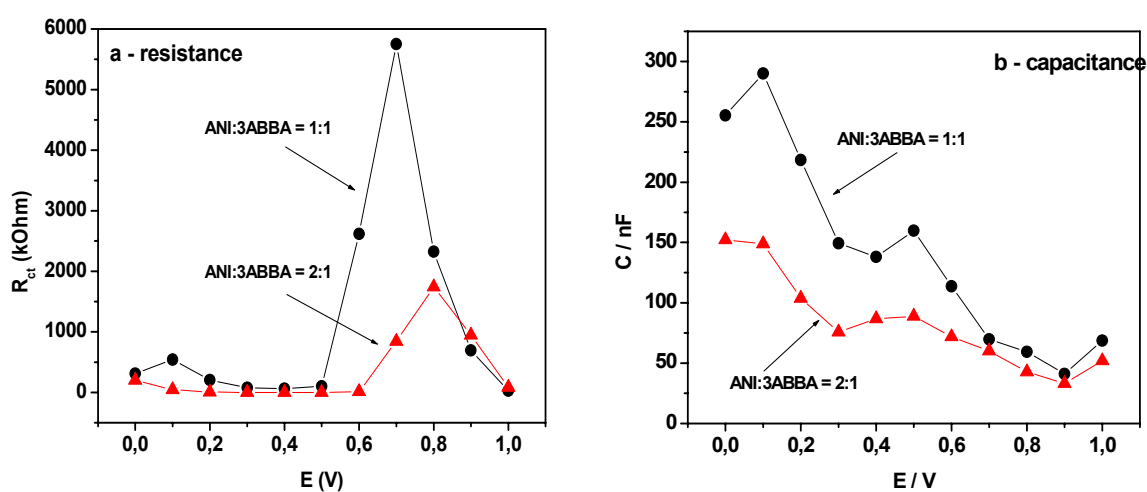
Fig. 3.8.2-2 Potential dependence of R_{ct} (a) and C_l (b) for copolymer P(ANI-3ABBA) in 0.5 M H_2SO_4

By using Electrochemical Impedance Spectroscopy, the range of potentials corresponding to the conductive states of PANI and its copolymers have been evaluted in this work. This state of the polymers is of importance for the applications in HCl sensors.

3.9 Influence of pH and Electrode Potential on Conductivity of OCPs

Pure PANI and its copolymer P(ANI-3ABBA) films (about 1 μm thick) deposited on four-interdigitated platinum electrodes were prepared for investigating the changes of conductivity in a series of universal buffers with different pH value. Buffer A and B contain 5mM of the respective buffer substance, and 100 mM or 1M KCl (The preparation is described in Chapter 2.1).

For studying potential dependence of polymer conductance, a potential source (Type: S-11, Berlin) was used to provide a direct potential in the range of 0V ~ 0.9 V vs SCE. The anode of this potential source was connected to the "low source" of work electrodes, and its cathode was linked to a SCE reference electrode.

Resistance measurement was recorded automatically by using simultaneous 2- and 4-piont methods. To make it comparable, the value was taken after the electrodes coated with studied polymer films were immersed in buffer solution for 30min. Buffers were changed every 30 min, and the electrode was rinsed with a large amount of MILLIPORE water, then dried in high purity N_2 flow before it was dipped into the buffer. For investigating the potential influence, the resistance value was recorded for 2 min after the working electrodes were equilibrated in the buffer at fixed potential for 30 min. Buffers were changed from the lower to the higher pH value.

3.9.1 Influence of pH
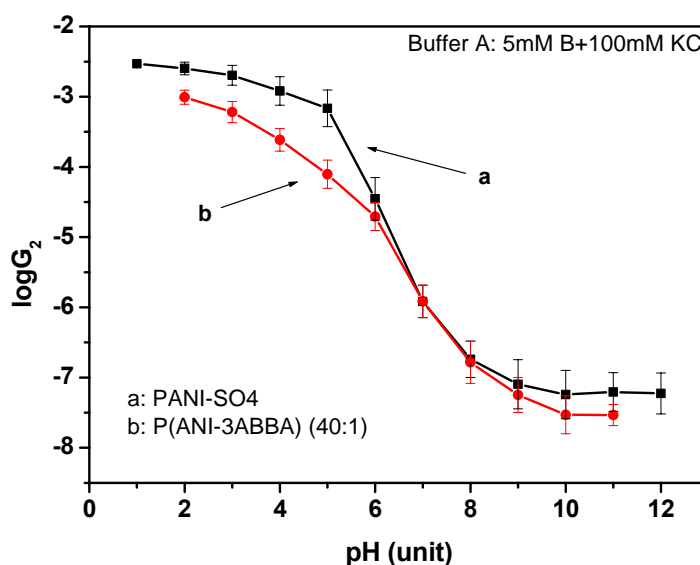
Fig. 3.9.1-1 Conductance of PANI and P(ANI-3ABBA) (40:1) at various pH

Fig. 3.9.1-1 presents the changes in conductance of PANI sulfate (a) and its copolymer of P(ANI-3ABBA) (ANI:3ABBA, 40:1) (b) with the variation of pH. In both cases, the polymer conductance decreases with increasing the pH value. This results from increasing percentage of PANI base with decreasing of the concentration of [H^+]. Generally, curve *a* (PANI) shows two slight platforms in the lower and higher pH range; curve b decreases smoothly from pH 1 to 10. The conductance drop in curve *a* is much slower than that in *b*

from pH 1 to 5. The sharp drop in conductance for PANI appears in the range of pH 5 ~7 from 10^{-3} to 10^{-6} S; while the curve slope of P(ANI-3ABBA) in this range is generally lower than that of PANI. In addition, curve *a* is located above of *b*, indicating that the conductance of copolymer P(ANI-3ABBA) is lower than PANI conductance.

It was reported that the substitution of aniline led to reduced conductivity compared to PANI,[78;249-253] and reduced the influence of pH.[254] So the observed result implies that the incorporation a low conductive component −3ABBA into PANI chains causes its conductivity to decrease. The copolymer with a higher ratio of aniline to 3-ABBA possesses higher conductivity than that with a lower ratio.

Additionally, the influence of ionic strength of buffer on the polymer conductance has been studied. Buffer A and B were used. The results are presented in Fig. 3.9.1-2.
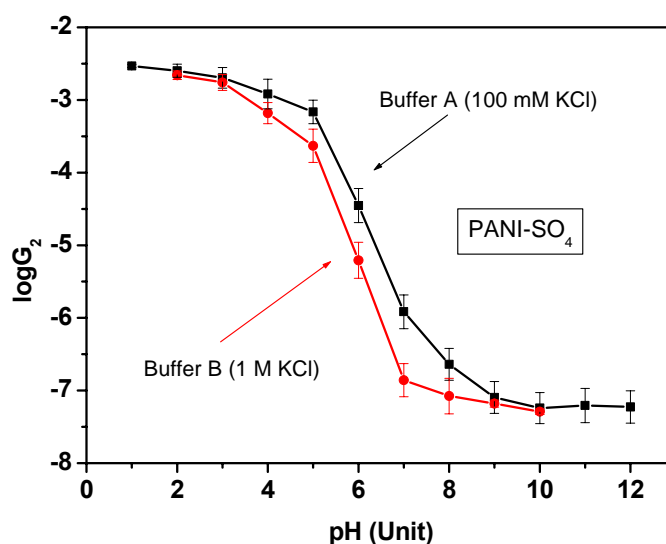
Fig. 3.9.1-2 Influence of Ionic strength of buffer on PANI conductance

It was shown that the conductance of polymers under the condition of higher ionic strength is lower than that in the buffer of lower ionic strength. Surprisingly, an increase of the ionic strength shifted the curve to the left. Taking into account that the surface pH ($pH_{surface}$) and bulk pH (pH_{bulk}) are correlated by this equation:

$$pH_{surface} = pH_{bulk} + \Delta\psi \ / \ (2.3RT/zF) \hspace{3cm} Eq3.9-1$$

where $\Delta\psi$ is the surface potential. Taking into account that an increase of the ionic strength leads to the screening of the surface potential, the only possibility to explain the shift of the curve (Fig. 3.9.1-2) to the left at higher ionic strength is the conclusion that the surface

is negatively charged. This rather paradoxical fact can be explained by adsorption of multi-valent buffer anions in the solution (phosphate, hydrogen phosphate, borate, and citrate).

3.9.2 Model for pH dependence of PANI conductance

The model is built on the basis of the acid / base doping causing PANI conductive/insulating for explanation pH dependence of PANI conductance. PANI is suggested as a combination of n parallelly connected chains with many units (n) which can be switched either to conductive states (g_w^{on}) or to low conductive states (g_w^{off}). Each chain can be in one of the two states. The maximum of PANI conductance (n* g_w^{on}) is the conductance got at the lowest pH value used in the experiment (usually 1); and the minimum value (n* g_w^{off}) is what we measured at highest pH (usually 12). g_w^{on} and g_w^{off} are constants.

Let's consider poly(emeraldine salt) (PES) of PANI as one acid HA, and poly (emeraldine base) PEB as the base of HA (A$^-$). At different pH, physical state of PANI film can be expressed at a sum of states (*on +off*), and conductance of PANI is relative to the doping level of PANI, i.e. the concentration of HA, on the other side, nonconductive state is response to the concentration of dedoped PANI (A$^-$). Therefore, such physical conversion of PANI at different pH can be explained by the following chemical equilibrium:

Conducting state $\longleftrightarrow$ Non-conducting state $\qquad\qquad$ Eq 3.9-2

$$[HA] \xleftrightarrow{ka} [A^-] + H^+ \qquad\qquad \text{Eq 3.9-3}$$

where k_a ('a' refers to PANI) represents the equilibrium constant of dissociation of doped PANI (HA) to dedoped PANI (A$^-$) and hydrogen ions. According to the equilibrium between acid and base, Eq 3.9-3 can be expressed as:

$$[H^+] = k_a * \frac{[HA]}{[A-]} \qquad\qquad \text{Eq 3.9-4}$$

$$pH = pK_a - \log \frac{[HA]}{[A-]} \qquad\qquad \text{Eq 3.9-5}$$

Conductance of PANI in buffer can be expressed as:

$$G = [HA] * (g_w^{on}) + [A] * (g_w^{off}) \qquad\qquad \text{Eq 3.9-6}$$

In the system of PANI in buffer,

$[HA] + [A^-] = n$ $\qquad$ Eq 3.9-7

where n represents the numbers of switch segments, and it is a constant. Therefore, Eq 3.9-6 can be rearranged to,

$G = [HA]* (g_w{}^{on}) + (n-[HA])* (g_w{}^{off})$ $\qquad$ Eq 3.9-8

$G = [HA] (g_w{}^{on}) + n(g_w{}^{off}) - [HA](g_w{}^{off})$ $\qquad$ Eq 3.9-9

We have derived:

$$[HA] = \frac{g - ng(\text{off})}{g(\text{on}) - g(\text{off})}$$ $\qquad$ Eq 3.9-10

$$[A] = n - [HA] = \frac{ng(on) - ng(off) - g + ng(off)}{g(on) - g(off)}$$ $\qquad$ Eq 3.9-11

$$[A] = \frac{ng(on) - g}{g(on) - g(off)}$$ $\qquad$ Eq 3.9-12

So Eq 3.9-5 is rearranged to:

$$pH = pk_a + \log\{ \frac{ng(on) - g}{g(on) - g(off)} / \frac{g - ng(\text{off})}{g(\text{on}) - g(\text{off})} \}$$ $\qquad$ Eq 3.9-13

$$pH = pk_a + \log(\frac{ng(on) - g}{g - ng(off)})$$ $\qquad$ Eq 3.9-14

$$\log(\frac{ng(on) - g}{g - ng(off)}) = pH - pk_a$$ $\qquad$ Eq 3.9-15

$$\frac{ng(on) - g}{g - ng(off)} = 10^{(pH - pka)}$$ $\qquad$ Eq 3.9-16

and then,

$g (10^{(pH - pka)} + 1) = n(g_w{}^{on}) + n(g_w{}^{off})* (10^{(pH - pka)})$ $\qquad$ Eq 3.9-17

$g = \{n(g_w{}^{on}) + n(g_w{}^{off})* (10^{(pH - pka)})\}/(10^{(pH - pka)} + 1)$ $\qquad$ Eq 3.9-18

where $n(g_w{}^{on}) = g_{max}$ (at pH 1) and $n(g_w{}^{off}) = g_{min}$ (at pH 12) are constants.

The pH ~ log$G$ curves obtained in this part were fitted with this equation Eq 3.9-18 and the results are shown in Fig. 3.9.2-1 (a, b).
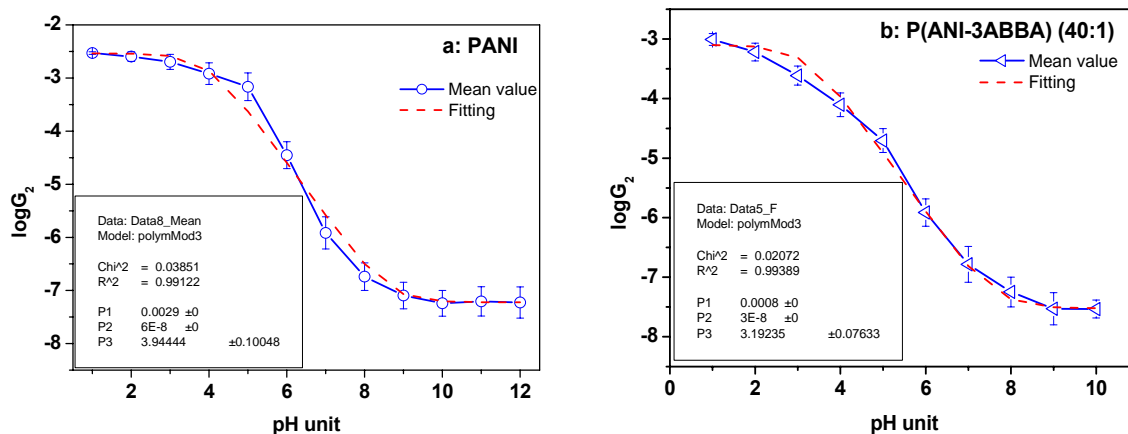
Fig. 3.9.2-1 Fitting (dash) of OCP model for conductance changes
of PANI and P(ANI-3ABBA) at various pH.
a: PANI; b: P(ANI-3ABBA)

From the fitting curves in Fig. 3.9.2-1 (*a and b*), we can conclude that the OCP model generally fits to our results. A slight difference between fitting and experimental curves was observed in both cases of PANI and its copolymer; this implies that some unknown parameters influence the effect. One of possible reasons for this deviation is that the surface electrostatics was ignored at this model.

3.9.3 Influence of Electrode Potential

Fig. 3.9.3-1 presents the influence of the electrode potential on conductance changes of PANI in buffer at different pH. The pH value was varied between 2 and 6 in this experiment. The conductivity of PANI at higher pH than 6 is already too low to be measured by our device in the potential range of 0 V ~ 0.9 V. From this plot, following conclusions can be drawn:

First of all, conductance of PANI at every pH in Fig. 3.9.3-1 is much lower than that obtained at the same pH without potential drop (OCP) in Fig. 3.9.1-1 (a). The conductance of polymer film almost reaches the scale of 10^{-6} Sm at pH 4. This indicates that the polymer film is not electro - active at pH values higher than 5. In case of pH = 3, the highest conductance of PANI film was observed only 10^{-4} Sm at 0.2 V. This explains why electrochemical polymerization of aniline in aqueous solution can be carried out at pH value less than 3.[31] Secondly, at a given potential, the conductance decreased dramatically with an increase of pH, especially at 500 mV, the conductance dropped sharply from 10^{-3} to 10^{-7} Sm when pH was

changed from 2 to 3. Thirdly, the given potential causing highest conductance for each pH shifts successively from 0.3 V to 0.2 V, 0.1 V and 0 V with the pH increasing from 2 to 6. In addition, PANI film at pH 2 possesses a relatively wide potential range of conductive state, from 0.1 V to 0.6 V, which agrees with the results of cyclic voltammetry in Chapter 3.2.1. PANI is in the state of conductive emeraldine salt.[51;255]
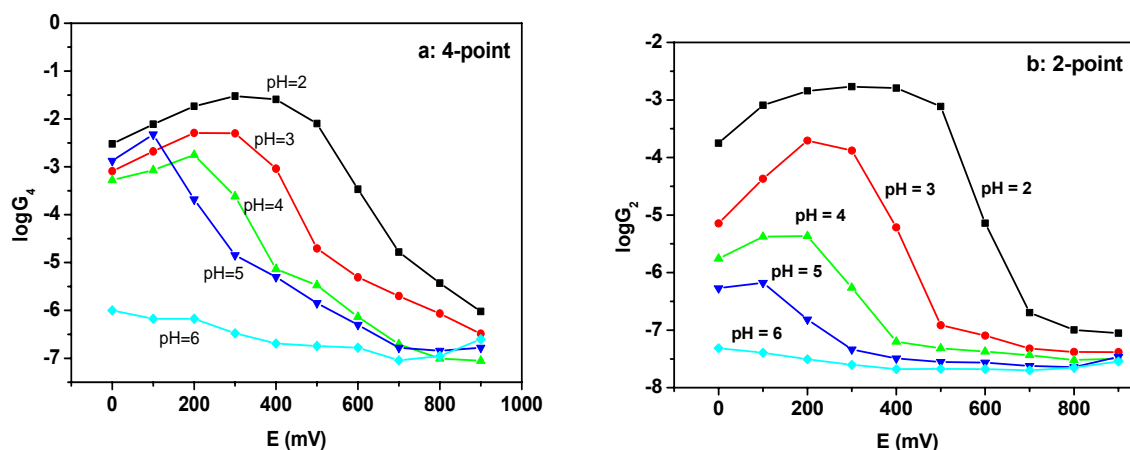
Fig. 3.9.3-1 Potential dependence of PANI conductance in buffers with various pH

In summary, the electrical state of PANI is influenced greatly by pH and applied potential. This is associated with the properties of PANI which can be controlled by acidic doping (reversibly protonated/deprotonated doping)[18;55;256;257] and electrochemical oxidative doping (intrinsic redox states)[28;46].

3.10 Investigation of Temperature Effects on PANI-HCl Binding

Although there are lots of studies about thermal properties of PANI,[258-262] only a few of them are based on PANI films doped with gases.[146;147;263] No studies on gaseous HCl sensors based on conducting polymers in thermal properties have been found. So it is of significance to study the thermal properties of the PANI - gaseous HCl micro-system in this field. The useful methods are thermogravimetric analysis (TGA) and differential scanning calorimetry (DSC). Both adsorption and desorption of gaseous HCl to PANI films were studied in a certain temperature range by using the setups described in Chapter 2.4.7.

PANI sulfate films were deposited on interdigitated platinum electrodes with the thickness about 1μm. Before used for the thermal study, the electrodes with polymer films

were treated with alkaline for 15 min, dried, rinsed with large amount of MILLPORE water, and heated at 150°C for ten minutes.

3.10.1 Thermal Analysis (TG, DSC) of PANI-HCl Binding

To study thermal desorption of PANI doped with HCl gas, four kinds of probes were post-treated as following. Probe 1 was placed in air for 12 hours to adsorb moisture in air after heated at 150 ºC for 15 min; Probe 2 was put in a vacuum container immediately after heating (without moisture); Probe 3 was put in the closed container containing dry gaseous HCl (200 ppm diluted with N_2) for 12 h (saturated with dry HCl gas without moisture); Probe 4 was treated as Probe 3, and then left in the open air for 12 h (saturated with dry HCl and moisture).

Thermal stability of the polymers was measured using TGA 7 (Perkin Elmer) at a heating rate of 1 ºC / min in nitrogen atmosphere, from 25 ºC up to 210 ºC or 800 ºC. DSC measurements were performed in DSC 7 (Perkin Elmer), between 25 ºC and 400 ºC, with the heating rate of 1 ºC/min, under nitrogen. Additionally, two measuring cycles were done for Probe 3 by using of DSC. It was performed as follows: for the1st cycle, starting from 25°C up to 250°C with a heating rate of 1°C/min, then cooling down until 25°C in the N_2 flow; repeating the same cycle. A platinum cell was used for the high temperature test on TGA. The others were carried out in open aluminum cells. The results from DSC and TGA are shown in Fig. 3.10.1-1(a, b) and Fig. 3.10.1-2, respectively.

The DSC information of PANI-HCl (g) (Probe 3) is shown in Fig. 3.10.1-1 (*a, b*). There are three endothermic peaks in the range of 25°C ~ 800°C (the sharp peak at 225 °C was caused by device). A wide peak at 100°C is probably the loss of analyte HCl since there is no moisture in Probe 3. The second peak appears at about 160°C. The peak at 380°C ~ 450°C in (*a*) results from the decomposition of PANI after loss of dopant (HCl), according to literature on PANI salts doped with other dopants.[92;264] The decomposition of PANI base occurs in the similar range near 400°C.[90;265] Fig. 3.10.1-1 (b) presents that two endothermic peaks are irreversible. The small peak at 160°C probably resulted from the loss of carbonate dopant which remained in the polymer after buffer treatment.

The loss of HCl dopant from polymer chain starts from lower temperature compared to the range of 200 ~ 300°C observed for other dopant in PANI. The loss of dodecyl benzene sulfonic acid (DBSA) in PANI is around 280°C reported by Chen Cheng-Ho;[92] the loss of p-toluene sulfonic acid from PANI was reported at 200-300°C by Gazotti W. A. *et al* [266] and the

release of HCl dopant at 320°C by Li X.W. *et al* [264]. This indicates the binding energy between HCl molecule and PANI body bone is weaker than sulfuric acids.
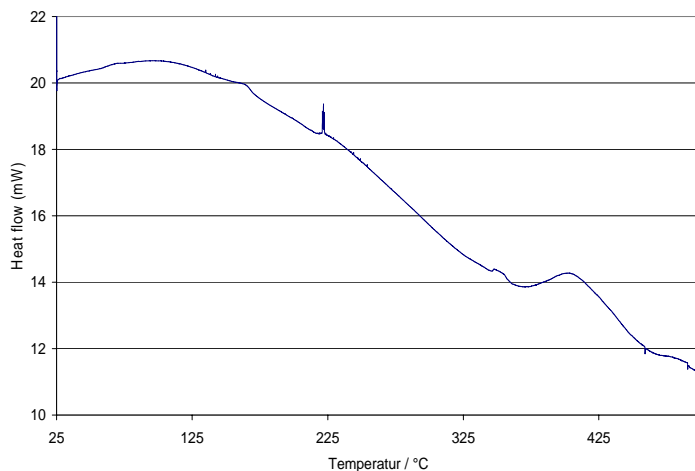
a
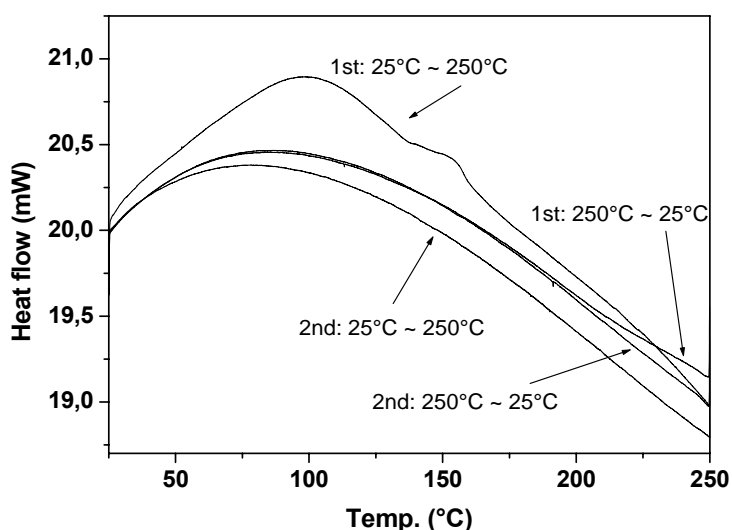
b

Fig. 3.10.1-1 DSC curves of PANI doped with gaseous HCl

a. 25°C ~ 450°C; b. 25°C ~ 250°C (two cycles)

To prove the loss of HCl at relatively low temperature, TGA experiments were performed in the range of 25 ~ 210 °C for the Probe 1, 3 and 4. The results are presented in Fig. 3.10.1-2. The weight loss of 3.67%, 17.32% and 19.1% were observed for Probe 1 (loss of moisture), Probe 3 (loss of dry HCl) and Probe 4 (the loss of HCl and moisture), respectively. The theoretical value for the loss of HCl dopant from PANI in the salt state is 16.8%. This is close to the experimental value 17.3%. The experimental value is slightly higher than the calculated one. It could be due to physical adsorption of free HCl molecules and carbonate residue. Additionally, the difference between the curves of Probe 3 and Probe 4,

corresponding to the moisture contribution into the probe weight, is comparable with the curve of Probe 1. Therefore, HCl dopant (probably together with other residue) in PANI films can be removed completely at 200°C, or even at 150°C according to the results from DSC.
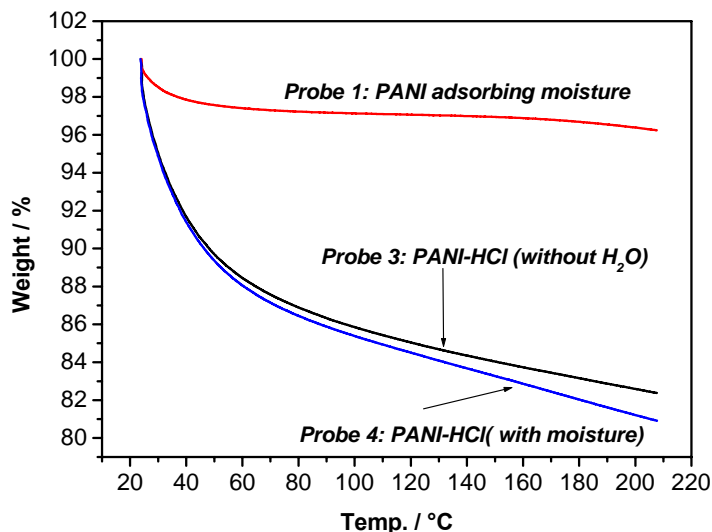
Fig. 3.10.1-2 TGA of PANI probes before (Probe 1) and after (Probe 3 and 4) adsorption of gaseous HCl.

Infrared Spectroscopy (IR) and Elemental Analysis (EA)

The FT-IR spectra of PANI base and Probe 4 after heating up to 250°C were acquired, and compared each other. The results are shown in Fig. 3.10.1-3. The adsorption peaks related to the quinoid ring (~ 1580, 1380, 1301 cm^{-1}) and benzenoid ring (1500 cm^{-1}) were observed in both cases. According to literature[85], the peak at 1163 cm^{-1} belongs to the mode of N=Q=N, and 1500 cm^{-1} corresponds to benzenoid ring. In Fig. 3.10.1-3 (a), the relative height between the peaks at 1163 cm^{-1} and 1500 cm^{-1} is reduced for PANI heated at 250°C compared with the curve of PANI base. The peak at 1500 cm^{-1} became stronger than other peaks in the same IR curve. This means the chemical structure of PANI base was changed slightly after heating to 250°C, and part of the backbone (quinoid group) is cross-linked.[85] MacDiarmid et al. reported that the cross-linking reaction occurred when EB powder was heated up to 300°C.
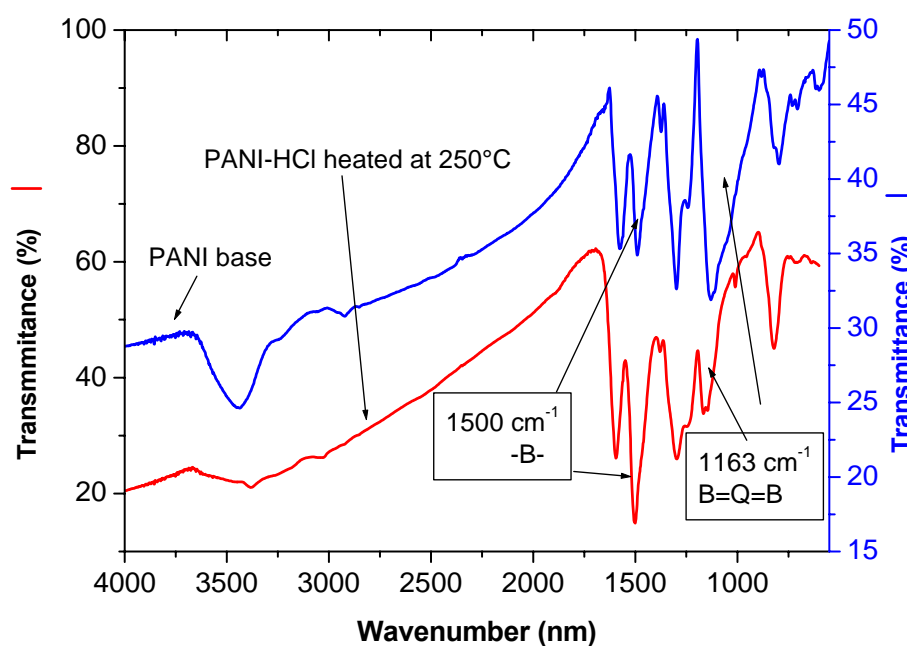
Fig. 3.10.1-3 Comparison of infrared spectra between PANI base
and PANI- gaseous HCl heated at 250°C

The result from EA indicated that a little amount of sulfate remained in the sample after the buffer treatment. The analytical (and calculated) values of C, H, N, S elements for EB ($C_{24}H_{18}N_4$) are: C, 66.59 (79.56) %; H, 4.91 (4.97) %; N, 12.73 (15.47) %; S, 2.46 (0.0) %, respectively. For the probe of PANI-gaseous HCl heated at 150°C, the analytical (and calculated for EB) values are: C, 65.98 (79.56) %; H, 4.67 (4.97) %; N, 12.85 (15.47) %; S, 2.68 (0.0) %. This means lightly doped PANI (ES state) remains in PANI base after buffer treatment. According to literature[267], slightly protonated PANI base has higher response than complete PANI base. Therefore, buffer treatment probably could be helpful for gaseous HCl sensor.

3.10.2 Temperature Effects on PANI-HCl Binding

3.10.2.1   Adsorption of Gaseous HCl

Setup 2 described in the chapter 2.4.7 was used to investigate the influence of temperature on the change of conductance of PANI films on exposure to 80 ppm HCl. The PANI-coated electrode inserted into a holder was put into a glass gas cell which was closed with the rear of the holder. The gas cell with a steel tube for transporting gases was preheated for 5min at each temperature before gas flow was started. Resistance changes were measured

and recorded. The response of PANI on exposure to gaseous HCl for 3 min was acquired in the range of 30 ~ 120 °C. Afterwards, N_2 flow with high flow rate of 1000 ml/min was employed for cooling down the system and for removing the rest HCl gas remaining in the tubes. The sensor was treated with alkaline after adsorbing HCl gases to remove HCl dopants for the next experiment, and heated at 100 °C for removing moisture. The normalized results at 30 ~ 80°C are shown in Fig. 3.10.2.1-1.
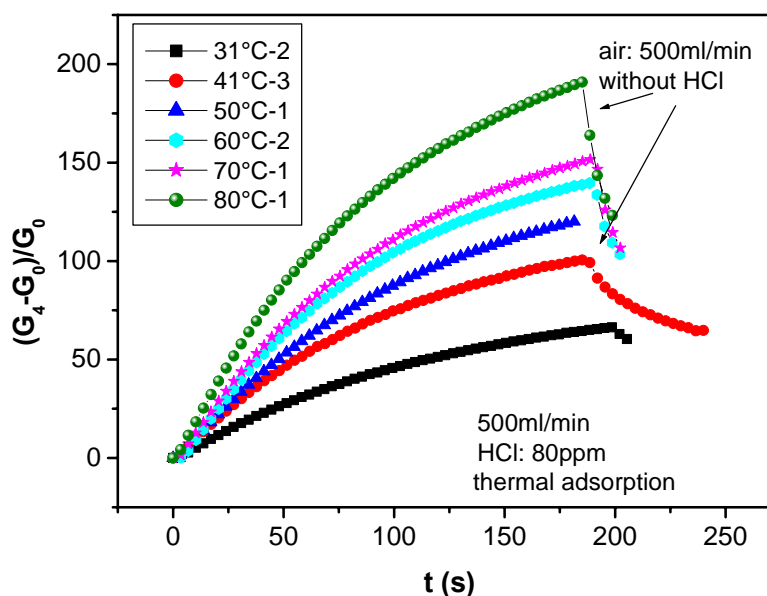
Fig. 3.10.2.1-1 Response of PANI film on exposure to gaseous HCl
at different temperatures (Gas Flow rate: 500 ml/min)

Fig.3.10.2.1-1 presents relative changes in conductance of PANI at various temperatures. From 30 °C to 80 °C, the conductance changes of PANI (i.e. the sensitivity of tested sensor to 80 ppm gaseous HCl) are obviously increasing with the temperature. In the temperature range of 90 °C ~ 120 °C, however, the sensitivity was observed to be decreasing with increasing temperature (not shown here). This results from the influence of temperature on the equilibrium between adsorption and desorption in the gaseous–solid phase. As described before, adsorption of gaseous HCl to PANI may include both chemical and physical adsorption. At lower temperatures, the chemical adsorption prevailed in the equilibrium, and PANI base was doped by HCl, leading to an increase of conductivity. However, for temperatures higher than 90°C, the desorption of gaseous HCl was getting stronger, therefore the sensitivity decreases relatively.

3.10.2.2   Desorption of Gaseous HCl

The similar studies have been done for studying the influence of temperature on the conductance of PANI after doping with gaseous HCl. The temperature range of 60 °C~180 °C was investigated. PANI films were pretreated in 80 ppm HCl for 3 min before heating. We heated the sensor at defined temperature for the certain time, and then measured its resistance after cooling down in the air. The time step of heating was 5 min for the experiments in the temperature range of 60 ~ 120°C, 2min for those at 150°C and 180°C. The normalized results are shown in Fig. 3.10.2.2-1.
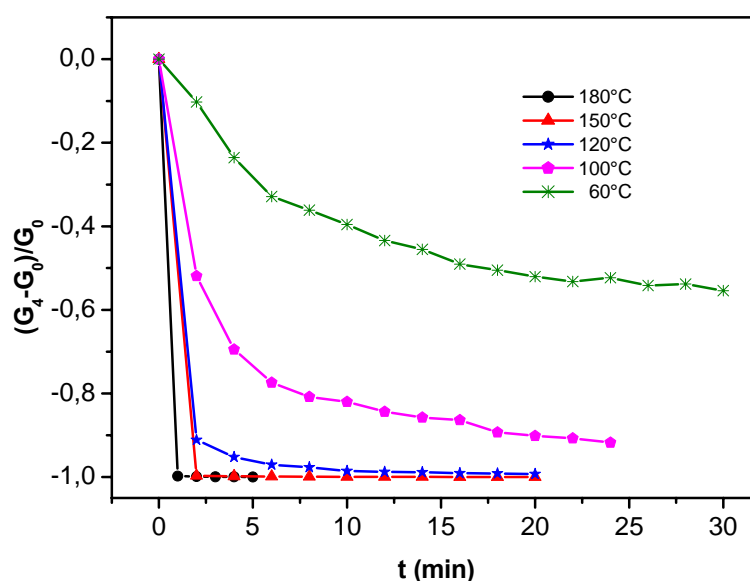
Fig.3.10.2.2-1 Kinetic scheme of normalized conductance of PANI-based sensor (at room temp.) for thermal desorption of gaseous HCl in the range of 60°C ~ 180°C. (G_0 is the conductance of polymer before thermal desorption)

The kinetic curves at different temperatures in the range of 60 ~ 180°C are presented in Fig. 3.10.2.2-1. All curves at various temperatures are decreasing with the increase of the heating time. Moreover, the drop of conductance decreases faster and faster with increasing of the heating temperature. It increased from 10% at 60°C to about 100% at 150°C during the fist two minutes. The drop of conductivity results from the decrease of dopant content of PANI due to the loss of HCl dopants from PANI-HCl. At the temperature higher than 150 °C, the dopant of HCl was almost completely removed. This coincides very well with the results from thermal analysis in chapter 3.10.1.

3.10.3 Calculation of Activation Energies and Binding Energy for Adsorption and Desorption Processes

According to the results from Fig. 3.10.2.1-1 and Fig. 3.10.2.2-1, the activation energy (E_{act}) of PANI with gaseous HCl was calculated for both adsorption and desorption processes. This analysis has been done for the data obtained in both adsorption and desorption process at different temperatures. To exclude a contribution of the reverse reactions, we investigated kinetics at the initial stages for the reversible reactions as following.

$$\text{PANI} + \text{HCl (g)} \quad \underset{\text{Desorption}}{\overset{\text{Adsorption}}{\rightleftharpoons}} \quad \text{PANI-HCl}$$
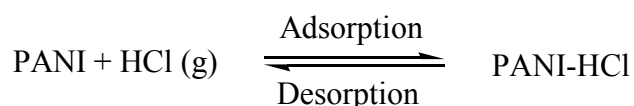
The reaction rate can be expressed as:

$$d[\text{PANI-HCl}] / dt = k_{ads}*[\text{PANI}]*[\text{HCl}] - k_{des}*[\text{PANI-HCl}] \qquad \text{Eq 3.10.3-1}$$

where k_{ads} and k_{des} are the rate constants for the adsorption and desorption processes. Let us assume the conductance (G) of polymer is proportional to the amount of PANI-HCl at the initial stages of adsorption or desorption processes, i.e. $G \approx \alpha*$ [PANI-HCl], where α is a constant. Thus, in each initial adsorption process ($t = 0$, [PANI-HCl] = 0), the reaction system only involves the same amount of PANI film ([PANI]) and the same gaseous HCl with constant pressure ([HCl]). So the reaction systems in initial processes remain under the same conditions at different temperatures. Therefore, only the initial part in each curve (about 30s) was taken into account in the adsorption process for calculating activation energy. Similarly, in the initial stage of desorption (t = 0, and [PANI] = 0), the initial state of reaction system is constant for each temperature studied.

Since the change of polymer conductance is proportional to the change amount of coordinate PANI-HCl, the initial slopes of conductance changes in Fig. 3.10.2.1-1 and Fig. 3.10.2.2-1 at each temperatures have been calculated. These slopes are considered to be proportional to the reaction rate (v) of adsorption or desorption of HCl, i. e. proportional to the rate constant of reaction, k_{ads} and k_{des}.

The Arrhenius plots ($\ln k \sim 1/T$) in both cases are shown in Fig. 3.10.3-1 and Fig. 3.10.3-2, together with their linear fitting.
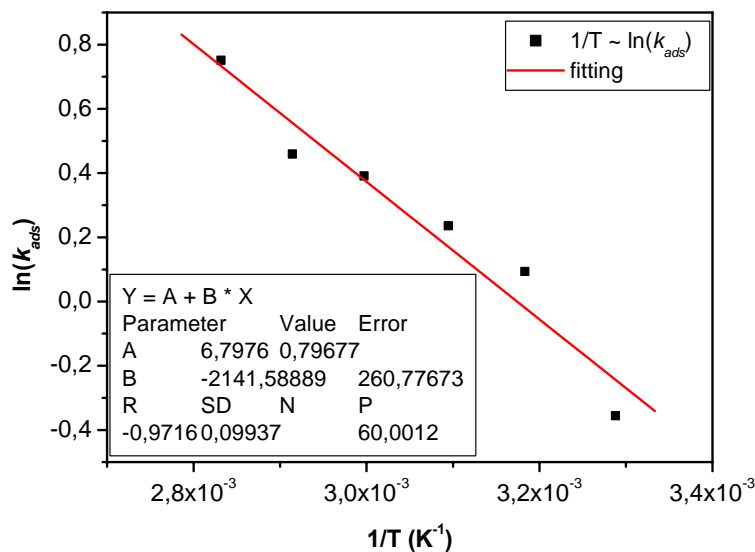
Fig. 3.10.3-1 Temperature dependence of the adsorption rate (its initial slope during the first 30 seconds.) in Arrhenius coordinates. Solid line is the fitting of $1/T \sim \ln k$, here k is the rate constant of adsorption at different temperatures.
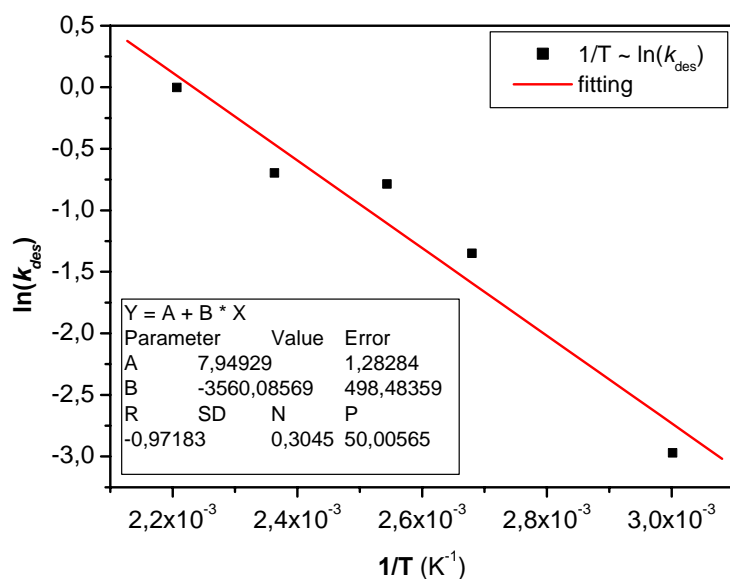
Fig. 3.10.3-2 Temperature dependence of the desorption rate (its initial slope during the first 2 min.) in Arrhenius coordinates. Solid is the fitting of $1/T \sim \ln k$, here k is the rate constant of desorption at different temperatures.

According to the empirical Arrhenius Rate Law, $\ln k = - E_{act} / (RT) + B$, where E_{act} is the activation energy of the reaction and $R = 8.314$ J / (mol*K), the slopes $(-E_{act} / R)$ of both fitting curves in Fig. 3.10.3-1 and Fig. 3.10.3-2 are response to the activation energy of

processes, $E_{act}{}^{ads}$, and $E_{act}{}^{des}$. Therefore, the activation energies for both adsorption and desorption processes can be calculated as:

$E_{act}{}^{ads} \approx 18$ kJ/mol ≈ 0.20 eV, i.e. ($3.0e^{-20}$ J/molecule)

$E_{act}{}^{des} \approx 30$ kJ/mol≈ 0.31 eV, i.e. ($4.9e^{-20}$ J/molecule)

$\Delta E = 12$ kJ/mol

The estimated value of activation energy for adsorption and adsorption heat is slightly lower than those obtained for ammonia adsorption on PANI film (Hu et al [120]).
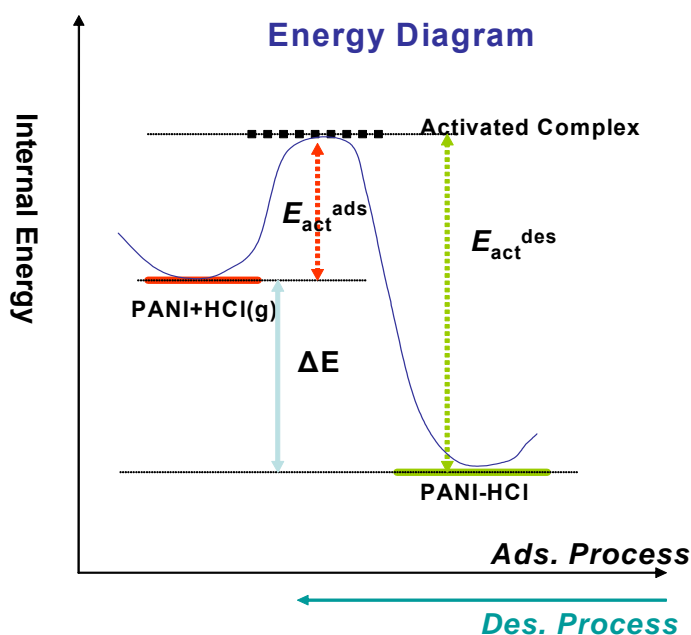
Scheme 3.10.3-1 Reaction energy diagram in both adsorption and desorption processes

The energy diagram is described in Scheme 3.10.3-1. The binding energy (12 kJ/mol) of PANI-HCl is very weak, which is much less than covalent N-H bond energy (390.8 kJ/mol). It is in the range of hydrogen bond energy (usually from 4 kcal/mol to 20 kcal/mol). However, there is no environment for the formation of real hydrogen bonds. As known from MacDiarmid A.G.,[268] PEB can be doped with aqueous protonic acids to poly(emaraldine salt) state. But, here, the interface is only gas and solid. So we assume that the weak binding is classified as coordinate covalent bond. Therefore, we may draw a conclusion that the formation of coordinate covalent bonds between gaseous HCl and nitrogen atom in PANI chain cause the increase in the conductance of PANI. The reaction steps are assumed as following.
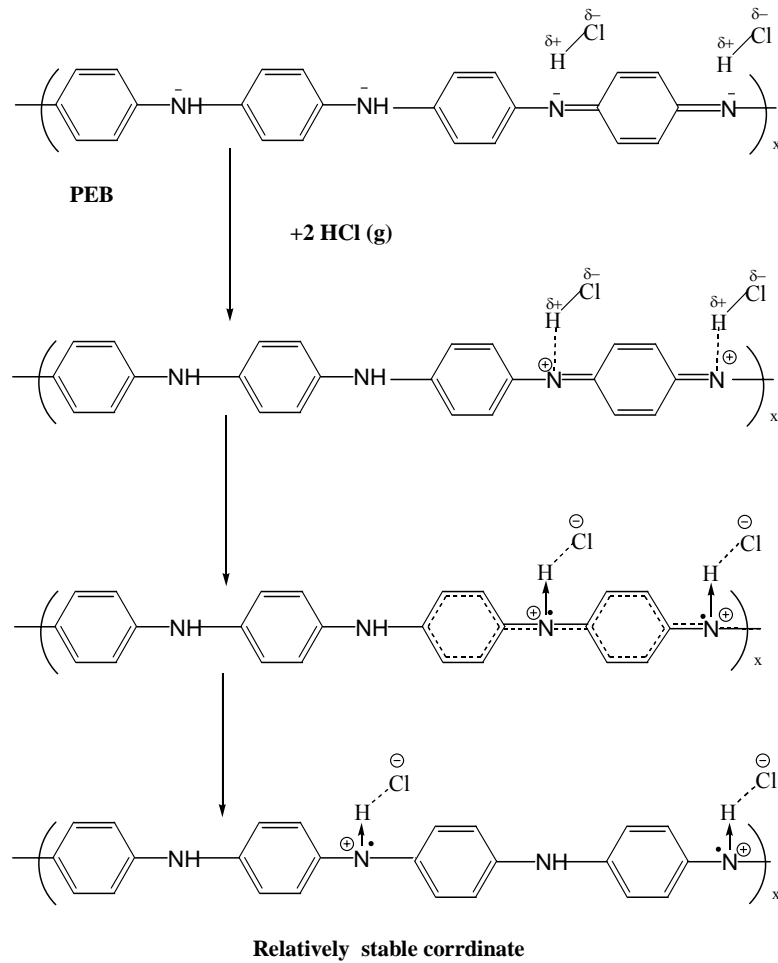
Scheme 3.10.3-2 Reaction between PANI base and HCl gas

The calculated E_{act}^{des} can be used to estimate the required desorption time to remove HCl dopant from PANI films at different temperatures. Desorption rate can be expressed according to the Arrhenius reaction rate equation by:

$$v = v_0 * \exp(-E_{act}^{des} / RT) \qquad \text{Eq. 3.10.3-2}$$

Therefore, the desorption time,

$$\tau = \tau_0 * \exp(E_{act}^{des} / RT) \qquad \text{Eq. 3.10.3-3}$$

is induced, where E_{act}^{des} is 30 kJ/mol, and τ is the desorption time. According to the results of desorption experiments, $\tau = 120s$ for 150°C (about 90% HCl in PANI-HCl was desorbed), τ_0 is estimated to be 22ms. Therefore, when the desorption reaches about 90%, the function for the required desorption time is

$$\tau = 0.22 * \exp(3608 / T) \qquad \text{Eq. 3.10.3-4}$$

The required desorption time for other temperatures was calculated from this function:

At 100°C, $\tau \approx 350$ s

180°C, $\tau \approx 63$ s

120°C, $\tau \approx 112$ s

In summary, the thermal properties of PANI – gaseous HCl system have been acquired by studying adsorption and desorption of HCl at different temperature. The loss of HCl covers a wide temperature range from 50°C ~ 200°C. This result is helpful for the improvement of reversibility of gas sensors. The activation energy for adsorption and desorption processes was calculated. The formation of coordinated covalent bond between HCl and nitrogen in PANI backbone has been first proposed by calculating activation energy for both processes.

3.11 Development of HCl Gas Sensors

3.11.1 Optimal Materials with Good Sensitivity to Gaseous HCl - *Sensitivity*

Sensitivity is the most important factor for sensors.[269] For the development of HCl gas sensors (or a fire alarm sensor) based on OCPs, all conducting polymers synthesized in our work were tested the response to gaseous HCl for 3min. The concentration range of HCl in the first experiments was varied from 20 ppm to 80ppm. Then it was shifted to the lower concentrations. All polymer films used here were deposited electrochemically on gold or platinum interdigitated electrodes. The thickness for all polymer films on electrodes we used for single experiments is about 1 μm, controlled with the polymerization charge. The polymer films were treated with alkaline (pH = 9.0) overnight; afterward they were rinsed with MILLIPORE water and dried in N_2. Gas testing was carried out in a home-made gas system (described in Chapter 2.4.8), and gas flow was controlled by software. Resistance measurement was done by two and four-point simultaneous methods. Since all studied polymers have similar volume (diffusion polymers out of electrode windows were ignored and probably irrealizable), conductance or resistance of polymers can be used instead of conductivity. The normalized change of conductance $(G-G_0)/G_0$ was calculated for all data obtained in this part, Here, G_0 and G are the conductance of polymer films before and after exposure to gaseous HCl. The results in the case of 20 ppm HCl are listed in Table 3.11.1-1.

Table 3.11.1-1 Response of conducting polymers on exposure to 20 ppm HCl

Polymer	$(G_4-G_0)/G_0$	Polymer	$(G_4-G_0)/G_0$
PANI-SO$_4$	160	P(ANI-NMA 1:1)-SO$_4$	2.5
PANI-ClO$_4$	7	P(ANI-NMA 1:2)-SO$_4$	0.6
PANI-DSA	0	P(EDOT-3ABBA 1:1)-SO$_4$	0
PANI-LiClO$_4$	0	P(ANI-3ABSA 3:2)-SO$_4$	2.0
PNMA-SO$_4$	~0	P(ANI-3ABSA 2:1)-SO$_4$	2.0
PNMA-ClO$_4$	~0	P(ANI-3ABSA 1:1)-SO$_4$	1.0
PNMA-SO$_4$(80ppm HCl)	0.2	P(ANI-3ABBA 40:1)-SO$_4$	6.0
PNMA-ClO$_4$ (80ppm HCl)	1.5	P(ANI-3ABBA 30:1)-SO$_4$	2.5
PPy	0	P(ANI-4ABA 7:3)-SO$_4$	70
DPA-SO$_4$	0.02	P(ANI-4ABA 1:1)-SO$_4$	7.0
DPA-SO$_4$ (without Buffer)	-0.02	P(ANI-3ABA 2:1)-SO$_4$	30
AA-SO$_4$	28	P(ANI-3ABA 1:1)-SO$_4$	23
3ABA-SO$_4$	~1	P(ANI-AA 1:1)-SO$_4$	65
1st layer: (PANI-ClO$_4$) 2nd layer: PEDOT	0.1	P(ANI-PY 1:1)-SO$_4$	~0
P(ANI-EDOT 1:1)	~0	P(ANI-Py 40:1)-SO$_4$	0
1st layer: (PANI-SO$_4$) 2nd layer: P(4-E-phenol)	0.5	P(ANI-Py 100:1)-SO$_4$	0

From Table 3.11.1-1, the highest sensitivity among those studied polymers (including individual, co-polymerized and multilayer polymers) belongs to PANI-SO$_4$, followed its copolymers with its derivatives, P(ANI-AA), P(ANI-4ABA), P(ANI-3ABA) and P(ANI-3ABSA). The conductance of PANI deposited from H$_2$SO$_4$ was increased almost 100 times,

after the film was exposed to gaseous HCl at 20ppm for 3min, and the polymer became conductive. This results from the formation of ES state of PANI protonated with gaseous HCl. The response of PANI-ClO_4 is much lower than that of PANI-SO_4. This is presumably due to the influence of film morphology. The morphology of PANI film formed from $HClO_4$ acid is solid and uniform, while PANI-SO4 films are more porous. As we discussed before, the morphology of PANI is not changed after buffer treatment. The porous structure is advantageous for the permeation of gas. So the conductance of porous PANI films increases very fast.

The sensitivity of PANI formed from H_2SO_4 is 2~3 orders of magnification higher than other single polymers due to the porous morphology; its derivatives and the copolymers from both are also sensitive to HCl to some degree, some of them with promising results. Therefore, PANI and its derivatives could be selected as sensitive materials and candidates for developing HCl gas sensors.

3.11.2 Response of PANI to Other Gases (HCl, NH_3, H_2O, CO_2) - *Selectivity*

An ideal sensor should be selective to its analyte even in mixtures and complex matrices. Therefore, to test the response of PANI to other gases is of significance. Gaseous HCl, NH_3, CO_2, humidity and their mixture with various concentrations have been tested on PANI films deposited from H_2SO_4 electrolyte. The generation of sensors was performed by using N_2 or synthetic air flow – the popular method. PANI films in emeraldine salt state were used for testing ammonia; Base state of PANI was used in the other cases. The response of PANI films on exposure to various gaseous under different conditions are shown in Fig. 3.11.2-1 ~5.

In the case of Fig. 3.11.2-1 (*a, b*), several cycles of adsorption and desorption process of 20 ppm HCl were done on PANI base sample. A great resistance drop in *a* was observed for the first cycle of gaseous HCl adsorption. It caused the conductance increasing as high as 150 times of original value during 2 min (shown in *b*). This is due to protonation of emeraldine base in the presence of gas HCl. After 3-minute desorption process by nitrogen flow of 250 ml/min, the PANI resistance reached to 10 kOhm, reduced by 2 orders of magnitude compared to the original value (1 MOhm) (shown in *a*); the following adsorption of gaseous HCl to the PANI film caused the conductance increasing again, but the increase of conductance was 3 orders of magnitude lower than the first circle (shown in *b*). The similar

phenomena were observed in the subsequent cycles. The electrical state of PANI film could not be regenerated completely after 3-min desorption in the nitrogen flow. The start resistance for the each adsorption circles in the figure 3.11.2-1(*a*) appears to be decreasing. As shown in *b*, the increase of PANI conductance is getting smaller with increasing of adsorption circles. Long time (24 h) test has also been performed for the regeneration of such probes of PANI films after adsorption of gaseous HCl, but it did not return to the original state of conductance. This phenomenon is associated with the non-complete dopant removing.
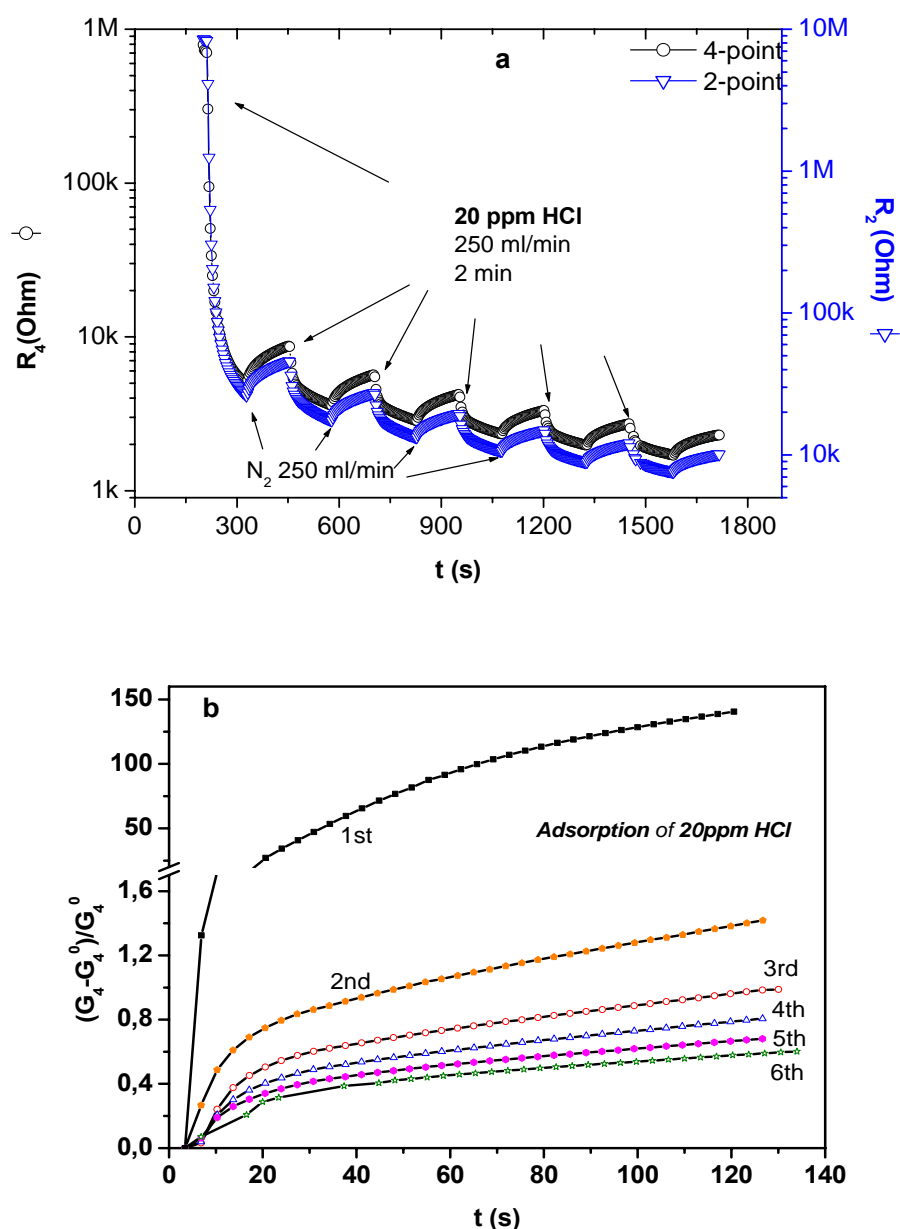
Fig. 3.11.2-1 Response of PANI on exposure to 20 ppm HCl gas

for 2 min with 3-min regeneration by N_2.

a, t~R; *b*, t ~ $(G_4-G_4^0)/ G_4^0$

In addition, the concentration dependence of relative change in conductance of PANI has been also investigated. The minimum concentration of HCl detected by PANI probe is less than 5 ppm. More sensitive experiments were complicated by poor reversibility.
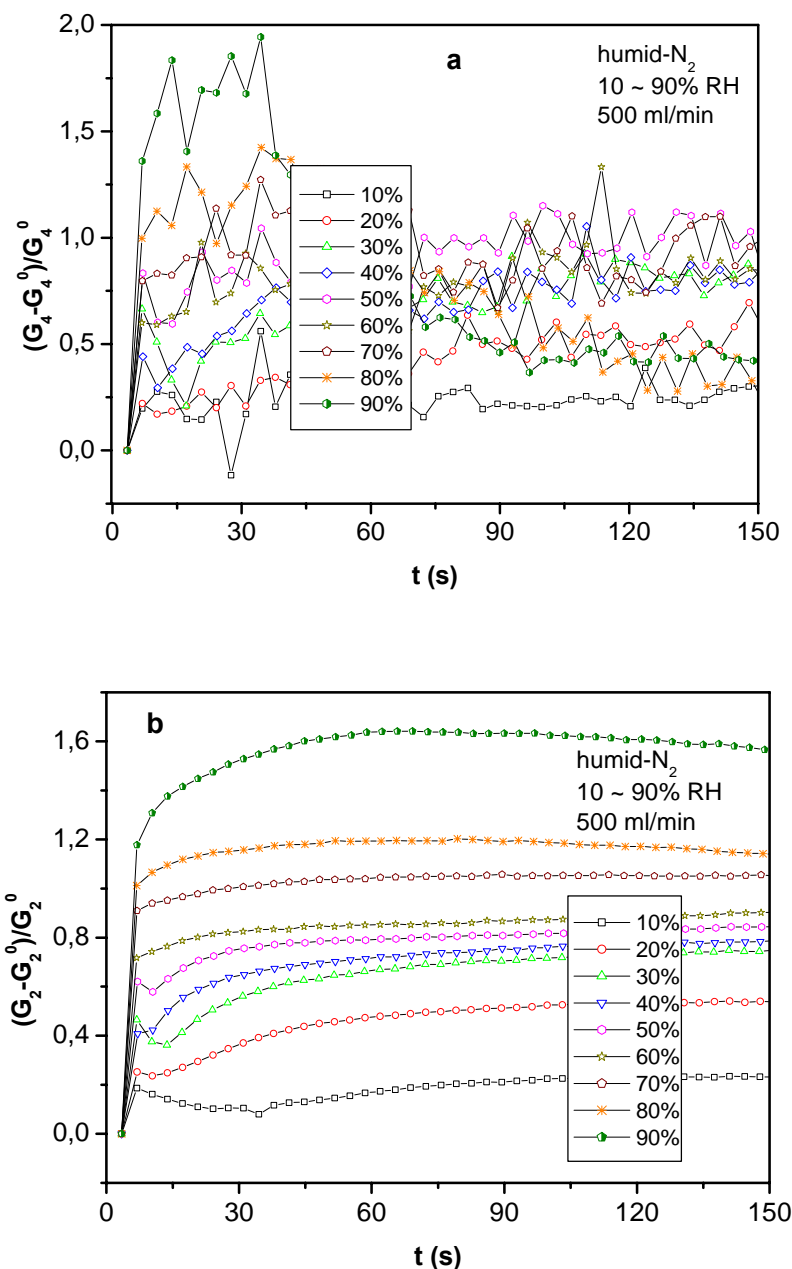
Fig. 3.11.2-2 Response of PANI to humid N_2 over the relative humidity range of 10%~ 90%

Fig. 3.11.2-2 (*a, b*) presents the response of PANI base prepared from H_2SO_4 electrode to humid N_2. The relative humidity (RH) was varied from 10 % ~ 90 %. The N_2 flow of 500 ml/min was used for the regeneration of sensors. The increase in conductance of PANI on exposure to humid N_2 from both four and two point methods are shown in *a* and *b*

respectively. However, the change in conductance from 4-point is not systematically dependent on the RH value, while that in Fig. 3.11.2-2 (b) increases with increasing RH. This indicates that the presence of water improves the contact in the interface greatly. This is in agreement with the other study.[34] From the normalized result obtained by 4-point technique (shown in *a*), a slight increase in polymer conductance, compared with the influence of dry HCl (Fig. 3.11.2-1), was observed for all cases of RH from 10% to 90%. The increased conductance of PANI is probably due to the formation of hydrogen bonds[270] between oxygen atom of water molecules and the hydrogen atoms in the PANI chains; on the other hand, it could also be explained as the similar mechanism to PANI-gaseous HCl system since water molecular can also be considered as Lewis acid. The similar semi-reversible process was observed in this experiment in case of desorption in the gas flow.
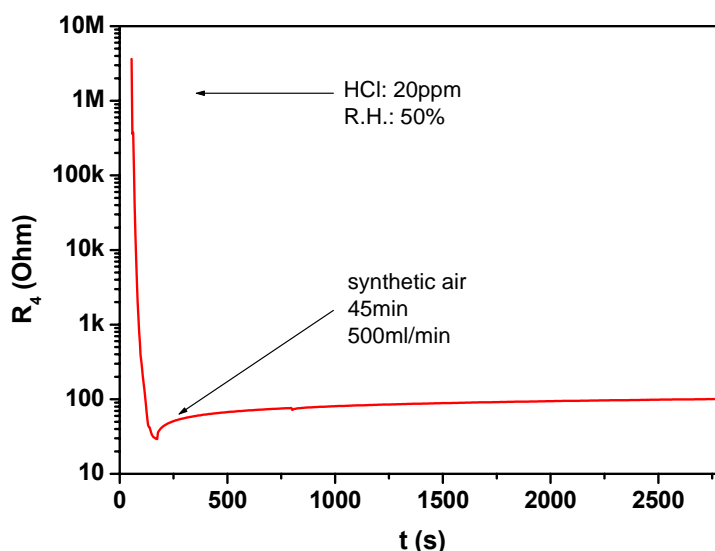
Fig. 3.11.2-3 Response of PANI to 20 ppm HCl with 50% relative humidity

Fig. 3.11.2-3 shows the change in resistance of PANI on exposure to 20 ppm HCl in the presence of moisture with 50 % RH. Three orders of magnitude change in the conductance of PANI base were enhanced quickly in the presence of an atmosphere containing HCl and moisture, but such sensor also cannot be regenerated by using N_2 at all. As shown in this plot, the resistance is still in the scale of hundred Ohm after 45 min N_2 flow. Gaseous HCl molecules can hydrolyse to H^+ and Cl^- ions in the presence of moisture. Dramatics increase in conductance is due to the faster and higher degree protonation of PANI from H^+ than from molecular HCl.
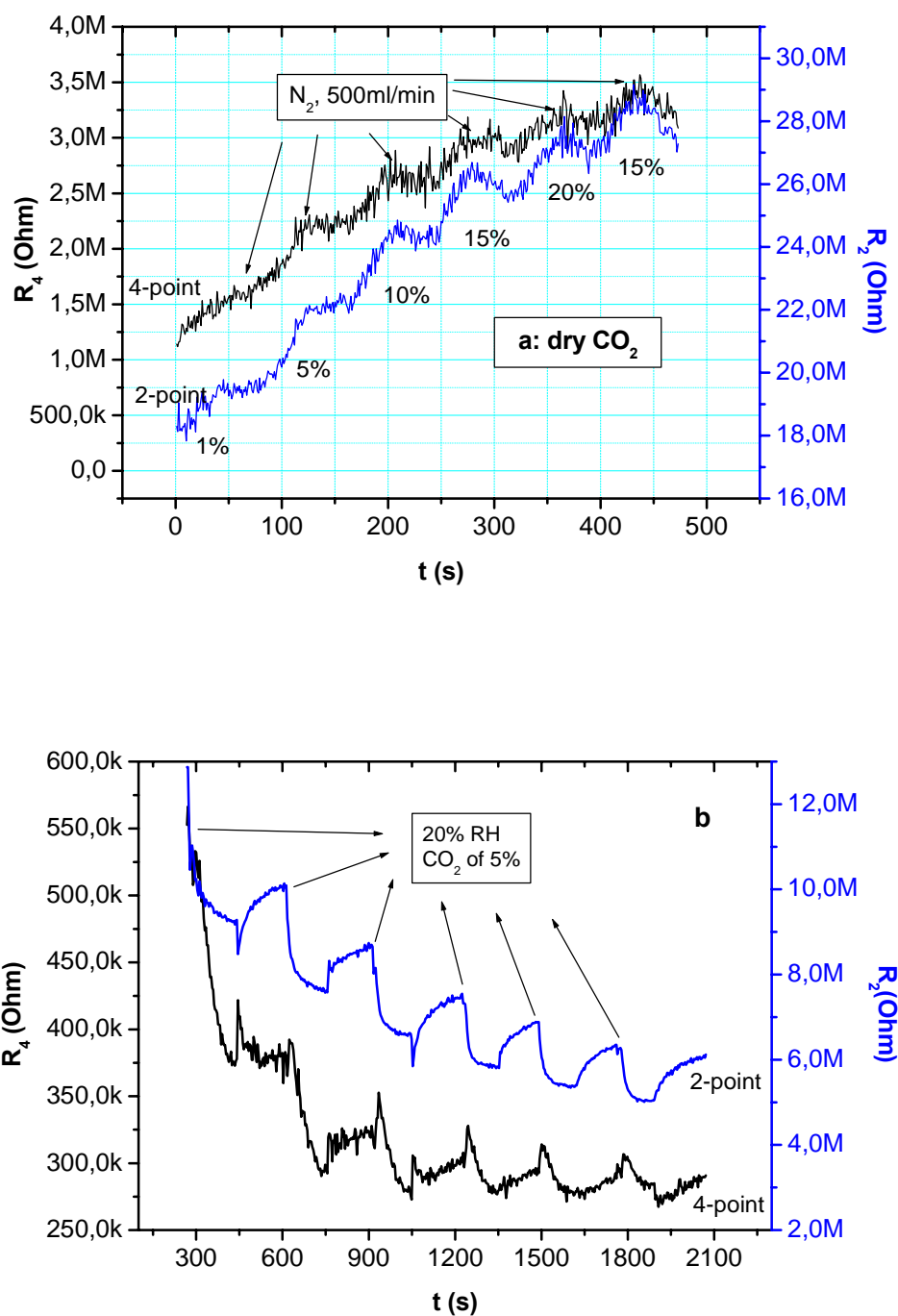
Fig. 3.11.2-4 Response of PANI to dry CO_2 (1% ~ 20%) (*a*)

or humid CO_2 (5 % CO_2 and 20 % RH) (*b*)

The response of PANI to dry and humid CO_2 is presented in Fig. 3.11.2-4 (*a*) and (*b*) respectively. The results for dry CO_2 show a slight decrease in conductance on exposure to CO_2 in the range of 1% ~20 %. While in the presence of humid CO_2, the response of PANI changed to the opposite direction. But the relative change in conductance of PANI on

exposure to 5 % CO_2 and 20 % RH is only 0.5 fold. This is similar to that in the case of moisture. Therefore, this effect is mainly caused by water.

Additionally, the influence of ammonia on both emeraldine base and salt of PANI was studied. There is no influence of ammonia to PANI base since there is no hydrogen on the quinonoid forms to be deprotonated. However, ammonia may cause the conductance of PANI salts to decrease, due to the competitive deprotonation of PANI salts as shown in Fig. 3.11.2-5. This is the reason that the PANI salt was used for ammonia sensors.[43;146;152;271-273]
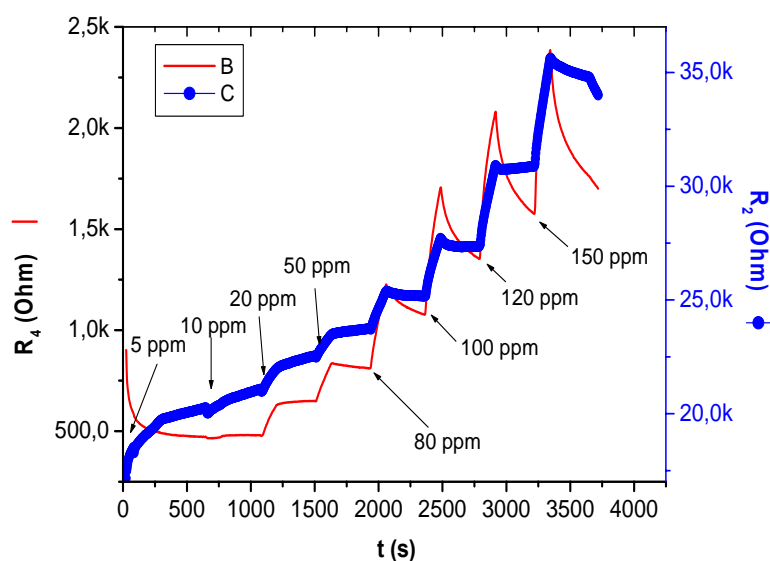
Fig. 3.11.2-5 Response of PANI-SO_4 salt on exposure to NH_3 in the concentration range of 5 ~ 150ppm. N_2 flow of 500 ml/min was used for regeneration.

In general, from the results above, we observed that conductivity of PANI base increases in the presence of gaseous HCl (Fig.3.11.2-1), moisture (Fig. 3.11.2-2), humid HCl (Fig. 3.11.2-3), and humid CO_2 (Fig. 3.11.2-4, *b*). However, it decreased on exposure to dry CO_2 (Fig. 3.11.2-4, *a*) and did not change in case of ammonia (Fig. 3.11.2-5) and N_2. Moreover, the sensitivity of PANI base to dry HCl or to humid HCl is much higher than to other studied analytes. However, a complete regeneration of such sensors based on PANI has not been achieved successfully by using the flow of N_2 or synthetic air. Only a partial reproducibility was reached. Many groups, who are working in this field, use this way for other sensors based on OCPs.[73;140;145;274;275]

3.11.3 Comparison of Sensor Regeneration by Gas Flow and Heating

- *Reversibility* and *Reproducibility*

Simple regeneration of sensors is important property for gas sensors. By now, a fast and high response of our probes on exposure to gaseous HCl has been observed, as well as a semi-reversible regeneration in the flow of N_2. But the regeneration of HCl sensors was not so complete as for reported other kinds of sensors,[131;188] especially when the analytic gas is humid HCl. Therefore, it is important to search for the better an optimal regeneration way. In principle, basic solution or gas could be used to regenerate PANI from its salt state to its base state, but it is not practical for the HCl sensors used as fire alarm.

From our study described in Chapter 3.10, we know that the gaseous HCl may be removed completely from PANI layers at temperatures higher than 150° during a short time. But the chemical structure would cross-link if the temperature is higher than 250°C. This results in the degradation of polymer. So ten-minute heating at 150 °C was used for regeneration instead of N_2 flow. The electrodes covered by PANI films were heated at 150°C for 10 min after adsorption of gaseous HCl. The change of the polymer resistance was recorded during gas adsorption after heating. The results are presented in Fig. 3.11.3-1.
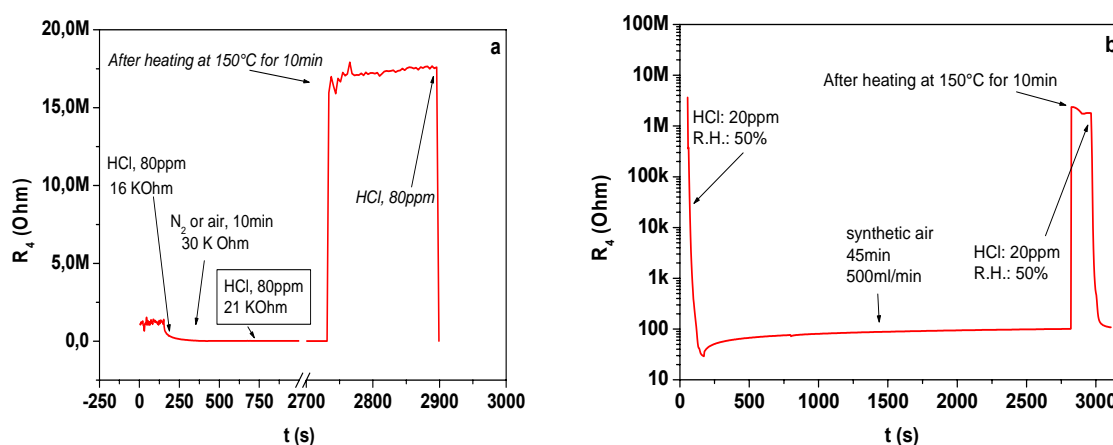
Fig. 3.11.3-1 Response of PANI polymers to dry (a) and wet (b) HCl by thermal desorption at 150 °C comparing with pressed N_2 or air.

In Fig. 3.11.3-1, the polymers appeared nonconductive after heating at 150 °C for 10 min, and the fast and extensive conductance change was observed in the presence of both dry and humid HCl (a and b). The response of these probes to HCl gas was within the seconds

scale. This is due to the formation of non-conductive state of PANI after thermal desorption. Moreover, heating at 150 °C can also remove moisture and other unspecified chemicals from polymer films. This causes the electrical state of PANI to be more insulating. This acts as a 'cleaning process' for non-conductive PANI. The state of PANI after heating is probably the EB state of PANI. Compared with the regeneration in the N_2 flow, heating is much more efficient. Moreover, according to our results in Fig. 3.11.3-1, heating regeneration improved the sensitivity of PANI to gaseous HCl. Therefore, thermal desorption can be used for regeneration of gaseous HCl sensor based on PANI polymers.
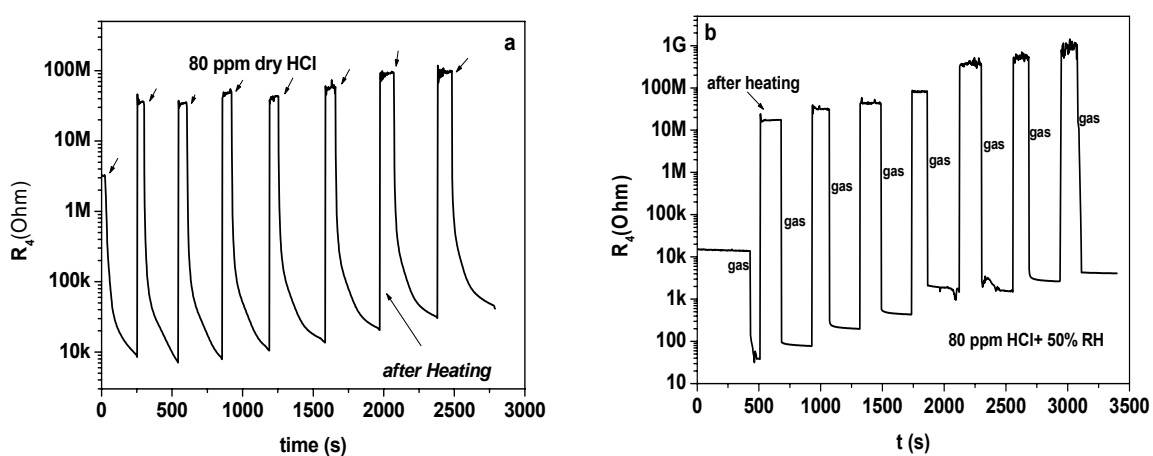
Fig. 3.11.3-2 Response of PANI films to dry (a) or wet (b) HCl
by thermal regenerated at 150°C

Fig. 3.11.3-2 shows the response of PANI films to dry (a) or humid (with 50% RH) (b) HCl of 80 ppm, thermally regenerated at 150°C. The sensors were preheated as described in the beginning of this chapter. In Fig. 3.11.3-2 (a), the vertical drop of resistance during initial fews of seconds was observed for each cycle, followed a sharp slope of response curve at the bottom of each cycle. This indicates that the doping level of PANI by HCl is increasing gradually with the exposure time to dry HCl. The probe response to the humid HCl (Fig. 3.11.3-1, a) was much faster and about 5 times higher than that to dry HCl (Fig. 3.11.3-2, a). A plateau of the $t \sim R$ curve appeared instead of a slope after a similar vertical drop of resistance. The almost stationary value of conductance in each plateau indicates that the protonation level of PANI films remained stable or completely. The equilibrium of the reactions already reached within the first minutes of gas exposure.

The sensor was quite reversible and reproducible with thermal regeneration.

3.11.4 Sensitivity and Selectivity of HCl Gas Sensors Based on PANI Films

The successful application of heating regeneration for gas sensors based on PANI has already been extended to other gases, for instance humidity, dry CO_2, humid CO_2 and humid HCl. The same polymer films of EB form were used as sensitive layers for above gases. After heating, the sensitivity and selectivity of PANI-based sensors to HCl were improved dramatically. The response to moisture was reduced.

Table 3.11.4-1 Sensitivity, selectivity and reversibility of sensors based on PANI film

(according to the function, $r = (G_4 - G_4^0)/ G_4^0$)

Sensor Parameter	Regeneration Mode	Analytes				
		CO_2, dry	CO_2 (5ppm) + H_2O (90%)	H_2O (10% - 90%)	HCl (80ppm), dry	HCl (80ppm) + H_2O (50%)
Sensitivity	In N_2 25°C	~ 0	0.2	0.1-1.0	2	~2000
	Heating 150°C	~ 0	0.4	-0.1~0.2	>1000	>5000
Reversibility	In N_2 25°C	~ 0	0.8	1-2	0.60-0.65	0.0001
	Heating 150°C	~ 0	>1	>1	>1	>1
Relative Selectivity HCl / test Analyte	in N_2 25°C	/	10	2-20	1	/
	Heating 150°C	/	>2500	>5000 ~10^4	1	/

The sensitivity (response) of PANI film to gaseous analytes was estimated by the following equation, $r = (G_4 - G_4^0)/ G_4^0$, where G_4 and G_4^0 are the current and initial conductance obtained by 4-point technique on exposure to analytes, respectively. Selectivity coefficients were determined as a ratio between sensor sensitivity to gaseous HCl and its sensitivity to other gases.[276] All the tests were performed on the electrodes based on PANI films. The results from both regeneration methods are compared in Table 3.11.4-1.

In Table 3.11.4-1, the comparison among various gaseous probes presents that pretreated PANI films have the higher sensitivity (response) to gaseous HCl, especially to

humid HCl, than the other analytes. The sensitivity and selectivity of HCl sensors based on PANI films have been greatly enhanced after heating regeneration; however, the sensitivity of PANI films to humid N_2 is reduced after heating. The selectivity of such HCl sensor against moisture is as high as three orders of magnitude fold by using thermal regeneration.

In order to test the response of our sensors to other gases, such as NO_2, SO_2 and ethanol vapor, additional experiments have been performed on PANI films by BOSCH GmbH. The probes based on PANI were prepared as before. The selectivity of the HCl gas sensor to those vapors complies with the requirement of DIN ((Deutsche Industrie Norm).

3.11.5 Long Time Monitoring of HCl Gas Sensors Based on PANI Films

Two sensors coated by PANI films were prepared as described in the last sub-chapter. The pretreated sensors were left in the office (Room Nr. 11.1.06; faced to the west side) and in the laboratory (Room Nr. 11.1.16; faced to the east side) air, respectively, for more than half a year to continuously monitor the air quality (HCl or other acidic vapours).
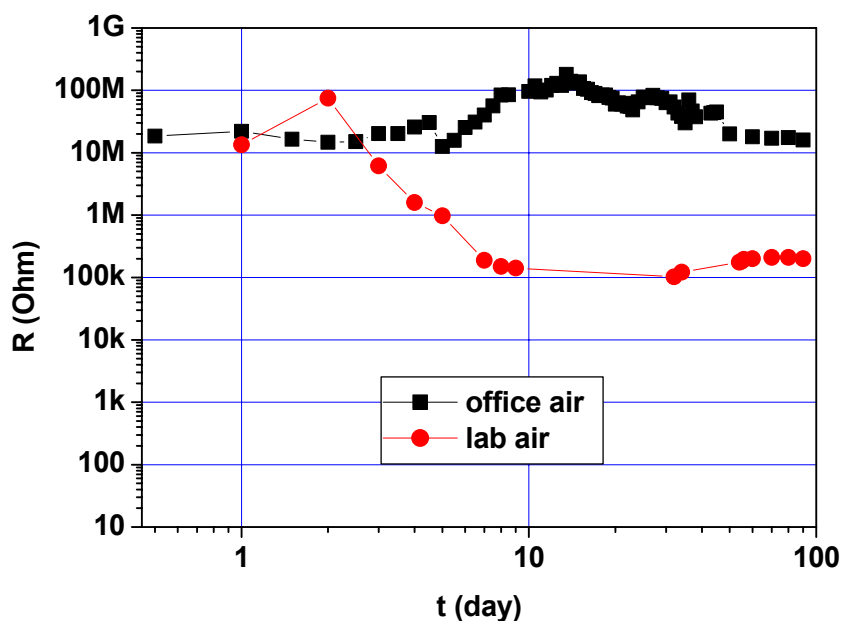
Fig. 3.11.5-1 Long time air monitoring by using HCl sensors based on PANI
(Note: Exposure of the sensor to HCl of 5ppm with humidity of 10% results in much lower resistance.)

After three months, two different curves were obtained. The results are shown in Fig. 3.11.5-1. It seems that the air quality from office is much better than laboratory. There are more acidic or humid gases causing the resistance of PANI to decrease, for example HCl in the laboratory. This seems reasonable, since lots of buffers and acidic solutions are stored in

that lab. According to the former results, exposure to HCl of 5ppm with humidity of 10% resulted in a lower resistance than 100 kOhm. Calibration showed that HCl concentration in the laboratory was much less than 1 ppm. This also implies that the detectable minimum concentration is in a sub-ppm range. The results demonstrate that, by application in the relatively pure conditions, the regeneration cycle can be 3 months or more. The results will be applied for Patent.

3.11.6 Advantages of HCl Sensors Based on PANI

In order to estimate the practical significance of the developed HCl sensor, the results were compared with relevant literature data (shown in Table 3.11.6-1).

Taking into account the requirements of industry, the sensor should possess a rapid and high response, high selectivity, stability, perfect reversibility, reproducibility and the possibility of regeneration. However, it has been a rather difficult aim to fulfil all the requirements. For instance, slow penetration of gases into bulk OCPs causes hysteresis and relatively long response time (tens of seconds to minutes);[187] poor reversibility was observed in traditional regeneration by the flows of nitrogen or air at room temperature.

In Table 3.11.6-1, the HCl detection is based on different principles: optical absorbance, optical transmission, and electrical conductance/resistance and amperometric mechanisms. Sensitive materials cover organic and inorganic chemicals; most of them belong to the family of OCPs. Interestingly, the sensors developed in our group display the most attractive properties of every analytical or even economical parameter. This result will be used for patent.

Table 3.11.6-1 Comparison of known HCl sensors

Reference	Rever-sibility	Analytical Sensitivity (Δsignal /Δ concentration)	Dimensionsless Analytical Sensitivity (Δ signal / background_signal / Δ concentration)	Material	Transducer Type	Detection limit.	Regeneration time
277	yes	~0.025 (abs / ppm) 20% (reflectance, I/I_0)	2 % / ppm	5, 10, 15. 20-tetrakis (3',5'-di-tert-butyl-4'-hydroxyphenyl) porphin-ethylcellulose composite	optical (transmission)	sub-ppm	increases with increase of HCl concentration (40 min for 11 ppm at 40°C)
278	no data	no data	10^7% / ppm	Nanofibers from PANI / Camphorsulfonic acid	electrical resistance	no data (the only experiment at 100 ppm)	no data
267	no data		up to $4*10^7$% / ppm	PANI; Poly(o-toluide)	electrical resistance	sub-ppm	no data
279	no data	0.5 mS / cm / ppm	up to 5% / ppm	PANI + Polyvinylacetate, Polystyrene or Polyvynilchloride	electrical conductance	no data (minimal concentration used: 200 ppm)	no data
280	yes	2.0 µA / ppm	~ 800 / ppm	MnO_2 **Disadvantage:** consumption of the sensor material (life time: 1000 h at 5 ppm)	amperometric (MnO2 reduction)	0.3 ppm	about 10 min
281	not reversible	no data	10^{10}% / ? ppm (the air was bubbled through 1 M HCl) in the first exposure to HCl, then much less	PANI/ calixarene (LB films)	conductance	~10 ppm	no complete regeneration within 5 hours
282	not reversible	no data	10^{-3} % / ppm	pH indicator, plasticizer, polymer	optical absorbance	~ 1000 ppm	-
Hao, Q-L; Mirsky, V.; Wolfbeis, O. S.	yes	> 1 GOhm / ppm	10^5 % / ppm for dry HCl or ~10^7 % / ppm for wet HCl	PANI (the heating for sensor regeneration was tested also for other copolymers on the base of PANI)	electrical conductance	at least sub ppm (was checked at 2.5 ppm)	10 min at 150 °C

3.11.7 Real–time Test Compared with Standard Fire Sensors (German, 2003)

HCl sensor based on PANI was prepared and tested as an alarm sensor for the detection of cable fire. It was tested according to DIN (Deutsche Industrie Norm) by Robert BOSCH (Germany). One of the results from the comparison of our sensor with the currently used industrial fire sensors (at German Market) is shown in Fig. 3.11.7-1. (Sorry! other results are not allowed to be published because they are internal secret of BOSCH.)

The result shows the signal of our sensor based on PANI is much faster and higher than those from currently used industrial sensors (Sensor 1 and Sensor 2). Therefore, it is promising to make it commercialize. This is in process.
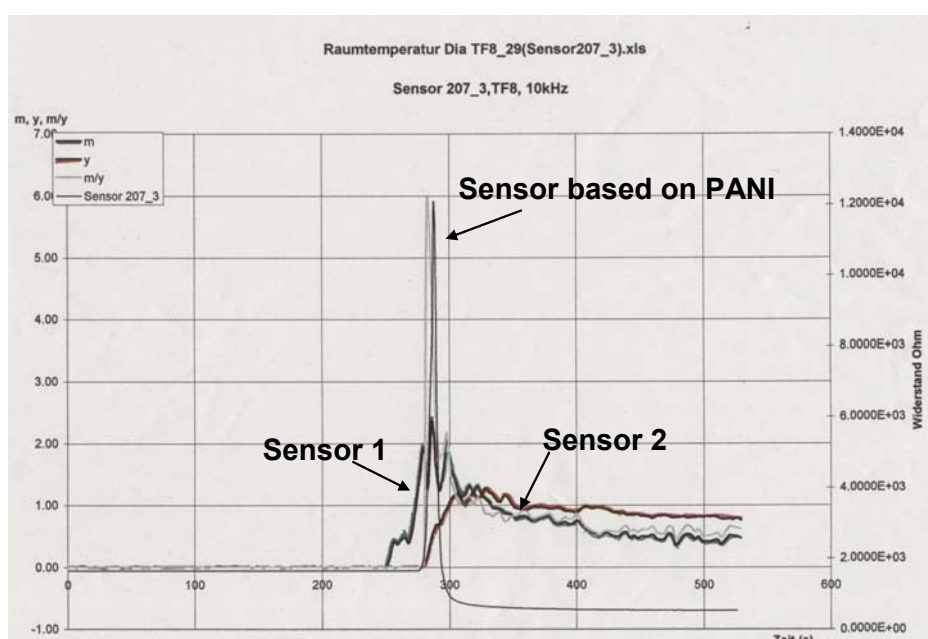
Fig. 3.11.7-1 Comparison of PANI based HCl sensor with commercial sensors from German market (2003)

3.12 Combinatorial Screening

3.12.1 Combinatorial Experiments

Further optimization of sensitive properties of PANI has been performed by its combinatorial copolymerization with different PANI derivatives: 4-aminobenzoic acid (4ABA), 2-aminobenzoic acid (AA), 3-aminobenzoic acid (3ABA), 3-aminobenzosulfonic acid (3ABSA). The investigation has been performed at 0.9V for the wide range (typically up to 30% of aniline derivative in the polymerization mixture) of molar ratio of aniline and its

derivative in the polymerization mixture. All the polymerization experiments were controlled by charge limitation of 120 C/cm^2. More than 30% of aniline derivatives in molar part would take too long to polymerize, since a gradual increase of electrical resistance of a polymer with poor conductive suppressed electropolymerization, leading to a principal limitation of the layer thickness.

All the polymerizations were done at 40°C to speed up the reaction rate and to reduce the duration of the experiment. The electrochemical process was performed at constant potential (0.9V); the film thickness of around 1μm controlled by the total charge through electrodes. After polymerization, washing with MILLIPORE water and drying under pressed N$_2$ have been done automatically. Then, the electropolymerization cell was replaced by a gas cell for the gas test. The whole gas test was done according to the protocol (See Appendix II) described elsewhere.[157] Gas concentration was varied from 2.5 ppm to 40 ppm with a total flow rate of 600 ml/min. Thermal regeneration was carried out at 120°C for 10 min. Measurements were carried out on both electrical properties of the synthesized materials: current-voltage characteristics and conductivity as measured by two and 4-point techniques (See Chapter 2.4.3).

3.12.2 Results and Discussion
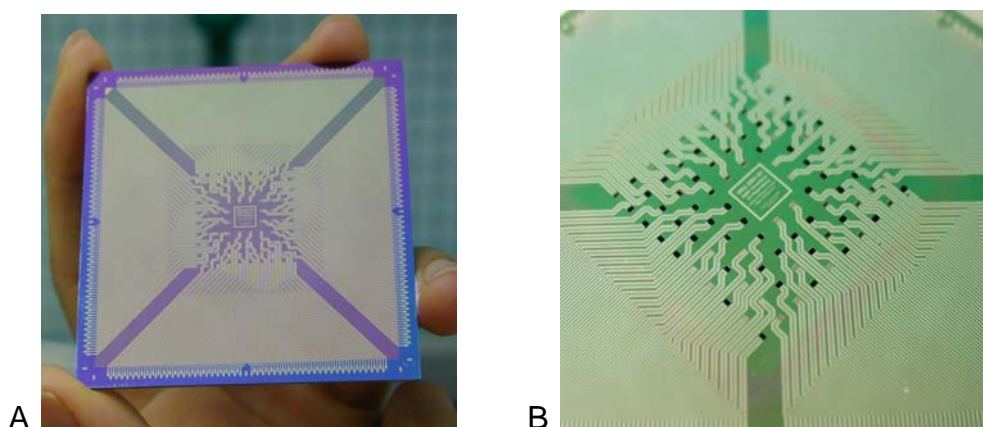
Fig. 3.12.2-1 Optical micrograph of electro-array before (A) and after (B) deposited electrochemically by PANI with different thickness

Fig. 3.12.2-1 shows the electropolymerized PANI films (B) on an electrode array with different thickness, from ~700nm to 1mm, in comparison with the blank electrode array (A).

The data obtained from the data library have been processed according to the protocol (See Table 2.5.3-2 in Chapter 2). The results containing all parameters were analyzed and compared according to the parameters in the protocol. The considered parameters are relative/absolute sensitivity, response, desorption efficiency, reversibility, reproducibility, and so on. The best results were calculated from the mean value of those parameters for five kind copolymers with the mixed ratio corresponding to the best value of the studied parameter. The selected 'optimal ratio' of each kind copolymer for each parameter was determined among various ratios according to the best value of the studied parameter.

The best results are shown in Fig. 3.12.2-1. In these plots, the values on the column indicate optimal molar part of the aniline derivate in the polymerization mixture. The results obey the following trends:

- The absolute sensitivity of aniline can be improved by copolymerization with 3ABA or 3ABSA. Other copolymers investigated shows decrease or only a modest increase of absolute sensitivity.
- P(3ABA-ANI) copolymers also have the best reproducibility, reversibility and response time and the lowest contact resistance between polymer and electrodes, besides the best absolute sensitivity.
- Pure polyaniline has the best desorption efficiency. Any modification of this polymer resulted in less of the regeneration efficiency.
- Most of polymers show very high linearity – the correlation coefficient for all investigated copolymers (except 3ABSA) for the optimal monomers ration was in the range between 0.995 (AA) and 0.999 (4ABA).

Therefore, among all copolymers studied here, P(3ABA-ANI) copolymer, as a sensitive layer to HCl, deposited from the mixture containing 30 % 3ABA presented the best abs. sensitivity, reversibility, response time, reproducibility and best contact. But it has the worse relative sensitivity. PANI has the best desorption efficiency. According to these analysis, P(3ABA-ANI) with ratio mentioned above (30% 3ABA) can be considered as the promising material for HCl gas sensor by thermal regeneration.
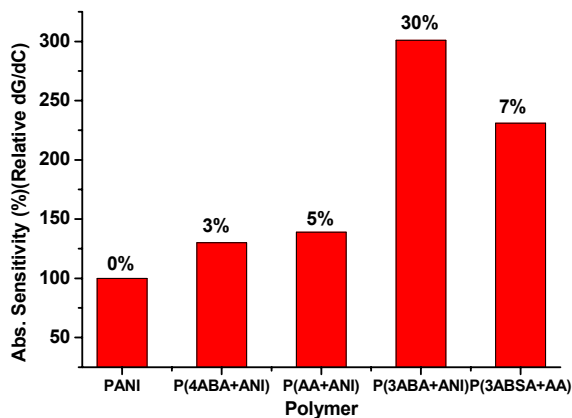
Best Sensitivity: P(3ABA-ANI) 30%
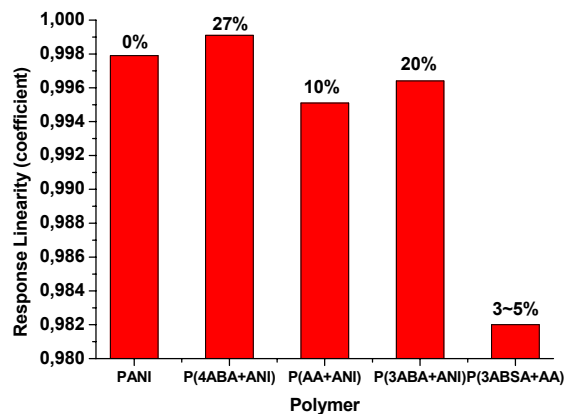
Best Linearity: P(4ABA-ANI) 20%
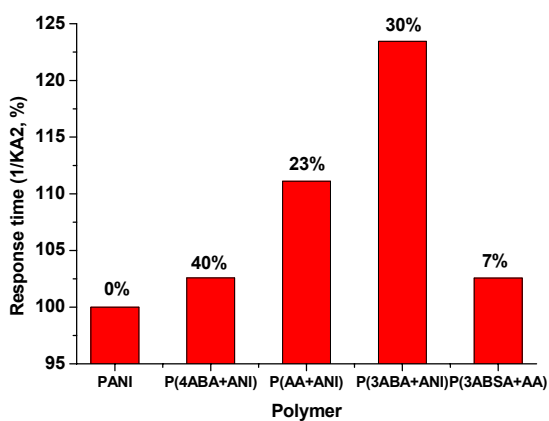
Best Response Rate: P(3ABA-ANI) 30%
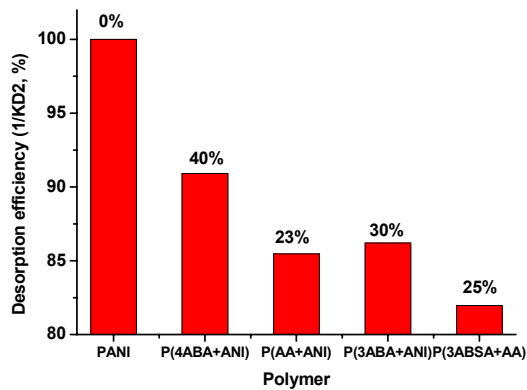
Best Desorption Efficiency: PANI
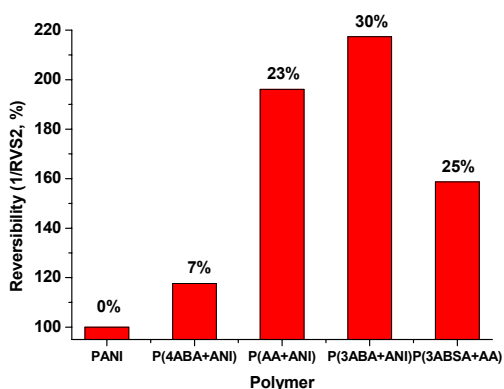
Best Reversibility: P(3ABA-ANI) 30%
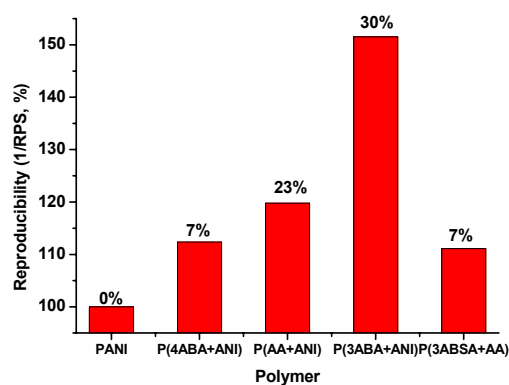
Best Reproducibility: P(3ABA-ANI) 30%
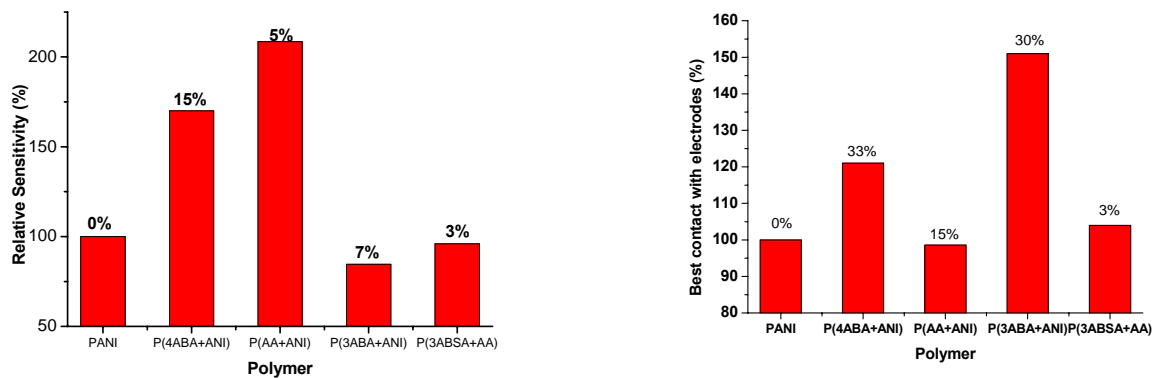
Best Relative Sensitivity: P(AA-ANI) 5%　　　**Best Contact with Electrodes: P(3ABA-ANI) 30%**

Fig. 3.12.2-1 Best statistic results (calculated mean value of five kinds of polymer samples, with the mixed ratio corresponding to the best value of the studied parameter)

4 Summary

- Electropolymerized thin films from polyaniline and its derivatives and more than thirty copolymers with the derivatives were studied. Mainly, electrochemical methods were used. Anion-exchange and the influence of pH and electrode potential on the electrical parameters of the polymer films were studied. The results were also evaluated by the newly developed technique of simultaneous applications of two- and four point measurements. Optimization of polymerization conditions was further used for combinatorial electropolymerization.

- Systematic investigation of polymerization conditions on the morphology of N-methyl polyaniline resulted in a formation of glass-like polymer layers which are smooth in sub-micrometer scale.

- Multilayer polymer sensors where sensitivity and contact bonding were provided by different types of conductive polymers (polyaniline as the sensitive polymer and poly(3,4-ethylene-dioxythiophene) as inert conductive polymer) were prepared electrochemically.

- Surface plasmon resonance transducing was applied for gas sensing with conductive polymers. The detection of gaseous hydrogen chloride by N-methyl polyaniline was demonstrated.

- Temperature influence on the kinetics of polyaniline association with gaseous hydrogen chloride was investigated. Activation energy for the reaction was evaluated as 18 kJ/mol. Temperature influence on the kinetics of dissociation of hydrogen chloride from polyaniline was investigated. Activation energy for desoption process was evaluated as 30 kJ/mol. The comparison of activation energies for direct and reverse reactions was used for estimation of binding energy (12 kJ/mol). The results indicate the temperature dependent conversion of emeraldine salt into emeraldine base. Thermal analyses were performed by TG and DSC. The complete removal of HCl dopant can be performed by heating at about 150°C.

- The observation of temperature dependent conversion of the emeraldine salt into emeraldine base was used for development of thermoregeneration of sensors for gaseous hydrogen chloride. Ultra-sensitive highly reversible and highly selective sensors for applications in alarm systems for cable fire were developed. According to

the information from the industrial partner, the sensor test in DIN conditions confirmed that its properties exceed essentially currently produced sensors.

- Combinatorial electropolymerization was used for the comparison of sensitive polymers and further optimization of the sensor for gaseous hydrogen chloride. The best results were obtained for the copolymer formed from the mixture of aniline/3-aminobenzoic acid with molar ratio 3/7.

5 Zusammenfassung

- Elektropolymerisierte dünne Filme aus Polyanilin, Derivaten von Polyanilin und mehr als dreißig Colpoymeren dieser Derivate wurden untersucht. Dazu wurden hauptsächlich elektrochemische Methoden benutzt. Der Austausch der Anionen und die Einflüsse des pH-Werts und des Elektrodenpotentials wurden überprüft. Die Ergebnisse wurden mit der neu entwickelten Technik der gleichzeitigen Zwei- und Vierpunktmessung ausgewertet. Die Optimierung der Bedingungen für die Polymerisation wurde weiter zur kombinatorischen Elektropolymerisierung benutzt.

- Die systematische Untersuchung des Einflusses der Polymerisationsbedingungen auf die Morphologie von N-Methylpolyanilin resultierte in einer Ausbildung einer glasartigen Polymerschicht mit einer Glätte im Submikrometerbereich.

- Multischicht-Polymer-Sensoren deren Sensitivität und elektrische Kontaktierung aus verschiedenen leitenden Polymeren (z.B. Polyanilin als sensitives Polymer in Kombination mit Poly(3,4-ethylendioythiophen) als inertes leitendes Polymer) resultiert, wurden elektrochemisch erzeugt.

- Die Oberflächenplasmonresonanz wurde angewendet, um die Sensitivität von leitenden Polymerschichten für Gas zu prüfen. Eine Detektion von gasförmigem Chlorwasserstoff mit N-Methylpolyanilin konnte gezeigt werden.

- Der Einfluss der Temperatur auf die Kinetik der Assoziation von gasförmigem Chlorwasserstoff an Polyanilin wurde geprüft. Eine Aktivierungsenergie von 18 kJ/mol wurde für diese Reaktion ermittelt. Die Temperaturabhängigkeit der Kinetik der Dissoziation von Chlorwasserstoff von Polyanilin wurde ebenfalls untersucht. Die hierfür gefundene Aktivierungsenergie beträgt 30 kJ/mol. Der Vergleich der Aktivierungsenergien für beide Reaktionen erlaubt eine Abschätzung der Bindungsenergie (12 kJ/mol). Die Ergebnisse deuten auf eine Umwandlung des Emeraldin-Salzes in die Emeraldin-Base hin. Thermische Untersuchungen wurden mittels TG und DSC durchgeführt. Eine vollständige Entfernung der HCl Dotierung kann durch Erhitzen auf etwa 150 °C erreicht werden.

- Die Beobachtung der temperaturabhängigen Umwandlung des Emeraldin-Salzes in die Emeraldin-Base wurde zur Erzeugung eines thermoregenerativen Sensors für Chlorwasserstoffgas benutzt. Überaus sensitive, höchst reversible und äußerst selektive Sensoren zur Anwendung als Brandmelder für Kabelbrände wurden

entwickelt. Nach den Richtlinien der Industrie konnte gezeigt werden, dass dieser Sensor bei Tests unter DIN-Bedingungen besser abschnitt als bisherige Sensoren.

- Mit Hilfe der kombinatorischen Elektropolymerisierung wurden verschiedene sensitive Polymere verglichen und weitergehend optimiert hinsichtlich ihrer Verwendung als Sensor für Chlorwasserstoffgas. Die besten Ergebnisse wurden für Copolymere, erzeugt aus einer Mischung von Anilin und 3-Aminobenzoesäure bei einem molaren Verhältnis von 3:7, erhalten.

6 References

1. Shirakawa, Hideki; Louis, Edwin J.; MacDiarmid, Alan G.; Chiang, Chwan K.; Heeger, Alan J. *Journal of the Chemical Society, Chemical Communications* **1977,** 578-80.

2. Heeger, Alan J. *Reviews of Modern Physics* **2001,** *73*, 681-700.

3. MacDiarmid, Alan G. *Reviews of Modern Physics* **2001,** *73*, 701-12.

4. Shirakawa, Hideki *Reviews of Modern Physics* **2001,** *73*, 713-18.

5. Shirakawa, Hideki; McDiarmid, Alan; Heeger, Alan *Chemical Communications (Cambridge, United Kingdom)* **2003,** 1-4.

6. Kakuda, Satoko; Momma, Toshiyuki; Osaka, Tetsuya; Appetecchi, G. Battista; Scrosati, Bruno *Journal of the Electrochemical Society* **1995,** *142*, L1-L2.

7. Momma, Toshiyuki; Kakuda, Satoko; Yarimizu, Hideki; Osaka, Tetsuya *Journal of the Electrochemical Society* **1995,** *142*, 1766-69.

8. Osaka, Tetsuya; Nakajima, Toshiki; Shiota, Koh; Momma, Toshiyuki *Journal of the Electrochemical Society* **1991,** *138*, 2853-58.

9. Kawai, Tsuyoshi, Kuwabara, Takao, Wang, Shenglong, and Yoshino, Katsumi. *Japanese Journal of Applied Physics*, Part 1: Regular Papers, Short Notes & Review Papers. **1990**, *29*, 602-605.

10. Harry, B., Jr., Atta, N., Ma, Y. L., Petticrew, K. L., Zimmer, H., Shi, Y., Lunsford, S. K., Rubinson, J. F., and Galal, Ahmed. *Bioelectrochemistry and Bioenergetics* **1995**, *38*, 229-245.

11. Diaz, A. F., Rubinson, J. F., and Mark, H. B., Jr. *Advances in Polymer Science* **1988,** *84,* 113-139.

12. Kobayashi, Tetsuhiko; Yoneyama, Hiroshi; Tamura, Hideo *Journal of Electroanalytical Chemistry and Interfacial Electrochemistry* **1984,** *161*, 419-23.

13. Selampinar, Fatma; Toppare, Levent; Akbulut, Ural; Yalcin, Talat; Suezer, Sefik *Synthetic Metals* **1995,** *68*, 109-16.

14. Ahonen, H. J.; Kankare, J.; Lukkari, J.; Pasanen, P. *Synthetic Metals* **1997,** *84*, 215-16.

15. Partridge, A. C.; Jansen, M. L.; Arnold, W. M. *Materials Science & Engineering, C: Biomimetic and Supramolecular Systems* **2000,** *C12*, 37-42.

16. Shimano, J. Y.; MacDiarmid, A. G. *Synthetic Metals* **2001,** *123*, 251-62.

17. Shirakawa, Hideki *Synthetic Metals* **2001,** *125*, 3-10.

18. Nicolas-Debarnot, Dominique; Poncin-Epaillard, Fabienne *Analytica Chimica Acta* **2003,** *475*, 1-15.

19. Agbor, N. E.; Petty, M. C.; Monkman, A. P. *Sensors and Actuators, B: Chemical* **1995,** *B28*, 173-79.

20. Xie, Dan; Jiang, Yadong; Pan, Wei; Li, Dan; Wu, Zhiming; Li, Yanrong *Sensors and Actuators, B: Chemical* **2002,** *B81*, 158-64.

21. Li, Dan; Jiang, Yadong; Li, Yanrong; Yang, Xujie; Lu, Lude; Wang, Xin *Materials Science & Engineering, C: Biomimetic and Supramolecular Systems* **2000,** *C11*, 117-19.

22. Li, Dan; Ding, Wenyan; Wang, Xin; Lu, Lude; Yang, Xujie *Journal of Materials Science Letters* **2001,** *20*, 1925-28.

23. Rao, P. Swapna, Subrahmanya, S., and Sathyanarayana, D. N. *Synthetic Metals* **2002,** *128*, 311-316.

24. Rao, Palle Swapna; Sathyanarayana, D. N.; Palaniappan, S. *Macromolecules* **2002,** *35*, 4988-96.

25. Cruz, G. J., Morales, J., Castillo-Ortega, M. M., and Olayo, R. *Synthetic Metals* **1997,** *88*, 213-218.

26. Takeda, S. *Thin Solid Films* **1999,** *343-344*, 313-16.

27. Liao, Chuanping and Gu, Mingyuan. *Thin Solid Films* **2002,** *408*, 37-42.

28. MacDiarmid, A. G.; Chiang, J. C.; Richter, A. F.; Somasiri, N. L. D.; Epstein, A. J. *Conduct. Polym., Proc. Workshop*, Dep. Chem.,Univ. pennsylvania, Philadelphia, PA, USA, **1987** .

29. Abalyaeva, Valentina V. and Efimov, Oleg N., *Polymers for Advanced Technologies* **2000,** *11*, 69-74.

30. Malinauskas, A. Chemical deposition of conducting polymers. *Polymer* **2001**, *42*, 3957-3972.

31. Syed, Akheel A.; Dinesan, Maravattickal K. *Talanta* **1991,** *38*, 815-37.

32. Picart, Sebastien, Miomandre, Fabien, and Launay, Vincent. *Bulletin de l'Union des Physiciens* **2001**, *95*, 581-592.

33. Syed, Akheel Ahmed, Dinesan, Maravattickal Kunjan, and Genies, Eugene Marie. *Bulletin of Electrochemistry* **1988,** *4*, 737-742.

34. Hao, Qingli; Kulikov, Valentin; Mirsky, Vladimir M. *Sensors and Actuators, B: Chemical* **2003,** *94*, 352-57.

35. Laranjeira, Jane Maria Goncalves, De Azevedo, Walter Mendes, and De Araujo, Mario Cesar Ugulino *Analytical Letters* **1997,** *30*, 2189-2209.

36. Nyffenegger, Ralph M.; Penner, Reginald M. *Journal of Physical Chemistry* **1996,** *100*, 17041-49.

37. Noufi, Rommel; Frank, Arthur J.; Nozik, Arthur J. *Journal of the American Chemical Society* **1981,** *103*, 1849-50.

38. Noufi, Rommel; Tench, Dennis *Journal of the Electrochemical Society* **1980,** *127*, 188-90.

39. Bull, R. A.; Fan, F. R.; Bard, A. J. *Journal of the Electrochemical Society* **1983,** *130*, 1636-38.

40. Abrantes, L. M., Correia, J. P., Savic, M., and Jin, G. *Electrochimica Acta***. 2001,** *46*, 3181-3187

41. Lux, F.; Samuelsen, E. J.; Kang, E. T. *Synthetic Metals* **1995,** *69*, 167-69.

42. Genies, E. M.; Penneau, J. F.; Vieil, E. *Journal of Electroanalytical Chemistry and Interfacial Electrochemistry* **1990,** *283*, 205-19.

43. Dhawan, S. K.; Kumar, D.; Ram, M. K.; Chandra, S.; Trivedi, D. C. *Sensors and Actuators, B: Chemical* **1997,** *B40*, 99-103.

44. Genies, E. M.; Lapkowski, M.; Tsintavis, C. *New Journal of Chemistry* **1988,** *12*, 181-96.

45. Kang, E. T.; Neoh, K. G.; Tan, T. C.; Khor, S. H.; Tan, K. L. *Macromolecules* **1990,** *23*, 2918-26.

46. Kang, E. T.; Neoh, K. G.; Tan, K. L. *Progress in Polymer Science* **1998,** *23*, 277-324.

47. Shimano, J. Y.; MacDiarmid, A. G. *Synthetic Metals* **2001,** *119*, 365-66.

48. Epstein, A. J.; Ginder, J. M.; Zuo, F.; Woo, H. S.; Tanner, D. B.; Richter, A. F.; Angelopoulos, M.; Huang, W. S.; MacDiarmid, A. G. *Synthetic Metals* **1987,** *21*, 63-70.

49. Epstein, A. J.; MacDiarmid, A. G. *Materials Research Society Symposium Proceedings* **1990,** *173*, 293-303.

50. Kang, E. T.; Neoh, K. G.; Tan, K. L. *Surface and Interface Analysis* **1993,** *20*, 833-40.

51. MacDiarmid, A. G.; Chiang, J. C.; Richter, A. F.; Epstein, A. J. *Synthetic Metals* **1987,** *18*, 285-90.

52. MacDiarmid, Alan G., Mu, Shao Lin, Somasiri, Nanayakkara L. D., and Wu, Wanqun. *Molecular Crystals and Liquid Crystals* **1985,** *121*, 187-190.

53. MacDiarmid, Alan G. and Epstein, Arthur J. Polyanilines: *Faraday Discussions of the Chemical Society* **1989,** *88*, 317-332.

54. MacDiarmid, Alan G.; Epstein, Arthur J. *Macromolecular Symposia* **1995,** *98*, 835-42.

55. Ray, A.; Richter, A. F.; MacDiarmid, A. G.; Epstein, A. J. *Synthetic Metals* **1989,** *29*, E151-E156.

56. Ray, A.; Asturias, G. E.; Kershner, D. L.; Richter, A. F.; MacDiarmid, A. G.; Epstein, A. J. *Synthetic Metals* **1989,** *29*, E141-E150.

57. Heeger, Alan J. *Synthetic Metals*. **2001,** *125*, 23-42

58. Kang, E. T., Neoh, K. G., Tan, K. L., Kuok, M. H., and Tan, B. T. G. *Molecular Crystals and Liquid Crystals* **1990,** *178*, 219-230.

59. Kulikov, A. V.; Bogatyrenko, V. R.; Belonogova, O. V.; Fokeeva, L. S.; Lebedev, A. V.; Echmaeva, T. A.; Shunina, I. G. *Russian Chemical Bulletin* **2002,** *51*, 2216-23.

60. Chen, Wei Chih; Wen, Ten Chin; Gopalan, A. *Synthetic Metals* **2002,** *128*, 179-89.

61. Stilwell, David E.; Park, Su Moon *Journal of the Electrochemical Society* **1989,** *136*, 427-33.

62. Chen, Wei Chih; Wen, Ten Chin; Gopalan, A. *Electrochimica Acta* **2002,** *47*, 4195-206.

63. Stilwell, David E.; Park, Su Moon *Journal of the Electrochemical Society* **1988,** *135*, 2491-96.

64. Stilwell, David E.; Park, Su Moon *Journal of the Electrochemical Society* **1988,** *135*, 2254-62.

65. Ryu, K. S., Moon, B. W., Joo, J., and Chang, S. H. *Polymer* **2001**, *42*, 9355-9360.

66. Ball, I. J., Huang, S. C., Wolf, R. A., Shimano, J. Y., and Kaner, R. B. *Journal of Membrane Science* **2000**, *174*, 161-176.

67. Hu, Hailin, Saniger, Jose M., and Banuelos, Jose G. *Thin Thin Solid Films* **1999,** *347*, 241-247.

68. Jiang, Yadong; Li, Dan; Xie, Dan; Wu, Zhiming; Yang, Bangchao *Proceedings of SPIE-The International Society for Optical Engineering* **2001,** *4414*, 358-61.

69. Athawale, Anjali A., Kulkarni, Milind V., and Chabukswar, Vasant V. *Materials Chemistry and Physics* **2002,** *73*, 106-110.

70. Kang, E. T.; Neoh, K. G.; Huang, S. W.; Lim, S. L.; Tan, K. L. *Journal of Physical Chemistry B* **1997,** *101*, 10744-50.

71. Kang, E. T.; Ma, Z. H.; Tan, K. L.; Zhu, B. R.; Uyama, Y.; Ikada, Y. *Polymers for Advanced Technologies* **1999,** *10*, 421-28.

72. Beau, B.; Travers, J. P.; Banka, E. *Synthetic Metals* **1999,** *101*, 772-75.

73. Kiattibutr, P.; Tarachiwin, L.; Ruangchuay, L.; Sirivat, A.; Schwank, J. *Reactive & Functional Polymers* **2002,** *53*, 29-37.

74. Motheo, A. J.; Santos, J. R., Jr.; Venancio, E. C.; Mattoso, L. H. C. *Polymer* **1998,** *39,* 6977-82.

75. De Freitas, P. Scandiucci; De Paoli, Marco A. *Synthetic Metals* **1999,** *102*, 1012-13.

76. Morgan, H.; Foot, P. J. S.; Brooks, N. W. *Journal of Materials Science* **2001,** *36*, 5369-77.

77. Yang, C. Y., Smith, P., Heeger, A. J., Cao, Y., and Osterholm, J. E. *Polymer* **1994,** *35*, 1142-1147.

78. Dao, L. H., Leclerc, M., Guay, J., and Chevalier, J. W. *Synthetic Metals* **1989**, *29*, E377-E382.

79. Yue, J.; Epstein, A. J.; MacDiarmid, A. G. *Molecular Crystals and Liquid Crystals* **1990,** *189*, 255-61.

80. Cataldo, Franco; Maltese, Paolo *European Polymer Journal* **2002,** *38*, 1791-803.

81. Ng, S. C., Chan, H. S. O., Huang, H. H., and Ho, P. K. H. *Chemical Communications* **1995,** 1327-1328.

82. Neoh, K. G.; Kang, E. T.; Tan, K. L. *Polymer Degradation and Stability* **1994,** *43*, 141-47.

83. Chen, Show An; Hwang, Gue Wuu *Polymer* **1997,** *38*, 3333-46.

84. Al Ghamdi, Ali and Al Saigh, Zeki Y. *Journal of Chromatography*, **2002,** *A 969*, 229-243.

85. Ding, Lili; Wang, Xingwu; Gregory, R. V. *Synthetic Metals* **1999,** *104*, 73-78.

86. Jing, Xin li; Zhao, Wei bing; Zheng, Mao sheng *Shihua Jishu Yu Yingyong* **2001,** *19*, 225-28.

87. Wei, Yen; Hsueh, Kesyin F. *Journal of Polymer Science, Part A: Polymer Chemistry* **1989,** *27*, 4351-63.

88. Tan, Loon Seng; Simko, Sharon R.; Bai, Shih Jung; Vaia, Richard A.; Taylor, Barney E.; Houtz, Marlene D.; Alexander, Max D., Jr.; Spry, Robert J. *Journal of Polymer Science, Part B: Polymer Physics* **2001,** *39*, 2539-48.

89. Mathew, Raji; Mattes, Benjamin R.; Espe, Matthew P. *Synthetic Metals* **2002,** *131*, 141-47.

90. Ding, Lili; Wang, Xingwu; Gregory, R. V. *Synthetic Metals* **1999,** *104*, 73-78.

91. Conklin, Jeanine A.; Huang, Shu Chuan; Huang, Shiou Mei; Wen, Tianli; Kaner, Richard B. *Macromolecules* **1995,** *28*, 6522-27.

92. Chen, Cheng Ho *Journal of Polymer Research* **2002,** *9*, 195-200.

93. Lippe, Juergen and Holze, Rudolf. *Journal of Electroanalytical Chemistry* **1992,** *339*, 411-422.

94. Pron, Adam; Rannou, Patrice *Progress in Polymer Science* **2001,** *27*, 135-90.

95. Morales, G. M.; Miras, M. C.; Barbero, C. *Synthetic Metals* **1999,** *101*, 686.

96. Wang, Baochen; Tang, Jisong; Wang, Fosong *Synthetic Metals* **1987,** *18*, 323-28.

97. Zotti, G.; Cattarin, S.; Comisso, N. *Journal of Electroanalytical Chemistry and Interfacial Electrochemistry* **1988,** *239*, 387-96.

98. Desilvestro, Johann; Scheifele, Werner *Journal of Materials Chemistry* **1993,** *3*, 263-72.

99. Nunziante, P.; Pistoia, G. *Electrochimica Acta* **1989,** *34*, 223-28.

100. Duic, Lj; Mandic, Z.; Kovacicek, F. *Journal of Polymer Science, Part A: Polymer Chemistry* **1994,** *32*, 105-11.

101. Tang, Heqing; Kitani, Akira; Shiotani, Masaru *Electrochimica Acta* **1996,** *41*, 1561-67.

102. Janata, Jiri. *Critical Reviews in Analytical Chemistry* **2002,** *32*, 109-120.

103. Janata, Jiri, *Proceedings of the IEEE* **2003,** *91*, 864-869

104. Janata, Jiri and Josowicz, Mira. *Nature Materials* **2003,** *2*, 19-24.

105. Janata, J.; Josowicz, M.; DeVaney, D. M. *Analytical Chemistry* **1994**, *66*, 207R-28R.

106. McQuade, D. Tyler, Pullen, Anthony E., and Swager, Timothy M. *Chemical Reviews (Washington, D.C.)* **2000,** *100*, 2537-2574.

107. Gerard, Manju; Chaubey, Asha; Malhotra, B. D. *Biosensors & Bioelectronics* **2002,** *17*, 345-59.

108. Kros, Alexander, Nolte, Roeland J. M., and Sommerdijk, Nico A. J. M. *Advanced Materials* **2002,** *14*, 1779-1782

109. Santhanam, K. S. V. *Pure and Applied Chemistry* **1998**, *70*, 1259-1262.

110. Wallace, G. G., Smyth, M., and Zhao, H. *Trends in Analytical Chemistry* **1999,** *8*, 245-251.

111. Angelopoulos, M. *IBM Journal of Research and Development* **2001,** *45*, 57-75.

112. Conroy, Kenneth G.; Breslin, Carmel B. *Electrochimica Acta* **2003,** *48*, 721-32.

113. Moraes, S. R.; Huerta-Vilca, D.; Motheo, A. J. *Molecular Crystals and Liquid Crystals Science and Technology, Section A: Molecular Crystals and Liquid Crystals* **2002,** *374*, 391-96.

114. Santos, J. R., Jr.; Mattoso, L. H. C.; Motheo, A. J. *Electrochimica Acta* **1997,** *43*, 309-13.

115. Wessling, Bernhard; Posdorfer, Joerg *Electrochimica Acta* **1999,** *44*, 2139-47.

116. Heeger, Alan J. *Synthetic Metals* **2001,** *125*, 23-42.

117. Inzelt, G.; Pineri, M.; Schultze, J. W.; Vorotyntsev, M. A. *Electrochimica Acta* **2000,** *45*, 2403-21.

118. MacDiarmid, Alan G. *Synthetic Metals* **2001,** *125*, 11-22.

119. Pron, Adam; Rannou, Patrice *Progress in Polymer Science* **2001,** *27*, 135-90.

120. Hu, H.; Trejo, M.; Nicho, M. E.; Saniger, J. M.; Garcia-Valenzuela, A. *Sensors and Actuators, B: Chemical* **2002,** *B82*, 14-23.

121. Suri, Komilla; Annapoorni, S.; Sarkar, A. K.; Tandon, R. P. *Sensors and Actuators, B: Chemical* **2002,** *B81*, 277-82.

122. Leclerc, Mario. *Advanced Materials* **1999,** *11*, 1491-1498.

123. Milella, E. and Penza, M. *Thin Solid Films* **1998,** *327-329*, 694-697.

124. Hwang, B. J., Yang, J. Y., and Lin, C. W. *Sensors and Actuators, B: Chemical* **2001,** *B75*, 67-75.

125. Nicolas-Debarnot, Dominique; Poncin-Epaillard, Fabienne *Analytica Chimica Acta* **2003,** *475*, 1-15.

126. Kukla, A. L.; Shirshov, Yu; Piletsky, S. A. *Sensors and Actuators, B: Chemical* **1996,** *B37*, 135-40.

127. Matsuguchi, M.; Io, J.; Sugiyama, G.; Sakai, Y. *Synthetic Metals* **2002,** *128*, 15-19.

128. Nicho, M. E.; Trejo, M.; Garcia-Valenzuela, A.; Saniger, J. M.; Palacios, J.; Hu, H. *Sensors and Actuators, B: Chemical* **2001,** *B76*, 18-24.

129. Agbor, N. E.; Petty, M. C.; Monkman, A. P. *Sensors and Actuators, B: Chemical* **1995,** *B28*, 173-79.

130. Barker, P. S.; Di Bartolomeo, C.; Monkman, A. P.; Petty, M. C.; Pride, R. *Sensors and Actuators, B: Chemical* **1995,** *B25*, 451-53.

131. Do, J. S.; Chang, W. B. *Sensors and Actuators, B: Chemical* **2001,** *B72*, 101-07.

132. Xie, Dan; Jiang, Yadong; Pan, Wei; Li, Dan; Wu, Zhiming; Li, Yanrong *Sensors and Actuators, B: Chemical* **2002,** *B81*, 158-64.

133. Agbor, N. E.; Cresswell, J. P.; Petty, M. C.; Monkman, A. P. *Sensors and Actuators, B: Chemical* **1997,** *B41*, 137-41.

134. Takeda, S. *Thin Solid Films* **1999,** *343-344*, 313-16.

135. Sharma, Satish; Nirkhe, Chetan; Pethkar, Sushama; Athawale, Anjali A. *Sensors and Actuators, B: Chemical* **2002,** *B85*, 131-36.

136. Syritski, Vitali; Bereznev, Sergei; Opik, Andres *Proceedings of the Estonian Academy of Sciences, Chemistry* **1998,** *47*, 60-72.

137. Li, Dan; Jiang, Yadong; Li, Yanrong; Yang, Xujie; Lu, Lude; Wang, Xin *Materials Science & Engineering, C: Biomimetic and Supramolecular Systems* **2000,** *C11*, 117-19.

138. Barker, P. S.; Monkman, A. P.; Petty, M. C.; Pride, R. *Synthetic Metals* **1997,** *85*, 1365-66.

139. Krutovertsev, S. A.; Ivanova, O. M.; Sorokin, S. I. *Journal of Analytical Chemistry* **2001,** *56*, 1057-60.

140. Sharma, Satish; Nirkhe, Chetan; Pethkar, Sushama; Athawale, Anjali A. *Sensors and Actuators, B: Chemical* **2002,** *B85*, 131-36.

141. Sestak, Stephen; Conn, Costa; Lake, Michael; Baker, Anthony T.; Unsworth, Joe *Proceedings of SPIE-The International Society for Optical Engineering* **1997,** *3241*, 118-29.

142. Ogura, K.; Shiigi, H. *Electrochemical and Solid-State Letters* **1999,** *2*, 478-80.

143. Ogura, K.; Shiigi, H.; Oho, T.; Tonosaki, T. *Journal of the Electrochemical Society* **2000,** *147*, 4351-55.

144. Meijerink, M. G. H.; Strike, D. J.; de Rooij, N. F.; Koudelka-Hep, M. *Sensors and Actuators, B: Chemical* **2000,** *B68*, 331-34.

145. Matsuguchi, M.; Io, J.; Sugiyama, G.; Sakai, Y. *Synthetic Metals* **2002,** *128*, 15-19.

146. Kukla, A. L.; Shirshov, Yu; Piletsky, S. A. *Sensors and Actuators, B: Chemical* **1996,** *B37*, 135-40.

147. Kemp, N. T.; Flanagan, G. U.; Kaiser, A. B.; Trodahl, H. J.; Chapman, B.; Partridge, A. C.; Buckley, R. G. *Synthetic Metals* **1999,** *101*, 434-35.

148. Ingleby, P., Gardner, J. W., and Bartlett, P. N. *Sensors and Actuators, B: Chemical* **1999,** *B57,* 17-27.

149. Hosseini, S. Hossein; Entezami, Ali A. *Polymers for Advanced Technologies* **2001,** *12*, 482-93.

150. Ghita, M.; Gheorghe, M.; Visinoiu, A. *Proceedings - International Conference on Microelectronics, 22nd, Nis, Yugoslavia, May 14-17, 2000,* Bucharest, Rom, **1999**.

151. Collins, G. E. and Buckley, L. J. *Synthetic Metals* **1996,** 78, 93-101.

152. Chabukswar, V. V.; Pethkar, S.; Athawale, A. A. *Sensors and Actuators, B: Chemical* **2001,** *B77*, 657-63.

153. Cataldo, Franco; Maltese, Paolo *Polymers for Advanced Technologies* **2001,** *12*, 293-99.

154. Campos, M.; Bulhoes, L. O. S.; Lindino, C. A. *Sensors and Actuators, A: Physical* **2000,** *A87*, 67-71.

155. Athawale, A. A.; Kulkarni, M. V. *Sensors and Actuators, B: Chemical* **2000,** *B67*, 173-77.

156. V.M.Mirsky; V.Kulikov, Kluwer Academic/Plenum publishers: **2003**.

157. Kulikov, V.; Hao, Q.; Donoval, D.; Mirsky, V. M. *ASDAM '02, International Conference on Advanced Semiconductor Devices and Microsystems, Conference Proceedings, 4th, Smolenice Castle, Slovakia, Oct. 14-16, 2002*, **2002** .

158. Hao, Q.; Kulikov, V.; Mirsky, V. M.; Wolfbeis, O. S. **2002,** 15-9-2002; 755-56.

159. Athawale, Anjali A.; Deore, Bhavana; Vedpathak, Mahesh; Kulkarni, Sulabha K. *Journal of Applied Polymer Science* **1999,** *74*, 1286-92.

160. Timofeeva, O. N.; Lubentsov, B. Z.; Sudakova, E. Z.; Chernyshov, D. N.; Khidekel, M. L. *Synthetic Metals* **1991,** *40*, 111-16.

161. Costantini, Nicola; Capaccioli, Simone; Geppi, Marco; Ruggeri, Giacomo *Polymers for Advanced Technologies* **2000,** *11*, 27-39.

162. Han, Moon Gyu; Byun, Sung Woen; Im, Seung Soon *Polymers for Advanced Technologies* **2002,** *13*, 320-28.

163. Hung, Shiue Liang; Wen, Ten Chin; Gopalan, A. *Materials Letters* **2002,** *55*, 165-70.

164. Jousseaume, V.; Morsli, M.; Bonnet, A. *Journal of Applied Polymer Science* **2002,** *84*, 1848-55.

165. Omastova, Maria; Pavlinec, Juraj; Pionteck, Jurgen; Simon, Frank *Polymer International* **1997,** *43*, 109-16.

166. Amrani, M. E. H.; Payne, Peter A.; Persaud, Krishna C. *Sensors and Actuators, B: Chemical* **1996,** *B33*, 137-41.

167. Jin, Zhe; Su, Yongxuan; Duan, Yixiang *Sensors and Actuators, B: Chemical* **2001,** *B72*, 75-79.

168. Nicho, M. E.; Trejo, M.; Garcia-Valenzuela, A.; Saniger, J. M.; Palacios, J.; Hu, H. *Sensors and Actuators, B: Chemical* **2001,** *B76*, 18-24.

169. El Sherif, Mahmoud A.; Yuan, Jianming; MacDiarmid, Alan, *Journal of Intelligent Material Systems and Structures* **2001,** *11*, 407-14.

170. Agbor, N. E.; Cresswell, J. P.; Petty, M. C.; Monkman, A. P. *Sensors and Actuators, B: Chemical* **1997,** *B41*, 137-41.

171. Josowicz, Mira; Janata, Jiri *Analytical Chemistry* **1986,** *58*, 514-17.

172. Liess, Martin; Chinn, Douglas; Petelenz, Danuta; Janata, Jiri *Thin Solid Films* **1996,** *286*, 252-55.

173. Domansky, Karel, Li, Jing, and Janata, Jiri. *Journal of the Electrochemical Society* **1997,** *144*, L75-L78.

174. Domansky, Karel; Baldwin, David L.; Grate, Jay W.; Hall, Thomas B.; Li, Jing; Josowicz, Mira; Janata, Jiri *Analytical Chemistry* **1998,** *70*, 473-81.

175. Barker, P. S.; Di Bartolomeo, C.; Monkman, A. P.; Petty, M. C.; Pride, R. *Sensors and Actuators, B: Chemical* **1995,** *B25*, 451-53.

176. Barker, P. S.; Monkman, A. P.; Petty, M. C.; Pride, R. *Synthetic Metals* **1997,** *85*, 1365-66.

177. Do, J. S.; Chang, W. B. *Sensors and Actuators, B: Chemical* **2001,** *B72*, 101-07.

178. Josowicz, Mira *Chemia Analityczna (Warsaw, Poland)* **2001,** *46*, 161-74.

179. Syu, Mei Jywan; Liu, Jwo Ying *Sensors and Actuators, B: Chemical* **1998,** *B49*, 186-94.

180. Lavrik, N. V.; De Rossi, D.; Kazantseva, Z. I.; Nabok, A. V.; Nesterenko, B. A.; Piletsky, S. A.; Kalchenko, V. I.; Shivaniuk, A. N.; Markovskiy, L. N. *Nanotechnology* **1996,** *7*, 315-19.

181. Syritski, Vitali; Bereznev, Sergei; Opik, Andres *Proceedings of the Estonian Academy of Sciences, Chemistry* **1998,** *47*, 60-72.

182. Matsuguchi, M.; Izumi, K.; Okamoto, A.; Sakai, Y. *Chemical Sensors* **2001,** *17*, 215-17.

183. Li, Dan, Jiang, Yadong, Wu, Zhiming, Chen, Xiangdong, and Li, Yanrong. *Sensors and Actuators, B: Chemical* **2000,** *B66*, 125-127.

184. Ando, Masanori; Swart, Claudia; Pringsheim, Erika; Mirsky, Vladimir M.; Wolfbeis, Otto S. *Solid State Ionics* **2002,** *152-153*, 819-22.

185. Syu, Mei Jywan; Liu, Jwo Ying *Sensors and Actuators, B: Chemical* **1998,** *B50*, 1-8.

186. Cui, Gang; Lee, Jin Seo; Kim, Sang Jin; Nam, Hakhyun; Cha, Geun Sig; Kim, Hai Dong *Analyst (Cambridge, United Kingdom)* **1998,** *123*, 1855-59.

187. Janata, Jiri; Josowicz, Mira *Nature Materials* **2003,** *2*, 19-24.

188. Jin, Zhe; Su, Yongxuan; Duan, Yixiang *Sensors and Actuators, B: Chemical* **2001,** *B72*, 75-79.

189. Koul, Saraswati; Dhawan, S. K.; Chandra, S.; Chandra, R. *Indian Journal of Chemistry, Section A: Inorganic, Bio-inorganic, Physical, Theoretical & Analytical Chemistry* **1997,** *36A*, 901-04.

190. Hao, Qingli, Kulikov, V., and Mirsky, Vladimir M. *Sensors and Actuators, B: Chemical,* **2003**, In Press

191. Jandeleit, Bernd, Schaefer, Dieter J., Powers, Timothy S., Turner, Howard W., and Weinberg, W. Henry. *Angewandte Chemie, International Edition* **1999,** *38*, 2494-2532.

192. Meredith, Carson, Sormana, Joe Lahai, Tona, Alex, Elgendy, Hoda, Karim, Alamgir, and Amis, Eric. *Polymer Preprints* **2001,** *42*, 649-650.

193. Potyrailo, Radislav A. and Pickett, James E. *Angewandte Chemie, International Edition* **2002,** *41*, 4230-4233.

194. Potyrailo, Radislav A., Lemmon, John P., and Leib, Terry K. *Analytical Chemistry* **2003,** *75*, 4676-4681.

195. Zhao, Ji Cheng. *Advanced Engineering Materials* **2001,** *3*, 143-147.

196. Beck-Sickinger, A.; Weber, P. *Kombinatorische Methoden in Chemie und Biologie,* Spektrum Akad. Verl.: Heidelberg, Berlin, 1999.

197. Croston, Glenn E. *Trends in Biotechnology* **2002,** *20*, 110-15.

198. Schiedel, Marc Steffen; Briehn, Christoph A.; Bauerle, Peter *Angewandte Chemie, International Edition* **2001,** *40*, 4677-80.

199. Briehn, Christoph A.; Schiedel, Marc Steffen; Bonsen, Eva M.; Schuhmann, Wolfgang; Bauerle, Peter *Angewandte Chemie, International Edition* **2001,** *40*, 4680-83.

200. Gallop, M. A. *Solid-phase synthesis of compound libraries and their applications in drug discovery,* Acros Organics nv: Geel, 2000.

201. De Mello, Andrew J. *Analytical and Bioanalytical Chemistry* **2002,** *372*, 12-13.

202. Salimi-Moosavi, Hossein; Tang, Thompson; Harrison, D. Jed *Journal of the American Chemical Society* **1997,** *119*, 8716-17.

203. Yudin, A. K.; Siu, T. *Current Opinon in Chemical Biology*, *5*, 269-72.

204. Pilard, J. F.; Marchand, G.; Simonet, J. *Tetrahedron* **1998,** *54*, 9401-14.

205. Niyazymbetov, M. *International Forum on Electrolysis in the Chemical Industry: The Power of Electrochemistry, 10th, Clearwater Beach, Fla., Nov. 10-14,* **1996**, USA Office,Zelinsky Institute,Bear,DE,USA, 1996 .

206. Hayes, William A.; Shannon, Curtis *Langmuir* **1996,** *12*, 3688-94.

207. Lukkari, Jukka; Kleemola, Kari; Meretoja, Minna; Ollonqvist, Tapio; Kankare, Jouko *Langmuir* **1998,** *14*, 1705-15.

208. Scheying, Gerd, Schulte, Thomas, Brinz, Thomas, Kulikov, Valentin, and Mirsky, Vladimir. Robert Bosch Gmbh, Germany. **2001**, 10131581[10131581], 10. 2-7-2001. DE.

209. Diaz, A. F.; Logan, J. A. *Journal of Electroanalytical Chemistry and Interfacial Electrochemistry* **1980,** *111*, 111-14.

210. Genies, E. M.; Boyle, A.; Lapkowski, M.; Tsintavis, C. *Synthetic Metals* **1990,** *36*, 139-82.

211. Mu, Shaolin; Kan, Jinqing *Synthetic Metals* **1998,** *92*, 149-55.

212. Sivakumar, R.; Saraswathi, R. *Synthetic Metals* **2003,** *138*, 381-90.

213. Yang, Hongjun; Bard, Allen J. *Journal of Electroanalytical Chemistry* **1992,** *339*, 423-49.

214. Mu, Shaolin; Kan, Jinqing *Electrochimica Acta* **1996,** *41*, 1593-99.

215. Shim, Yoon Bo; Won, Mi Sook; Park, Su Moon *Journal of the Electrochemical Society* **1990,** *137*, 538-44.

216. Nekrasov, A. A.; Ivanov, V. F.; Gribkova, O. L.; Vannikov, A. V. Bad Herrenalb, Germany, 3 A.D. **2003**.

217. Hao, Qingli, Rahm, Michael, Weiss, Dieter, and Mirsky, Vladimir M. *Microchimica Acta* **2003**, *143*, 147-153.

218. Sabatani, Eyal; Gafni, Yael; Rubinstein, Israel *Journal of Physical Chemistry* **1995,** *99*, 12305-11.

219. Sapurina, I.; Osadchev, A. Yu; Volchek, B. Z.; Trchova, M.; Riede, A.; Stejskal, J. *Synthetic Metals* **2002,** *129*, 29-37.

220. Pankratov, A. N.; Uchaeva, I. M.; Doronin, S. Yu.; Chernova, R. K. *Journal of Structural Chemistry (Translation of Zhurnal Strukturnoi Khimii)* **2001,** *42*, 739-46.

221. Planes, Gabriel A.; Miras, Maria C.; Barbero, Cesar *Polymer International* **2002,** *51*, 429-33.

222. Bedekar, A. G.; Patil, S. F.; Patil, R. C. *Polymer International* **1996,** *40*, 201-05.

223. Patil, S. F.; Bedekar, A. G.; Patil, R. C.; Deore, Bhavana *Materials Letters* **1995,** *25*, 43-48.

224. Mazur, Maciej; Krysinski, Pawel *Electrochimica Acta* **2001,** *46*, 3963-71.

225. Panasyuk, Tatiana L.; Mirsky, Vladimir M.; Piletsky, Sergey A.; Wolfbeis, Otto S. *Analytical Chemistry* **1999,** *71*, 4609-13.

226. Rubinstein, Israel; Rishpon, Judith; Sabatani, Eyal; Redondo, Antonio; Gottesfeld, Shimshon *Journal of the American Chemical Society* **1990,** *112*, 6135-36.

227. Mirsky, Vladimir M. *TrAC, Trends in Analytical Chemistry* **2002,** *21*, 439-50.

228. Qiu, Hongjin; Wan, Meixiang; Matthews, Barry; Dai, Liming *Macromolecules* **2001,** *34*, 675-77.

229. Liu, Jing; Wan, Meixiang *Journal of Materials Chemistry* **2001,** *11*, 404-07.

230. Swart, C. Dipl. Thesis, University of Regensburg, 2001.

231. Wang, Baochen; Tang, Jinsong; Wang, Fosong *Synthetic Metals* **1986,** *13*, 329-34.

232. Thiemann, C.; Brett, C. M. A. *Synthetic Metals* **2001,** *123*, 1-9.

233. Estes, Richard H., Ito, Koji, Akita, Masanori, Mori, Toshihiro, and Wada, Minoru. Polymer Flip Chip Corp. and Toray Engineering Co.. 99-378847[6189208], 12. 23-8-**1999**. US.

234. Estes, Richard H. Polymer Flip Chip Corporation. **2001**-US26436[0217392], 38. WO.

235. Unger, Eugen and Weber, Werner. Infineon Technologies Ag, Germany. **2000**-10038125[10038125], 8. 4-8-2000. DE.

236. Akundy, Gouri Smitha; Rajagopalan, Ramakrishnan; Iroh, Jude O. *Journal of Applied Polymer Science* **2002,** *83*, 1970-77.

237. Cha, S. K., *Journal of Polymer Science, Part B: Polymer Physics* **1997,** *35*, 165-72.

238. Wang, Yanju; Wang, Xianhong; Li, Ji; Zhang, Hongfang; Mo, Zhishen; Jing, Xiabin; Wang, Fosong *Journal of Polymer Science, Part B: Polymer Physics* **2002,** *40*, 605-12.

239. Bartlett, Philip N.; Birkin, Peter R.; Wang, Jin Hai; Palmisano, Francesco; De Benedetto, Giuseppe *Analytical Chemistry* **1998,** *70*, 3685-94.

240. Misoska, V.; Price, W. E.; Ralph, S. F.; Wallace, G. G.; Ogata, N. *Synthetic Metals* **2001,** *123*, 279-86.

241. Kranz, Christine; Wohlschlaeger, Heidi; Schmidt, Hanns Ludwig; Schuhmann, Wolfgang *Electroanalysis* **1998,** *10*, 546-52.

242. Hirata, Mistutoshi; Sun, Liangyan *Sensors and Actuators, A: Physical* **1994,** *40*, 159-63.

243. Koul, Saraswati; Dhawan, S. K.; Chandra, S.; Chandra, R. *Indian Journal of Chemistry, Section A: Inorganic, Bio-inorganic, Physical, Theoretical & Analytical Chemistry* **1997,** *36A*, 901-04.

244. Hayes, William A.; Kim, Hyun; Yue, Xiaohui; Perry, Scott S.; Shannon, Curtis *Langmuir* **1997,** *13*, 2511-18.

245. Panasyuk, Tatiana L.; Mirsky, Vladimir M.; Piletsky, Sergey A.; Wolfbeis, Otto S. *Analytical Chemistry* **1999,** *71*, 4609-13.

246. Salamon, Zdzislaw; Macleod, H. Angus; Tollin, Gordon *Biochimica et Biophysica Acta* **1997,** *1331*, 117-29.

247. Chegel, Vladimir, Raitman, Oleg, Katz, Eugenii, Gabai, Rachel, and Willner, Itamar. *Chemical Communications* **2001,** *10*, 883-884.

248. Janek, Richard P.; Fawcett, W. Ronald; Ulman, Abraham *Langmuir* **1998,** *14*, 3011-18.

249. Gazotti, W. A., Jr., Faez, R., and De Paoli, Marco A. *Journal of Electroanalytical Chemistry* **1996,** 415, 107-113.

250. Pullen, Anthony E. and Swager, Timothy M. *Macromolecules* **2001,** 34, 812-816.

251. Ranger, M. and Leclerc, M. *Synthetic Metals* **1997,** *84*, 85-86.

252. Wang, X. H.; Geng, Y. H.; Wang, L. X.; Jing, X. B.; Wang, F. S. *Synthetic Metals* **1995,** *69*, 263-64.

253. Xu, L. G., Ng, S. C., and Chan, H. S. O, *Synthetic Metals* **2001,** *123*, 403-410.

254. Brett, Christopher M. A. and Thiemann, Carolin. *Journal of Electroanalytical Chemistry* **2002,** *538-539*, 215-222.

255. Focke, Walter W.; Wnek, Gary E. *Journal of Electroanalytical Chemistry and Interfacial Electrochemistry* **1988,** *256*, 343-52.

256. Neoh, K. G.; Kang, E. T.; Tan, K. L. *Polymer* **1993,** *34*, 1630-36.

257. Noeh, K. G.; Tan, K. L.; Tan, T. C.; Kang, E. T. *Journal of Macromolecular Science, Chemistry* **1990,** *A27*, 347-60.

258. Conklin, Jeanine A.; Huang, Shu Chuan; Huang, Shiou Mei; Wen, Tianli; Kaner, Richard B. *Macromolecules* **1995,** *28*, 6522-27.

259. Abell, L.; Pomfret, S. J.; Adams, P. N.; Monkman, A. P. *Synthetic Metals* **1997,** *84*, 127-28.

260. Bondarenko, V. E.; Zhuravleva, T. S.; Bibikov, S. B. *Khimicheskaya Fizika* **1999,** *18*, 96-100.

261. Chandrakanthi, Nayana; Careem, M. A. *Polymer Bulletin (Berlin)* **2000,** *44*, 101-08.

262. Kumar, D.; Chandra, R. *Indian Journal of Engineering & Materials Sciences* **2001,** *8*, 209-14.

263. Cochet, M.; Buisson, J. P.; Wery, J.; Jonusauskas, G.; Faulques, E.; Lefrant, S. *Synthetic Metals* **2001,** *119*, 389-90.

264. Li, Xingwei; Bian, Chaoqing; Chen, Wei; He, Jinbo; Wang, Zhaoquen; Xu, Ning; Xue, Gi *Applied Surface Science* **2003,** *207*, 378-83.

265. Pandey, S. S.; Gerard, Manju; Sharma, Amit L.; Malhotra, B. D. *Journal of Applied Polymer Science* **2000,** *75*, 149-55.

266. Gazotti, Wilson A., Jr.; Faez, Roselena; De Paoli, Marco A. *European Polymer Journal* **1998,** *35*, 35-40.

267. Jang, Guang Way.. Gumbs Associates, Inc. 96-704375[5869007], 12. 22-8-1996. US.

268. MacDiarmid, Alan G. *Angewandte Chemie, International Edition* **2001,** *40*, 2581-2590.

269. Diamond, Dermot and Editor. *Chem. Anal*, **1998**, *150*, 334.

270. Alix, A.; Lemoine, V.; Nechtschein, M.; Travers, J. P.; Menardo, C. *Synthetic Metals* **1989,** *29*, E457-E462.

271. Athawale, Anjali A.; Chabukswar, V. V. *Journal of Applied Polymer Science* **2001,** *79*, 1994-98.

272. Koul, S.; Chandra, R.; Dhawan, S. K. *Sensors and Actuators, B: Chemical* **2001,** *B75*, 151-59.

273. Matsumura, K.; Matsuguchi, Masanobu; Sakai, Yoshiro *Chemical Sensors* **1997,** *13*, 9-12.

274. Matsuguchi, M.; Okamoto, A.; Sakai, Y. *Sensors and Actuators, B: Chemical* **2003,** *B94*, 46-52.

275. Prissanaroon, W.; Ruangchuay, L.; Sirivat, A.; Schwank, J. *Synthetic Metals* **2000,** *114*, 65-72.

276. Krutovertsev, S. A.; Ivanova, O. M.; Sorokin, S. I. *Journal of Analytical Chemistry (Translation of Zhurnal Analiticheskoi Khimii)* **2001,** *56*, 1057-60.

277. Nakagawa, Katsuhiko; Kitagawa, Takahiro; Sadaoka, Yoshihiko *Sensors and Actuators, B: Chemical* **1998,** *B52*, 10-14.

278. Huang, Jiaxing; Virji, Shabnam; Weiller, Bruce H.; Kaner, Richard B. *Journal of the American Chemical Society* **2003,** *125*, 314-15.

279. Hosseini, S. Hossein; Entezami, Ali A. *Polymers for Advanced Technologies* **2001,** *12*, 482-93.

280. Chviruk, V. P., Linuycheva, O. V., and Zaverach, E. M. *Sensors and Actuators, B: Chemical* **2003,** *B92*, 60-66.

281. Lavrik, N. V.; De Rossi, D.; Kazantseva, Z. I.; Nabok, A. V.; Nesterenko, B. A.; Piletsky, S. A.; Kalchenko, V. I.; Shivaniuk, A. N.; Markovskiy, L. N. *Nanotechnology* **1996,** *7*, 315-19.

282. Morales, J. Alberto and Cassidy, John F. *Sensors and Actuators, B: Chemical* **2003,** *B92*, 345-350.

7 Abbreviations Used

AA	Anthranilic acid
3-ABA	3-Aminobenzoic acid
4-ABA	4-Aminobenzoic acid
3-ABBA	3-Aminobenzoboric acid
3-ABSA	3-Aminobenzenesulfonic acid
2sBA	2-*sec*.Butylaniline
2tBA	2-*tert*-Butylaniline
Borax	sodium tetraborate
BQ	*p*-Benzoquinone
CE	Counter Electrode
CV	Cyclic Voltammogram
DIN	Deutsche Industrie Norm
DPA	Diphenylamine
DSC	Differential scanning calorimetry
2EA	2-Ethylaniline
3EA	3-Ethylaniline
E_{ac}	Activation energy
EB	Emeraldine Base
EDOT	3,4-Ethylenedioxythiophene
EIS	Electrochemical Impedance Spectroscopy
ES	Emeraldine Salt
HQ	Hydroquinone
LB	Leucoemeraldine base
NB	Nigraniline Base
NBA	N-butylanline
NEA	N-ethylaniline
MA	N-methyl aniline
OCPs	Organic Conducting Polymers
2PA	2-Propylaniline
Pac	Polyacetylene
PANI	Polyaniline
P(ANI-3ABA)	Poly(aniline-3-aminobenzoic acid)
P(ANI-3ABBA)	Poly(aniline-3-aminobenzoboric acid)
PB	Pernigraniline Base
PEB	Poly(emeraldine base)
PEDOT	Poly(3,4-ethylenedioxythiophene)
PLB	Poly(leucoemeraldine base)
PNMA	Poly(N-methyl aniline)
PPY	Polypyrrole
PY	pyrrole
RE	Reference Electrode
TGA	Thermogravimetric analysis
Tris	Trishydroxymethylaminomethane
WE	Working Electrode

8 List of Publications and Presentations

8.1 Publications

1   **Qingli Hao,** Valentin Kulikov, Vladimir M. Mirsky, Investigation of contact and bulk resistance of conducting polymers by simultaneous two- and four-point technique**,** *sens. & Actuat. B*, 2003, 94(3), 352-357.

2   **Qingli Hao**, Michael Rahm, Dieter Weiss, Vladimir M. Mirsky, Morphology of electropolymerized poly (N-methylaniline) films**,** *Microchimica Acta.* 2003, 143(2-3), 147–153.

3   Valentin Kulikov, **Qingli Hao**, Otto S. Wolfbeis, Vladimir M. Mirsky*
Multiparameter High Throughput Characterization of Combinatorial Chemical Microarrays of Chemosensitive Polymers. *Macromolecule rapid Communications.* (2003) (accepted).

4   **Qingli Hao**, V. Kulikov, V.M. Mirsky A highly response and sensitive gas sensor based on conducting polymer performed by thermal desorption, In preparation(2003).

5   **Qingli Hao,** V. Kulikov, V.M. Mirsky Gas sensors based on multilayer structures of conducting polymers deposited electrochemically**.** In preparation (2003).

6   A. V. Samoylov, Y.M. Shirshov, C. Swart, **Qingli Hao,** Vladimir V. Mirsky, Chemical sensor for gaseous HCl based on surface plasmon resonance Prepared for publication, (2003).

8.2 Poster Presentations and Conferences

1   **<u>Qingli Hao,</u>** Valentin Kulikov, Vladimir M. Mirsky, Otto S. Wolfbeis, Gas sensors based on bi-layer structures of conductive polymers, Eurosensors XVI, the 16th European Conference on Solid-State Transducers, *Conference Proceedings*, Prague, Czech Republic, Sept. 15-18, 2002. 2002 (part 3) 749.

2   **<u>Qingli Hao</u>**, Michael Rahm, Dieter Weiss, Vladimir M. Mirsky, Morphology of electropolymerized poly (N-methyl aniline) films, International workshop on Electrochemistry of Electroactive Materials (WEEM-2003), Abstracts, Bad Herrenalb, Germany, July 22-27, 2003.

3   Valentin Kulikov, **<u>Qingli Hao</u>**, Daniel Donoval, Vladimir M. Mirsky, Set-up for combinatorial electrochemical synthesis and high-throughput investigation of organic semiconductor polymers for electronic devices, ASDAM '02, international Conference on Advanced Semiconductor Devices and Microsystems, *Conference Proceedings*, 4th, Smolenice Castle, Slovakia, Oct. 14-16, 2002. (2002), 63-66.

4   Valentin Kulikov, **<u>Qingli Hao</u>**, Vladimir M. Mirsky, Otto S. Wolfbeis**,** Set-up for combinatorial electropolymerization and investigation of polymer properties, Eurosensors XVI, the 16th European Conference on Solid-State Transducers, *Conference Proceedings*, Prague, Czech Republic, Sept. 15-18, 2002. 2002 (part 3) 765.

CONFERENCE PARTICIPATIONS:

15-18, Sept. 2002	Eurosensors XVI, Prague, Czech Republic
22-27, July 2003	WEEM-2003, Bad Herrenalb, Germany

9 Acknowledgements

I would like to thank the following people who contributed to the success of my work:

Generally I wish to give my grateful acknowledgements to all members of our institute, who provide a pleasant atmosphere where I spent two years of happy time.

First of all, I appreciate my supervisor, *PD. Dr. Vladimir M. Mirsky*. I would like to thank him for giving me this opportunity to study and work under his instruction, for his selfless supervision and assistance, for his intelligent guidance and discussion. I also would like to acknowledge *Prof. Dr. Otto. S. Wolfbeis*, our chief, for offering this chance for me, for his valuable discussion and his warm assistance;

Dipl. Ing. Valentin Kulikov, my cooperator in the Kombisens Project, who designed the setups and software for electrical measurements and gave me lots of help both in physical science and life;

Dr. Tanya Panasyuk-Delaney, *Mrs. Angela Haberkern*, *Mr. Thomas Hirsch* and *Joachim Rewitzer*, my lab colleagues, giving me plenty of valuable advice, warm help and care, with whom I had a happy time during the past period; Thank *Miss Claudia Swart* for introducing me to this project at the beginning;

Mr. Hubert Kettenberger, my former colleague, who gave me urgent assistance;

Mr. Athanas Apostolidis and *Dr. Damian Andrzejewski*, who designed the setup and software for gas measurements, supporting me with technical help;

Dr. S. Woelki, *Mr. Jürgen Keller and Mr. Alexander Wagner*, from the group of Prof. Dr. H.-H. Kohler, who offered their kind assistance to me; moreover, thank *Mr. Jürgen Kell* for his helpful discussion;

Dr. Axel Dürkop, who gave me advice on how to write a thesis;

Mrs. A. Stoiber, *Mr. Dr. K.-P. Rueß*, *Mr. Dr. O. Lossen* and *Mr. K. Berghausen*, who often helped me search for chemicals without hesitation;

Miss Gisela Emmert and *Dr. W. Oestreicher*, who patiently assisted me to solve computer problems;

Mrs. Edeltraud Schmid, *Mrs. M. Bauer*, our secretaris, whom I always caused trouble;

Miss Martina Kreuzer, *Dr. Jochen Abke* and *Dr. Rainer Müller*, from the group of Prof. em. Dr. K. Heckmann, who kindly lend hands with thermal analysis for me;

Mr. Michael Rahm, from the group of Prof. Dieter Weiss, who lent a hand to me on the measurement of STM;

Mrs. E. Bogner and *Mrs W. Krutina*, who carried out elemental analysis for me;

Mr. Changkuo Zhao, from the group of Prof. Dr. O. Reiser, who acquired IR spectra for me;

Linzhi Hong, *Meng Wu* and *Yinghong Lu*, who gave me friendly advice, warm assistance in Regensburg, lending hands to expel the homesick feeling of mine. Here I also wish them to finish their doctor work soon and successfully.

Dr. Gang Xiong from Durham University, UK, who gave me good suggestions;

This work was supported by the project Kombisens from the German Ministry for Science and Technology.

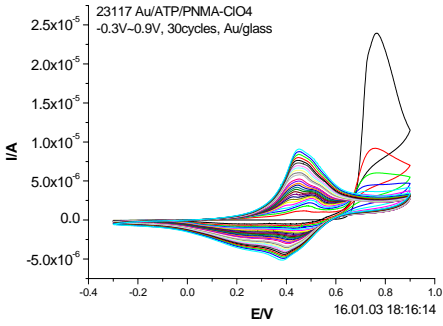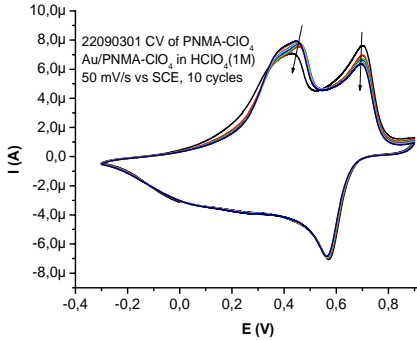Furthermore, **special appreciation** given to:
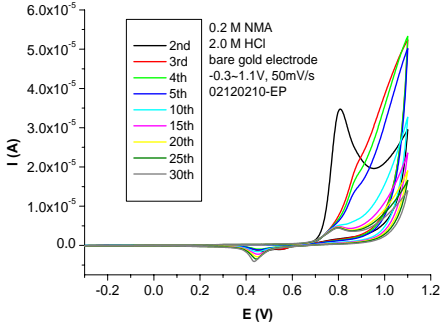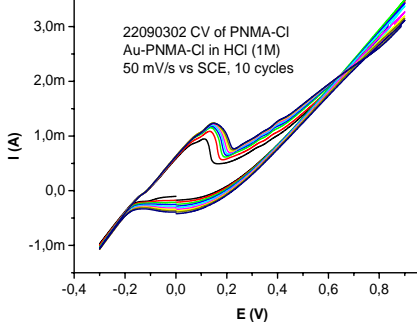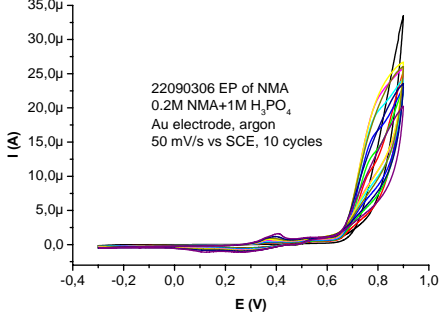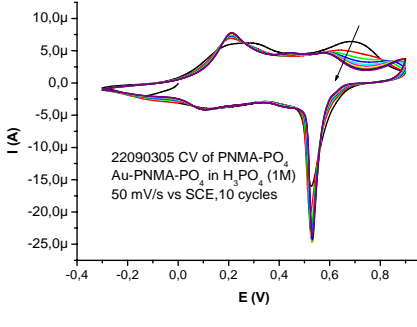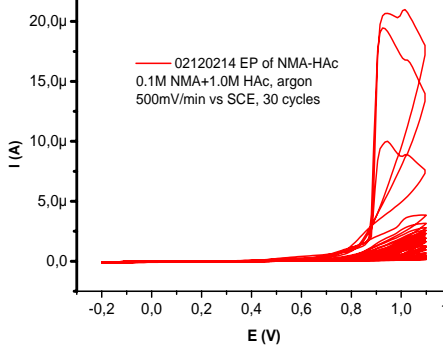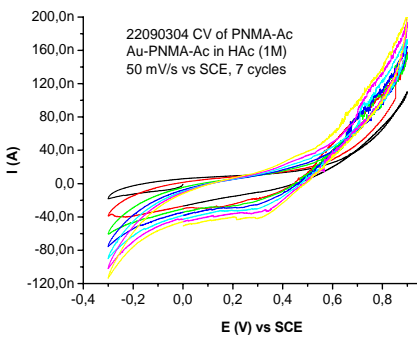
My German friends, *the family Dr. Albrecht* in Regensburg, who gave me great support in life and spirit, offering me warm hospitality and care, which presented me a feeling of home;

My husband and the whole family……

Table 3.1 Electrochemical synthesis of conducting polymers   Appendix

Appendix

Table 3.1 Electrochemical synthesis of conducting polymers

monomer	dopant	CV curve with monomer	CV curve without monomer
aniline	H_2SO_4		
aniline	$HClO_4$		
aniline	HCl		
NMA	H_2SO_4		

Table 3.1 Electrochemical synthesis of conducting polymers   Appendix

NMA	**HClO₄**		
NMA	**HCl**		
NMA	**H₃PO₄**		
NMA	**CH₃-COOH**		

Table 3.1 Electrochemical synthesis of conducting polymers   Appendix

4-ABA	**H_2SO_4**	23100201 4ABA-SO$_4$ (EP) 0.1M 4ABA + 0.1M H$_2$SO$_4$ 50 mV/S, 50 cycles	24100201 CV of P(4-ABA) 0.5M H$_2$SO$_4$ 10 cycles, 50 mV/s vs SCE
3EA	**H_2SO_4**	30090206 EP (3EA-ANI) + H$_2$SO$_4$ 50 mV/s, SCE, 10cycles	24100213 Poly3EA in H$_2$SO$_4$ 50 mv/s, 5th
NEA	**H_2SO_4**	14100202 EP of NEA 0.1M NEA + 0.5M H$_2$SO$_4$ 500 mv/s, 20 cycles Au electrode	Pt-PNEA-SO$_4$ 0.5V H$_2$SO$_4$ -0.3V ~ 1.2V
AA	**H_2SO_4**	15050306 EP of AA 0.1M AA + 0.5M H2SO4 50mv/s vs SCE, 50 cycles Au electrode, normal	Pt-PAA-SO$_4$ 0.5 M H$_2$SO$_4$ -0.3V ~ 1.0 V

®**DPA**	**(CH₃)₄N -ClO₄**		
NBA	**H₂SO₄**		
3ABSA	**H₂SO₄**		
3ABA	**H₂SO₄**		

Table 3.1 Electrochemical synthesis of conducting polymers   Appendix

3PA	**H₂SO₄**		
EDOT	**H₂SO₄**		
EDOT	**NaDBS;**		
EDOT	**SDS; LiClO₄**		

Table 3.1 Electrochemical synthesis of conducting polymers   Appendix

3ABBA	**H₂SO₄**		
2-tBA	**H₂SO₄**		
ANI-2EA	**H₂SO₄**		
ANI-3EA	**H₂SO₄**		

Table 3.1 Electrochemical synthesis of conducting polymers   Appendix

ANI-4ABA	**H₂SO₄**		
ANI-3ABBA	**H₂SO₄**		
ANI-3ABA	**H₂SO₄**		
ANI-3PA	**H₂SO₄**		

ANI-NMA	**H₂SO₄**		
ANI-2*t*BA (3:1)	**H₂SO₄**		
ANI-NEA	**H₂SO₄**		
ANI-AA	**H₂SO₄**		

Table 3.1 Electrochemical synthesis of conducting polymers Appendix

ANI-3ABSA	**H₂SO₄**		
EDOT-3ABBA	**H₂SO₄**		
EDOT-3ABBA	**SDS, LiClO₄, H₂SO₄**		
3ABBA-3ABSA	**H₂SO₄**		
ANI-3ABBA-3ABSA	**H₂SO₄**		

® All films were deposited in aqueous solutions except the marked in acetonitrile.